AD-A105 672 NATIONAL TELECOMMUNICATIONS/INFORMATION ADMINISTRATIO--ETC F/G 20/14
SHF-EHF PROPAGATION THROUGH VEGETATION ON COLORADO EAST SLOPE.(U)
JUN 81 E J VIOLETTE, R H ESPELAND

UNCLASSIFIED CECOM-81-CS020-F NL

1 OF 2
AD A105672

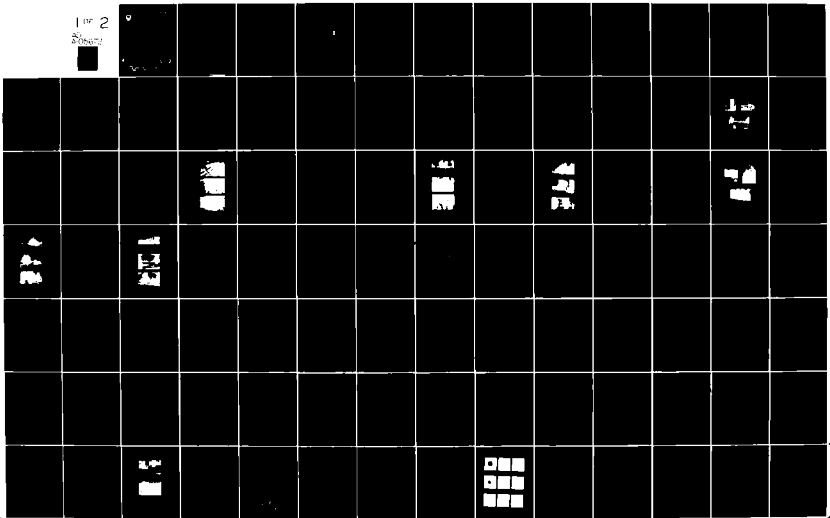

LEVEL II

12

RESEARCH AND DEVELOPMENT TECHNICAL REPORT
CECOM-81-CS020-F

AD A105672

SHF-EHF PROPAGATION THROUGH VEGETATION ON COLORADO EAST SLOPE

E.J. Violette, R.H. Espeland, A.R. Mitz
and F.A. Goodknight
U.S. DEPT. OF COMMERCE , NTIA/ITS
BOULDER, COLORADO

F. Schwering
CENTER FOR COMMUNICATION SYSTEMS

DTIC FILE COPY

June 1981

DTIC
ELECTE
OCT 16 1981
S D
D

DISTRIBUTION STATEMENT:
Approved for public release: distribution unlimited.

CFNA for contract only

CECOM
US ARMY COMMUNICATIONS - ELECTRONICS COMMAND
FORT MONMOUTH, NEW JERSEY 07703

81 10 16

NOTICES

Disclaimers

The citation of trade names and names of manufacturers in this report is not to be construed as official Government indorsement or approval of commercial products or services referenced herein.

Disposition

Destroy this report when it is no longer needed. Do not return it to the originator.

Unclassified

SECURITY CLASSIFICATION OF THIS PAGE (When Data Entered)

REPORT DOCUMENTATION PAGE		READ INSTRUCTIONS BEFORE COMPLETING FORM
1. REPORT NUMBER CECOM-81-CS020-F	2. GOVT ACCESSION NO. AD-A105672	3. RECIPIENT'S CATALOG NUMBER
4. TITLE (and Subtitle) SHF-EHF PROPAGATION THROUGH VEGETATION ON COLORADO EAST SLOPE		5. TYPE OF REPORT & PERIOD COVERED Final Report 1 Jan — 31 Oct 1980
		6. PERFORMING ORG. REPORT NUMBER
7. AUTHOR(s) Edmond J. Violette, Richard H. Espeland, Albert R. Mitz, and Frank A. Goodknight		8. CONTRACT OR GRANT NUMBER(s) CS-0-CS020-CS-WA
9. PERFORMING ORGANIZATION NAME AND ADDRESS US Dept. of Commerce, National Telecommunications & Information Administration, Institute for Telecommunication Sciences, Boulder, CO 80303		10. PROGRAM ELEMENT, PROJECT, TASK AREA & WORK UNIT NUMBERS 1L1 611102.H48.PM.11.01
11. CONTROLLING OFFICE NAME AND ADDRESS US Army Communications-Electronics Command ATTN: DRSEL-COM-RM-4, CENCOMS Ft Monmouth, NJ 07703		12. REPORT DATE June 1981
		13. NUMBER OF PAGES 90
14. MONITORING AGENCY NAME & ADDRESS (if different from Controlling Office)		15. SECURITY CLASS. (of this report) Unclassified
		15a. DECLASSIFICATION/DOWNGRADING SCHEDULE

16. DISTRIBUTION STATEMENT (of this Report)

Approved for Public Release; Distribution Unlimited.

17. DISTRIBUTION STATEMENT (of the abstract entered in Block 20, if different from Report)

18. SUPPLEMENTARY NOTES

19. KEY WORDS (Continue on reverse side if necessary and identify by block number)

Vegetation; propagation measurements; SHF-EHF; Colorado East Slope

20. ABSTRACT (Continue on reverse side if necessary and identify by block number)

An SHF/EHF measurement program was conducted to determine the effects on propagation through vegetation common to the Colorado East Slope. Presented in this reportare the frequency dependence of vegetation losses, polarization, depolarization, and backscatter on observed signal amplitude for three deciduous tree paths, two conifer tree paths, and one grass path at 9.6, 28.8, and 57.6 GHz. Some of the variables for these measurements were foliage depth, antenna position, antenna pointing, and antenna beamwidth. Time series data showing →

DD FORM 1473, 1 JAN 73 EDITION OF 1 NOV 65 IS OBSOLETE

Unclassified

SECURITY CLASSIFICATION OF THIS PAGE (When Data Entered)

410437

20. ABSTRACT
scintillation due to wind is displayed and discussed. A single rain event and a single snow event were recorded. Summer foliage measurements were compared to a wintertime defoliated state with identical terminal locations used for each condition.

TABLE OF CONTENTS

LIST OF FIGURES

LIST OF TABLES

SUMMARY

Instrumentation for measuring propagation effects caused by vegetation at frequencies in the micro-millimeter wave band was designed, constructed, and successfully operated. Both transmitting and receiving terminals are mounted in vans for mobility in rough terrain. The RF components are supported on erectable, track-mounted carriages to permit adjustment of the height above ground. In addition, the transmitter mounting permits two meters of horizontal travel to allow variability along this axis.

The directional antennas, scannable in elevation and azimuth angle by a remote-controlled positioner at the receiver terminal, provide data on the intensity of off-angle scatter from foliage and ground reflection effects.

Three frequencies, namely 9.6, 28.8, and 57.6 GHz, are used simultaneously to obtain frequency-dependent data to aid in developing transmission loss models for specific types of vegetation. Both vertical and horizontal antenna polarization are mechanically selectable at each terminal. Measurements also include cross polarization.

A computer-controlled data logger is incorporated into the receiver terminal. Also a computer-controlled data processing and plotting system facilitates the analysis efforts.

The three-frequency link described above was used to measure signal loss through vegetation, depolarization effects, and scattering characteristics for propagation through both deciduous and conifer groves. These measurements consist of 16 sets of data over 12 paths obstructed with trees in foliage and grass. Measurements were also made on the deciduous tree paths after the leaves had fallen.

The data recorded from these measurements consists of received signal amplitudes from both azimuthal and elevation scans at transmitter and receiver heights from 1 to 9 meters above ground. The transmitter antennas were normally fixed at a zero angle (on-path) pointing and the receiving antennas scanned a $\pm$ 20° angle in the azimuthal plane and $\pm$ 15° angle in the elevation plane. In addition to this basic mode of measurements, several special tests were conducted. These included both vertical and horizontal receiver antenna position displacements to evaluate spatial dependence, off-angle pointing of the transmitting antennas to assess off-path signal scatter, and one test to measure backscatter. Also, propagation effects for a path with vegetation during a rain and snow event are discussed and transmission through trees at EHF are compared to VHF and visible light transmission.

These measurements were made in the foothills region on the eastern slope of the Colorado Rocky Mountains. Tree coverage in this area for both deciduous and conifer trees is typified by sometimes sparse and non-uniform distribution. In this report, the measured signal loss (dB/m) through vegetation (called vegetation loss) means loss per meter of measured foliage depth on a path, independent of the total path length. With maximum total path lengths of just over 300 meters, a measurement of tree depth on a path was not difficult and signal loss per meter of foliage depth is a reasonable descriptor.

When comparing data in this report with data taken at lower frequencies (100 to 2000 MHz) consideration should be given the fact that for these lower frequencies path lengths are generally longer possibly resulting in a variation in density when defining foliage depth. Also a larger area of illumination occurs at lower frequencies i.e., more vegetation, ground, and tree tops are in view due to the wider antenna beamwidth at each terminal.

The following list of statements summarizes the results of this study. The figure or table number in some statements is used to detail the information in the statement:

1. The measured signal loss (vegetation loss) in dB/m through trees in foliage is higher than anticipated, based on measurements in the frequency range between 100 and 9000 MHz [1-16]. A wide range of values resulted from this study as well as from the experiments in the 100-9000 MHz band, but in all cases the measured dB/m loss between 10 and 60 GHz (Figure 4.23) exceeded predicted and/or extrapolated losses measured in the lower frequency band by a 2 to 1 ratio or greater [9,16].

2. Diffraction theory has a $\sqrt{f}$ dependence which sometimes is used to predict vegetation loss (dB/m) at higher frequencies. Although our results show that vegetation losses clearly increased (on the average) at these frequencies, the ratio was less than $\sqrt{f}$ over the 10 to 60 GHz frequency range (Table 4.3).

3. Normalized losses due to vegetation (dB/m) show a trend to decrease as the foliage path is lengthened, which appears consistent with measurements at lower frequencies (Table 4.3).

4. Deciduous groves in summer foliage produced about 2 to 3 times as much loss in dB/m as measured through these groves in their defoliated state (Figs. 5.1 through 5.6).

5. The measured vegetation loss, in nearly all cases, was less at the 1 and 2 meter heights than at heights greater than 2 meters. This is the result of no leaves or sparse leaves at the 1 and 2 meter height and the general absence of underbrush on the sites used for these tests. However, there is an important spatial

dependence at lower heights where large signal losses occur due to destructive interference produced when one or two signal components arrive by reflection from a tree trunk (Figures in Section IV).

6. An important factor is the dependence of received signal on spatial variance. Signal amplitude variation as large as 42 dB and typically 30 dB were observed for small displacements ($\approx$ 25 cm) of the transmitter antennas in either the horizontal or vertical plane (Figs. 4.16 through 4.18). There is considerable evidence that these deep fades are results of two relatively strong multipath signals reacting destructively. Exposed (free of leaf cover) trunks and branches appeared to be the source of the multipath.

7. An increase in vegetation loss was noted during a rain on a single observation when water covered or droplets formed on leaves and branches of a willow tree. The signal loss increase was 3 to 5 dB at 9.6 GHz and 15 to 20 dB at 28.8 GHz; however, these maximum losses occurred several minutes after the shower started, indicating perhaps a delay in wetting of leaves and branches. Moisture condensation in the waveguide prevented a measurement at 57.6 GHz (Fig. 4.37). A wet snow occurred while observing on a conifer path and much of it stayed on the branches; however, no detectable signal change was noted.

8. Vegetation loss difference as a function of antenna polarization (linear vertical or horizontal) was very slight. In making the mechanical rotation of antennas to change polarization, a small position displacement occurs. The resulting spatial variation probably masked any small signal change due to polarization. However, for tall grass, the horizontal polarization clearly provided less loss (Figures in Section IV and Table 4.8).

9. Depolarization of signals propagated at exposed tree trunk heights showed less change than through leafy foliage where depolarized signal level increased by as much as 20 dB (Table 4.7).

10. Lateral wave propagation and tree top diffraction enhancements were not detected; however, measurements were not conclusive due to uncertainties in canopy height, canopy roughness, and path geometry.

11. For a path with high loss due to foliage, a stronger received signal was observed when a common off-path volume (clear of tall trees) was illuminated. In the observed case, a common scatterer, perhaps a bush or terrain feature in a clearing, produced a side scatter signal level higher than the direct-path signal (Fig. 4.33 through 4.35).

12. Direct backscatter measurements from a willow and a pine grove produced an equivalent spherical radar cross section range of .008 to 0.5 square meters, depending on frequency (Figs. 4.25 through 4.27 and Table 4.4).

13. Observations during windy periods (10 to 15 mph) on a path with 10 or more meters of foliage depth produced signal variations (scintillations) of up to 15 dB with periods of less than 5 seconds. In addition, longer period (1 to 5 minutes) fades of as much as 8 dB were noted in gusting winds (Fig. 4.21).

14. On a defoliated path, narrowbeam illumination showed a slight decrease in vegetation losses and much reduced off-angle scattering components compared to wide-beam illumination on the same path. Also on a defoliated path, no detectable difference was found with placement of a narrowbeam terminal near foliage and a widebeam terminal in the clear compared to the reverse of these terminal locations.

I. INTRODUCTION

Measurements of millimeter wave propagation in vegetation have been made for the Army Communications-Electronics Command. The objective of the project has been to obtain information on signal loss, spatial, depolarization, and scattering characteristics for propagation through both deciduous and conifer groves for a variety of foliage density and moisture content at three frequencies in or near the millimeter wave band. This information is needed in the assessment of the feasibility of using trees for camouflage of one or both terminals of a communications link. A literature search [1-16] was conducted to determine the availability of experimental information on the effects of vegetation on millimeter wave propagation. The results of the search indicated a lack of data at frequencies above the UHF band and that modelling efforts were without the necessary empirical verification. The measurements described in this report are confined to foliage in the vicinity of Boulder, Colorado, and cover only a portion of the information needed to characterize millimeter wave propagation through vegetation because of the enormous variety of path geometry and conditions.

This report contains the results and analysis from measurement of single trees and groves during August and September with summer foliage. Additional measurements were made on paths with deciduous tree coverage in November and December when the leaves had fallen, with the transmitter and receiver carefully repositioned to duplicate the original paths. The data include measurements over path lengths of 92 to 320 meters with deciduous tree depths of 10 to 50 meters and measurements of conifer trees over paths of 150 to 300 meters with tree depths of 12 to 15 meters. Individual tree groupings and foliage density on each path varies from site-to-site. Vegetation depth was determined by measuring the maximum foliage depth on the direct path between the terminals.

An initial system gain calibration was made on a far-field path chosen to be free of obstructions and ground reflections, and additional calibrations were performed periodically during the measurement program to verify system gain stability.

In addition to these measurements to characterize propagation and transmission loss through foliage, one measurement near grazing angle through tall grass and shrubs was performed. Also a direct backscatter path was observed by illuminating a single deciduous grove and a conifer grove.

II. EQUIPMENT AND CALIBRATION

Millimeter wave instrumentation was developed to measure signal characteristics between two terminals positioned on paths obstructed by vegetation. Both terminals are mounted in four-wheel-drive van trucks with the rf hardware and antennas mounted on an elevator adjustable for heights above ground from 1 to 9 meters. The elevator towers can be extended to 12 meters, if needed.

The receiving antennas and the rf hardware are mounted on a remote-controlled positioner permitting both azimuthal and elevation scans at all elevator heights. All the antennnas are linearly polarized and can be readily changed from vertical, to horizontal, to cross polarization.

The link operates at three coherent frequencies: 9.6, 28.8., and 57.6 GHz. Beamwidths of the transmitting antennas are 10 degrees at all frequencies. Receiver beamwidths are 4.8 degrees at the 9.6 GHz frequency and 1.2 degrees at 28.8 and 57.6 GHz. A 60 dB dynamic range limited by the last IF amplifier stage and a minimum sensitivity of -100 dBm is available at all frequencies.

A. Instrumentation Description

A functional diagram of the transmitting terminal is shown in Figure 2.1. All three rf frequencies are derived from a 100 MHz temperature compensated crystal oscillator. A phased-locked, cavity-tuned (X96) multiplier is used to generate 30 mW at 9.6 GHz. An identical (X96) multiplier drives a varactor tripler which injection locks an 85 mW Gunn source at 28.8 GHz through a high isolation ferrite circulator. The Gunn power is fed to a directional coupler providing 20 mW to a 25 dB gain horn antenna, and the remaining power drives a varactor doubler. A directional coupler is used to inject a locking signal from the doubler into the 57.6 GHz IMPATT source. With a bias current of 260 ma, the IMPATT provides 120 mW to a 25 dB gain horn antenna. The entire transmitter is mounted in a temperature controlled enclosure which is held at 45°C $\pm$ 1°C to reduce power variation, in the worst case, to less than $\pm$ 0.5 dB at 57.6 GHz. The transmitter enclosure is attached to the vertical carriage of the van.

A functional diagram of the receiving terminal is given in Figure 2.2. All of the receiving rf components and the low noise IF preamplifiers are contained in a 45° $\pm$ 1°C temperature controlled enclosure. Three parabolic reflectors (18, 24, and 12-inch), in the order of ascending frequency are mounted on the enclosure with low-noise down converters coupled directly to the antenna feeds. This total assembly is mounted on the remote controlled positioner. The receiver noise figure is determined by the input down convertor, which is a double-balanced mixer at 9.6 GHz

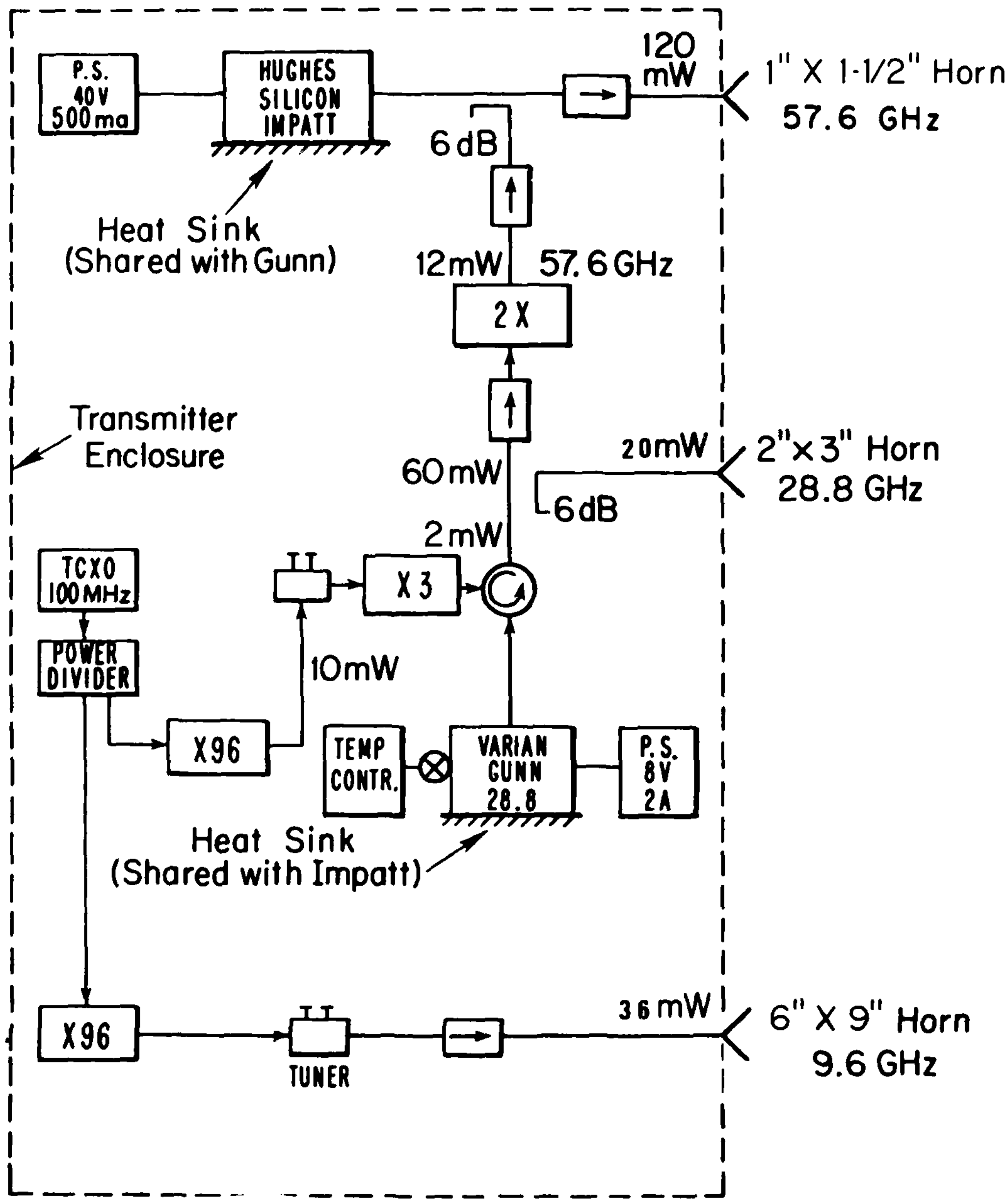

Fig. 2.1. A functional diagram of the transmitting terminal.

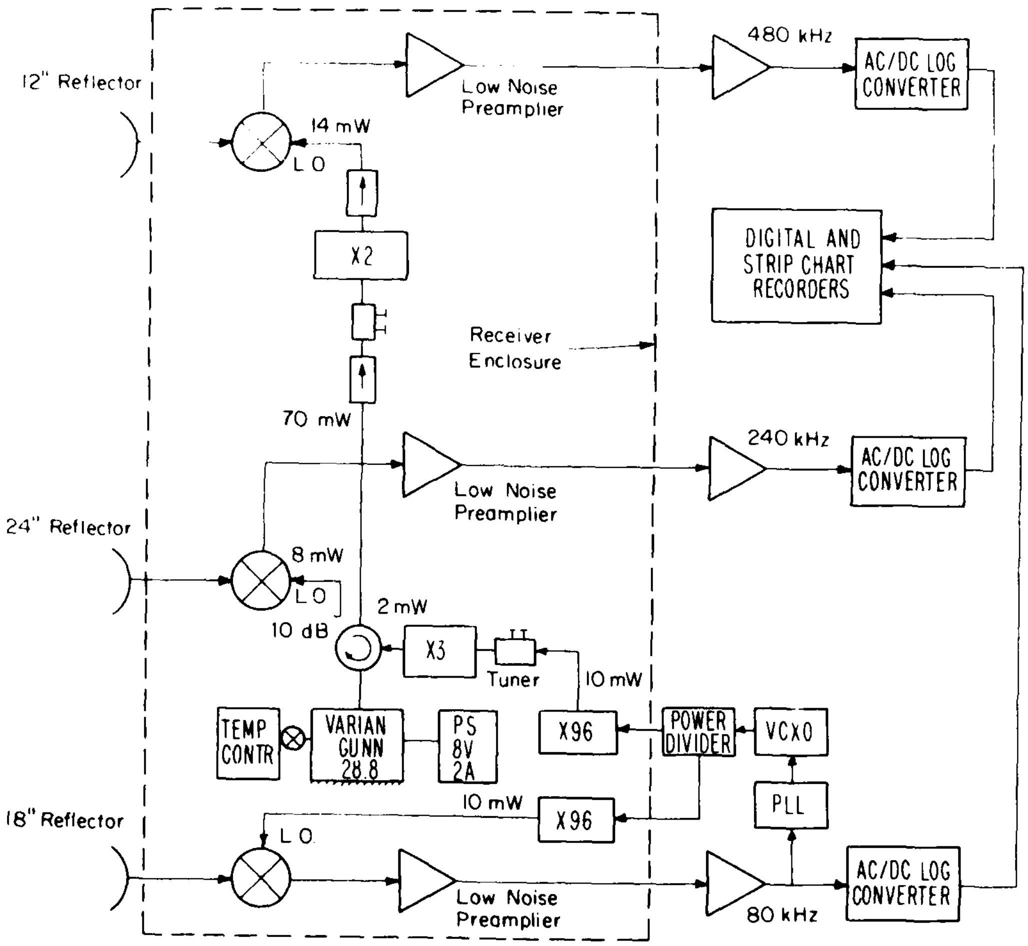

Fig. 2.2. A functional diagram of the receiving terminal.

with a 7.5 dB double side-band noise figure. The 28.8 and 57.6 GHz input mixers are of the strip guide-balanced type with double side-band noise figures of 5.5 and 6.0 dB, respectively. All local oscillator (LO) signals are generated from a voltage controlled crystal oscillator which is phase locked to the 9.6 GHz received signal with an 80 kHz reference offset frequency. The multipliers for the voltage controlled 100 MHz reference ($\pm$ IF/multiplying factor) to derive the LO injection signals are identical to the scheme used for the transmitter sources, except, at 57.6 GHz, the doubler alone provides sufficient LO level. Long term (weeks) gain stability for each receiver is less than $\pm$ 0.1 dB.

A block diagram of the data acquisition system is shown in Figure 2.3. The three IF frequencies of 80, 240, and 480 kHz are brought to the receiving van via co-axial cables, filtered, and amplified before entering an AC to DC log converter. The received IF signals are converted to a DC level which is logarithmically related to the rf signal amplitude. These DC levels drive a multi-channel strip chart recorder for monitoring, and they also appear at the input of a digital scanner which is capable of switching between each receiver level at rates of up to 100 times per second determined by the data-logging desk computer. The desk computer is also interfaced with a 5-1/2 digit voltmeter and is programmed to perform data collecting, data processing, tape storage, and data plotting functions.

B. Calibration and Path Characterization

The initial instrumentation calibration was performed on a far-field path of 97 meters. A definition of a minimum far-field distance is $d_{min} = 2D^2/\lambda$, where D is the receiving antenna aperture, and λ is the rf wavelength. The calibration path was chosen to be free of any significant reflecting components from either ground or above ground obstacles so that the on-path signal amplitude is not altered. For path lengths of less than 2 km and consistent with the system measurement accuracies, only the molecular oxygen absorption losses at 57.6 GHz need to be included. At Boulder, CO, where the elevation is 1600 meters above sea level, the attenuation at 57.6 GHz is 10.5 dB/km; that value is used for all path calculations. By comparison losses at 9.6 GHz are 0.006 dB/km and at 28.8 GHz are 0.017 dB/km at Boulder with an ambient temperature of 20°C and 50% relative humidity. The signal amplitude values presented in the later sections are relative to free space with molecular oxygen absorption loss corrections applied to the 57.6 GHz data only.

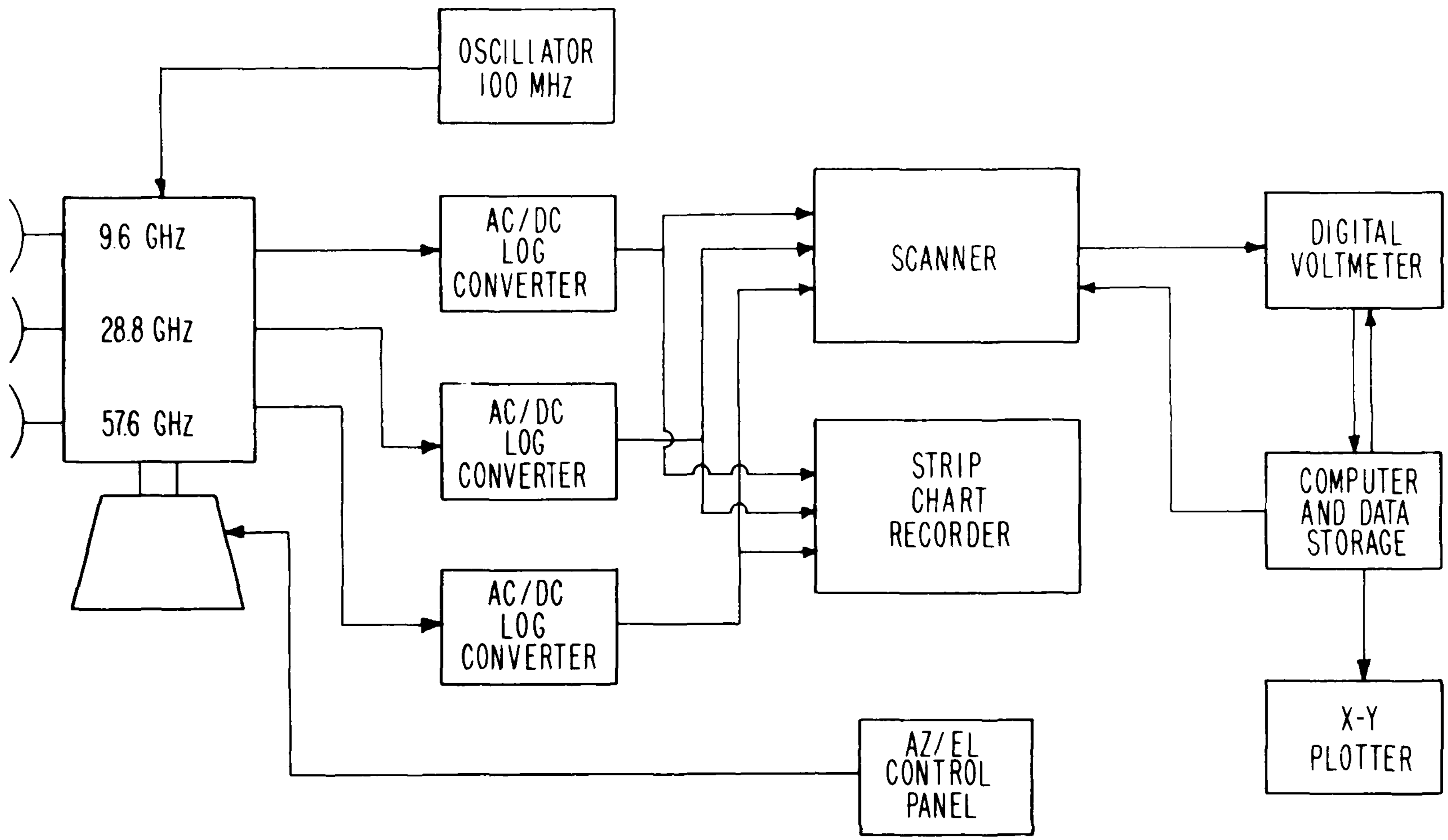

Fig. 2.3. A block diagram of the data acquisition system.

We found that at micro-millimeter wave frequencies, received signals propagated through vegetation are not only a function of attenuation, but of time and space. The time and space factor is the received signal dependence on multipath propagation and the composite vector sum of all signals seen at the receiver. Multipath reflections and scattering are important parameters in determining coherent channel bandwidth as well as signal characteristics, although the bandwidth consideration is not covered in this measurement series. In order to describe the effects of micro-millimeter wave propagation through vegetation, a special term is used. Vegetation loss is defined as the reduction in received rf signal over a path of distance R in excess of the factor 20 $\log_{10}$ R (plus any atmospheric attenuation) resulting from vegetation in a common volume illuminated by transmitting and receiving antennas.

1. Azimuthal Scans

Figure 2.4 shows the calibration measurement of signal amplitude versus azimuth angle for terminal heights of 1, 3, and 5 meters on a 97 meter calibration path. At zero pointing, the signal amplitude repeats exactly for all heights, indicating a valid calibration, not altered by reflection components. Of interest are the antenna pattern results seen in the azimuthal scans, which show the level of off-angle signals with slight variations for each height due primarily to surface reflections. Plots from data recorded on paths through foliage will show the above effects plus attenuation, diffraction, and scattering components resulting from the foliage. The scan rate of the antenna positioner is not absolutely uniform, and small shifts in signal peaks and nulls may occur on the azimuth scan due to this slightly non-linear rate; however, these effects are difficult to separate from those produced by low-level multipath signals.

With this calibration, the on-line, free-space signal level can be calculated for any path length used by a relation of 20 $\log_{10} d_c/d_f$, where d_c is the calibration path length and d_f is the foliage path to be measured. All other factors involving the free-space received signal level remain fixed: antenna gain, transmitter power, receiver gain, etc.

Since the final IF amplifier tends to saturate, the linear operating range for the received signal is selected by precision attenuators, which are inserted following the low noise preamplifiers. The noise level of the receiving system for the azimuthal calibration scans shown in Figure 2.4 is a maximum of -88 dB at 9.6 GHz, -105 dB at 28.8 GHz, and -83 dB at 57.6 GHz. These noise levels include atmospheric noise temperature and are relative to the free-space signal level, which is the 0 dB reference.

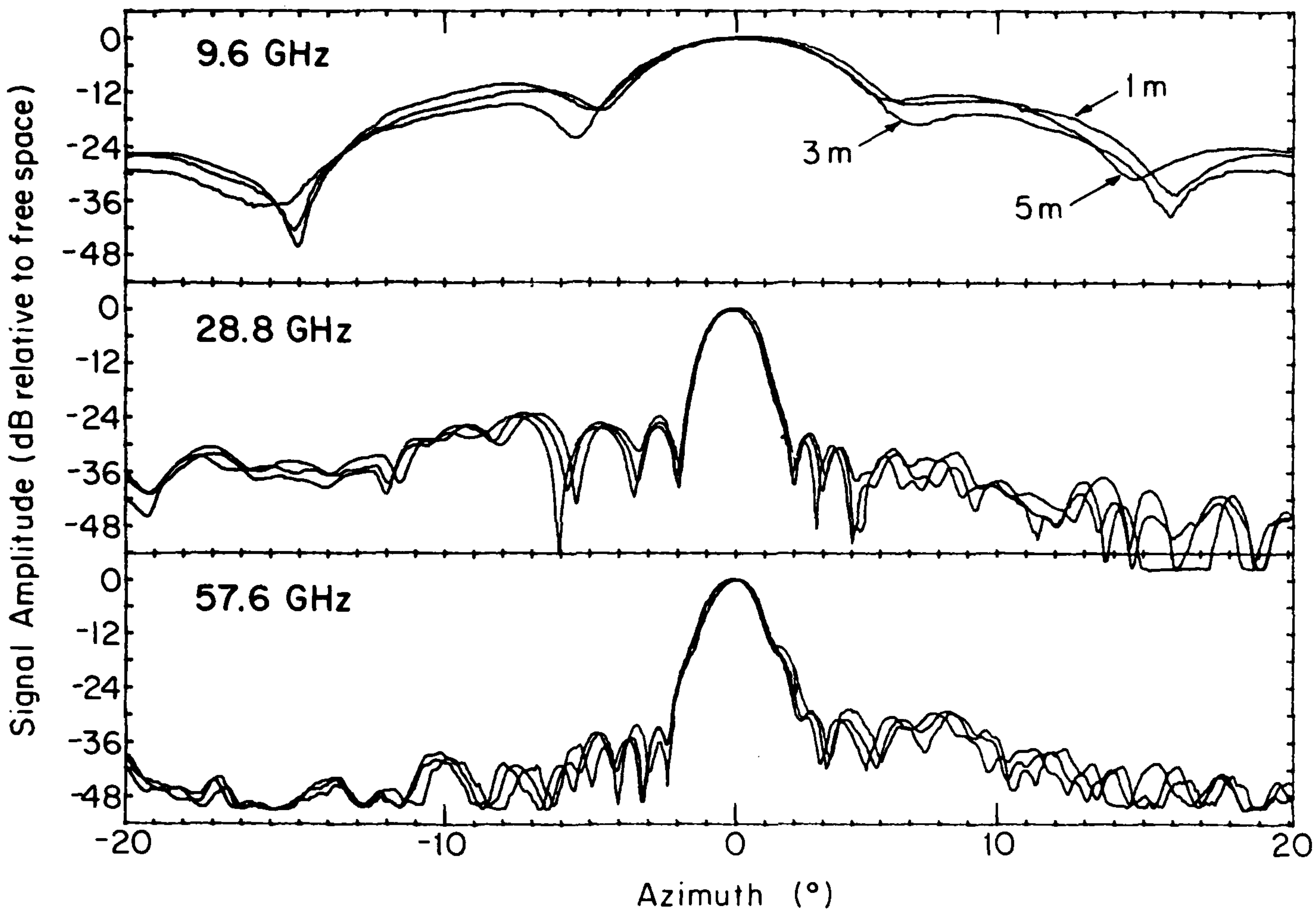

Fig. 2.4. Azimuthal calibration scans at heights of 1, 3, and 5 meters on a 97 meter clear path.

2. Elevation Scans

Azimuthal and elevation scans were made and the received signals were used to compose the data curves presented in section IV. Ground reflections are apparent in the elevation scan from several sets of free-space calibration data.

The data in Figure 2.5 show ground reflection effects in measurements from the free-space, 97-meter calibration path. The two plots for each frequency in Figure 2.5 are off-set by 10 dB. These plots are elevation scans which are basically antenna patterns in the vertical plane with transmitter and receiver positioned at 7 m for the upper plot and 3 m for the lower plot. Angles to the left of 0° represent angles above horizontal pointing and angles to the right represent angles lower than horizontal. Assuming approximate antenna symmetry, the change in signals with the antenna pointing down from zero, compared to signals with the antenna pointing an equal number of degrees up from zero, represent the contribution from ground reflection. These changes are manifested as either an increase or decrease in signal level as the reflected signal adds to or subtracts from the direct signal. Particularly apparent are the enhancements at approximately 10° below horizontal for all frequencies at the 7 meter height and the enhancements at approximately 6° below horizontal for all frequencies at the 3 meter height. Also apparent is a decrease in signal level at 2° to 3° below horizontal in the 9.6 GHz trace at the 3 meter height. The magnitude and pointing angle dependence of these enhancements and nulls are strongly dependent on transmitter and receiver height and path length.

Throughout this investigation, especially after changing measurement locations, calibration checks were performed on convenient clear paths, and after adjustment for path length and atmospheric losses, the calculated levels were consistently within one dB of the measured values.

The photographs in Figure 2.6 show the system terminals in an operating mode. Figure 2.6a is the transmitter, and Figure 2.6b shows the receiver. A calibration path is shown in Figure 2.6c, with the transmitter near the center of the photograph and the antenna mount of the receiver at the left of the photograph. The instrument in the lower left of the picture is used to electrically measure path length.

3. Cross-polarization Scans

The cross-polarization calibration scans are presented and discussed in section IV G.

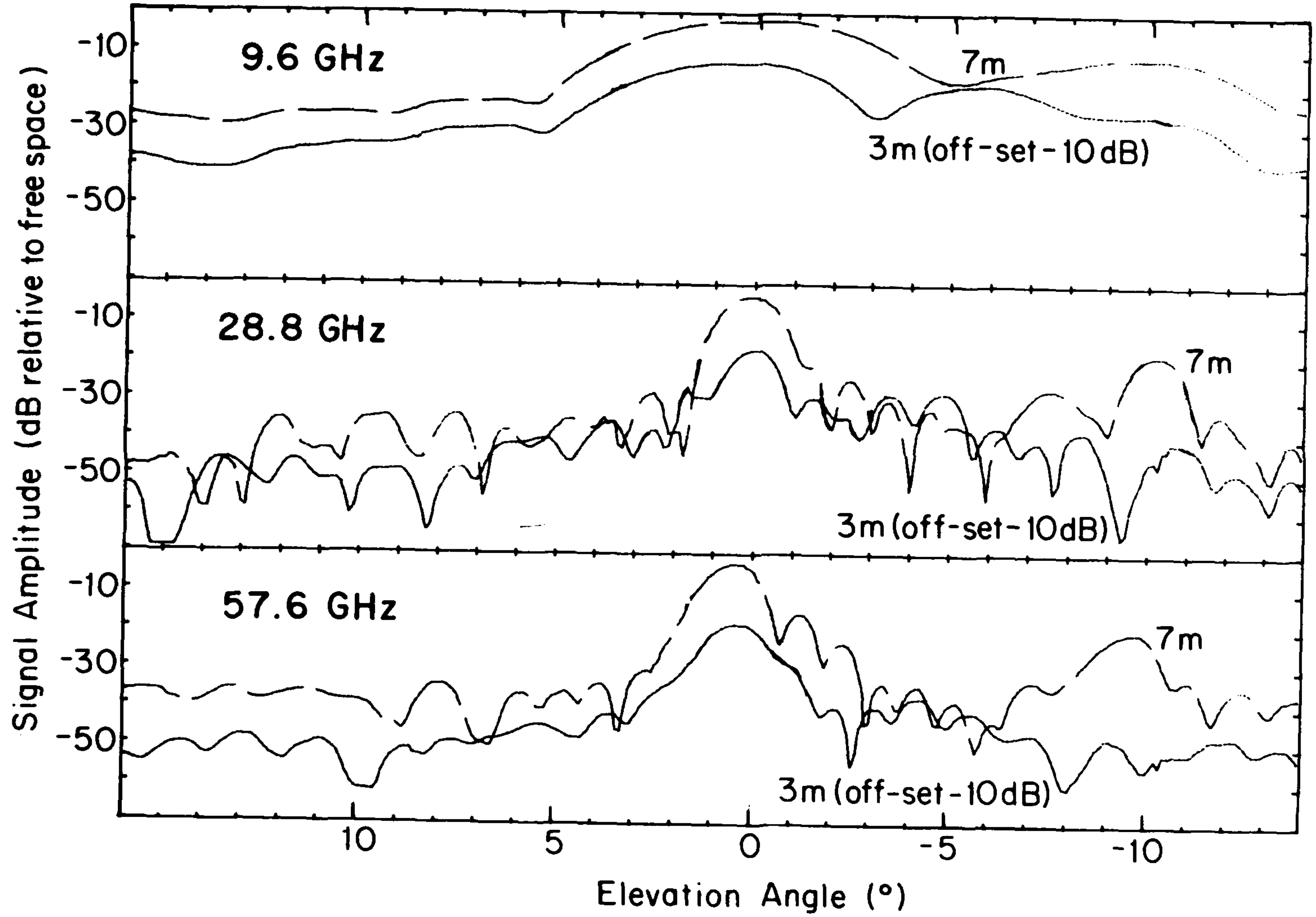

Fig. 2.5. Received signal amplitude from elevation scans at 3 meters and 7 meters. Ground reflections observed at a down angle of 10° on 7 m trace and at 5° on 3 m trace.

a

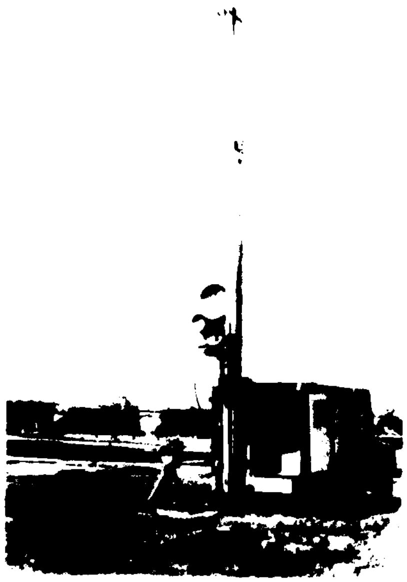

b

c

Fig. 2.6. Photographs of the transmitting and receiving equipment used for the vegetation measurements.

III. MEASUREMENTS

The measurement paths selected for this study can be grouped as deciduous, conifer, and grass. On each path, a number of data runs were made. Generally, these runs included azimuthal and elevation scans from four to six different heights with both horizontal and vertical antenna polarizations. Special data runs included vertical and horizontal off-set scans of the transmitter.

The data in Table 3.1 give a listing of the measurement paths according to type of path (foliage, structure), path length, path coverage, location code and location identification. The column on foliage depth indicates a measured depth of foliage between terminals. The trees on the path might be in a single group or randomly distributed. Reference will be made to this table in discussion of the data taken and in interpretation of the analyses.

TABLE 3.1

Measurement paths.

Path	Foliage type, structure	Grove/Forest	Total Length (meters)	Maximum Foliage Depth (meters)	Code	Location
Calibration	Free Space	---	92	---	BD01/01	Boulder
"	Free Space	---	150	---	BD05/01	"
"	Free Space	---	97	---	BD07/02	"
"	Free Space	---	172	---	MR02/01	Marshall Road
"	Free Space	---	320	---	MR03/02	" "
"	Free space	---	118	---	GM01/01	Green Mtn. Mesa
Deciduous	Willow - large trunk	Small group	92	10	BD02/01	Boulder
"	Cottonwood - large trunk	Groups - widely spaced	152	42	MR01/01	Marshall Road
"	Cottonwood - small trunk	Dense group	172	30	MR02/01	" "
"	Cottonwood - medium trunk	2-Dense groups	320	50	MR03/02	" "
"	Cottonwood - medium trunk	Dense group	320	30	MR04/02	" "
Conifer	Conifer - large trunk	Dense group	150	12	BD05/01	Boulder
"	Conifer - large trunk	Single trees widely spaced	181	15	GM02/01	Green Mtn. Mesa
Grass	Grass	Dense	320	75	MR03/02	Marshall Road
Conifer	Conifer - large trunk	Single trees	300	25	GM03/01	Green Mtn. Mesa

The data in Table 3.2 describes the foliage of the willow, cottonwood, and conifer trees used in the measurements. The description includes the length and width of leaves and needles and a definition of physical condition of the foliage.

TABLE 3.2

Description of foliage.

Tree type and size	Length of Leave (cm)	Width of Leave (cm)	Condition
Willow - Large	12 → 16	2 → 3.5	Good
Cottonwood - Large	4 → 8	5 → 9.0	Good
Cottonwood - Small	4 → 8	5 → 9.0	Good
Conifer - Large (dense)	12 → 20	dia. .15→ .3 needles dia. .8 → 1.3 supporting stems	Good
Conifer - Large (sparse)	8 → 14	dia. .1 → .3 needles dia. .7 → 1.3 supporting stems	≈ 15% Dead

Three maps shown in Figures 3.1 and 3.2 have been prepared as an aid to discussion and analysis of the recorded data. These maps represent the measurement locations at the Boulder Laboratories, Green Mountain Mesa, and Marshall Road. The transmitter (TX) and receiver (RX) sites for each path are indicated, and the path length and foliage type are given using the identification code from Table 3.1. These maps will be referred to in the next section in the discussion of data analyses.

Aerial photographs of the three measurement locations are shown in Figure 3.3. The transmitter and receiver sites are indicated on the photographs. These aerial photos were taken at about 10 AM and show long shadows which are identified, for the most part, by the darkest tone seen in the photograph.

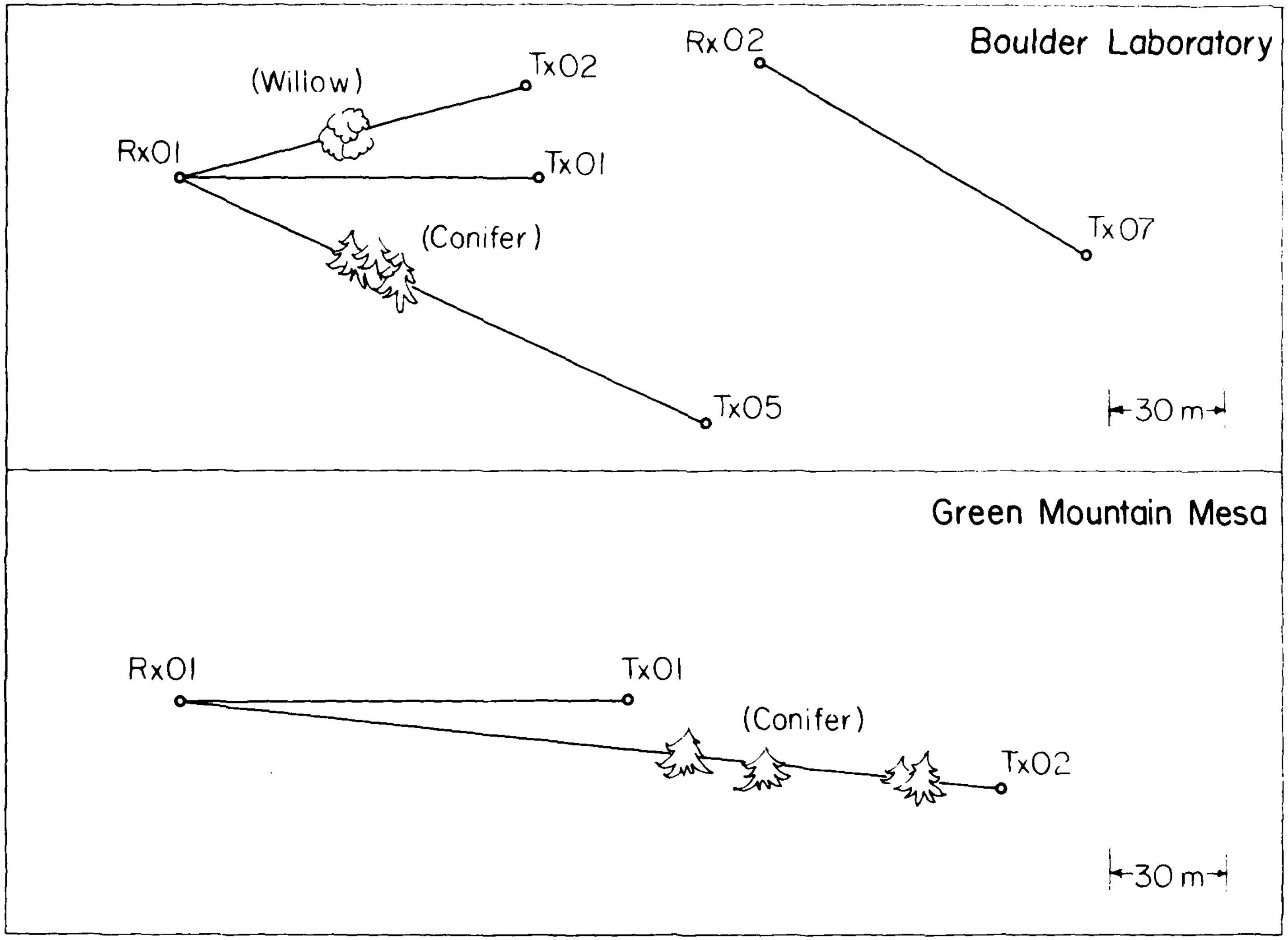

Fig. 3.1. Calibration and foliage paths at Boulder Laboratories and Green Mountain Mesa.

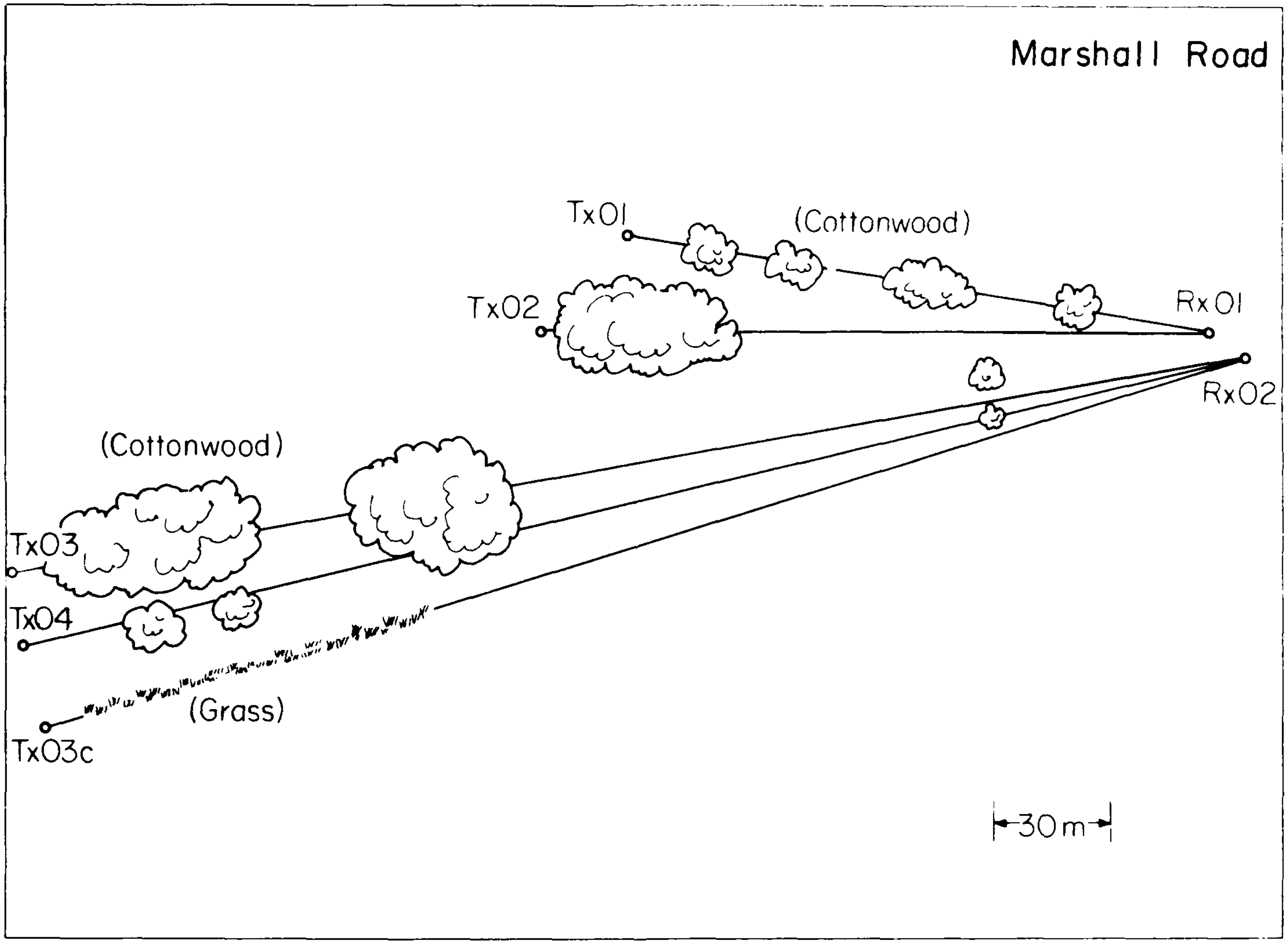

Fig. 3.2. Calibration and foliage paths at Marshall Road.

Boulder
Laboratories

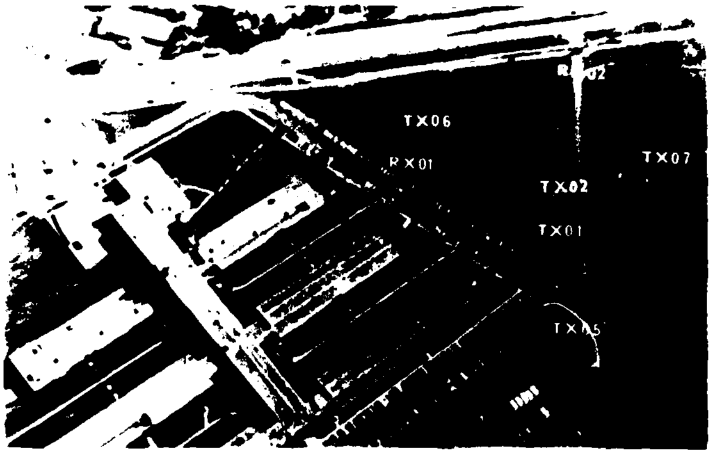

Green
Mountain
Mesa

Marshall
Road

Fig. 3.3. Aerial photographs of the vegetation propagation measurement sites.

IV. ANALYSIS OF SIGNAL CHARACTERISTICS THROUGH FOLIAGE

The text and figures in this section describe the observation of signals propagated through several foliage paths in order to identify and assign values to path and propagation parameters where possible. These parameters include type and depth of foliage and, angle, temporal, spatial, polarization and frequency dependence on vegetation loss.

Discussions pertaining to the recorded data, graphs plotted from the data, and photographs of the trees and paths are separated into the following categories:

a) Signal amplitude vs. antenna height

These data are sets of curves (parallel-polarization) showing amplitude dependence on height for five tree or grove scenarios.

b) Signal amplitude vs. azimuthal pointing

These data are selected multi-scan plots (at specified heights) to show the signal amplitude characteristics as a function of receiver antenna pointing.

c) Signal amplitude vs. antenna positioning

Several measurements were made to assess the signal amplitude dependence on small horizontal and vertical position displacement of the transmitter terminal.

d) Scintillation effects

Special time-series measurements show the magnitude of signal scintillation caused by the motion of leaves and branches on-path or near the path.

e) Vegetation loss vs. foliage depth

These data show the measured vegetation loss as a function of estimated on-path foliage depth. The results are subject to numerous variables such as foliage condition and path geometry as described.

f) Signal backscatter measurements

These special measurements show effective backscatter levels from trees illuminated in a common volume of the transmitter and receiver antenna beam.

g) Signal depolarization

Calibration and foliage depolarization effects are presented.

h) Off-path signal enhancement

Off-path measurements for a select location demonstrated an enhancement in received signal level when compared to the received signal levels for a path with dense foliage coverage.

i) Rain and snow effects

These data show the measured transmission loss with rain and snow on foliage.

A. Signal Amplitude as a Function of Antenna Height

Signal amplitude curves as a function of antenna height were composed for three paths with deciduous trees and two paths of conifer. These curves show signal dependence relative to transmitter height with trees or groves of trees in the path.

1. Deciduous Trees

The data in Figure 4.1 show signal amplitude measured on the willow tree path at the Boulder Laboratories for horizontal-horizontal (HH) polarization and vertical-vertical (VV) polarization. This path is identified as TX02-RX01 on the map in Figure 3.1. Pictures of the path and of the trunk structure and foliage are shown in Figure 4.2.

The signal levels measured as a function of height for the two polarizations are very similar. Maximum vegetation loss occurs between 4 and 8 meters. The average signal reduction for 9.6, 28.8., and 57.6 GHz over this range of heights is, respectively, 26 dB, 34 dB, and 36 dB. The increase in signal level at the 2-meter antenna height coincides with the decrease in foliage depth at the 2 meter level. This foliage depth decrease can be observed in photograph (a) in Figure 4.2. Variation in signal level is not only a function of height, but also a function of antenna azimuthal pointing and horizontal antenna positioning. Signal variation as a function of pointing and positioning is discussed further in sections IV B and IV C.

The second set of curves showing signal variations s a function of antenna height come from measurements on a 152 meter path of tall (15 meter) cottonwood trees with a maximum on-path foliage depth totalling 42 meters. The trees on this path consisted of three groups of large trunk cottonwoods. Estimated trunk diameter is from 20 to 70 cm. The signal level curves for this path are in Figure 4.3, and the photographs showing typical tree coverage are in Figure 4.4. This path is indicated as TX01-RX01 on the map in Figure 3.2. The path runs through the row of trees starting at the center of photograph 4.4(a) to the transmitter located in the background near the left of the picture. Photographs (b) and (c) further display the foliage and trunk size.

Signals for this path show a strong similarity between HH and VV polarizations. Also, these two sets of curves show a nearly uniform decrease in signal with increased antenna height, which suggests uniform increase in foliage depth with tree height. A visual examination confirms this fact and the fact that the maximum height of observation of seven meters reaches approximately to the middle of the trees. The measured signal level relative to free space for this path ranges as shown in Table 4.1.

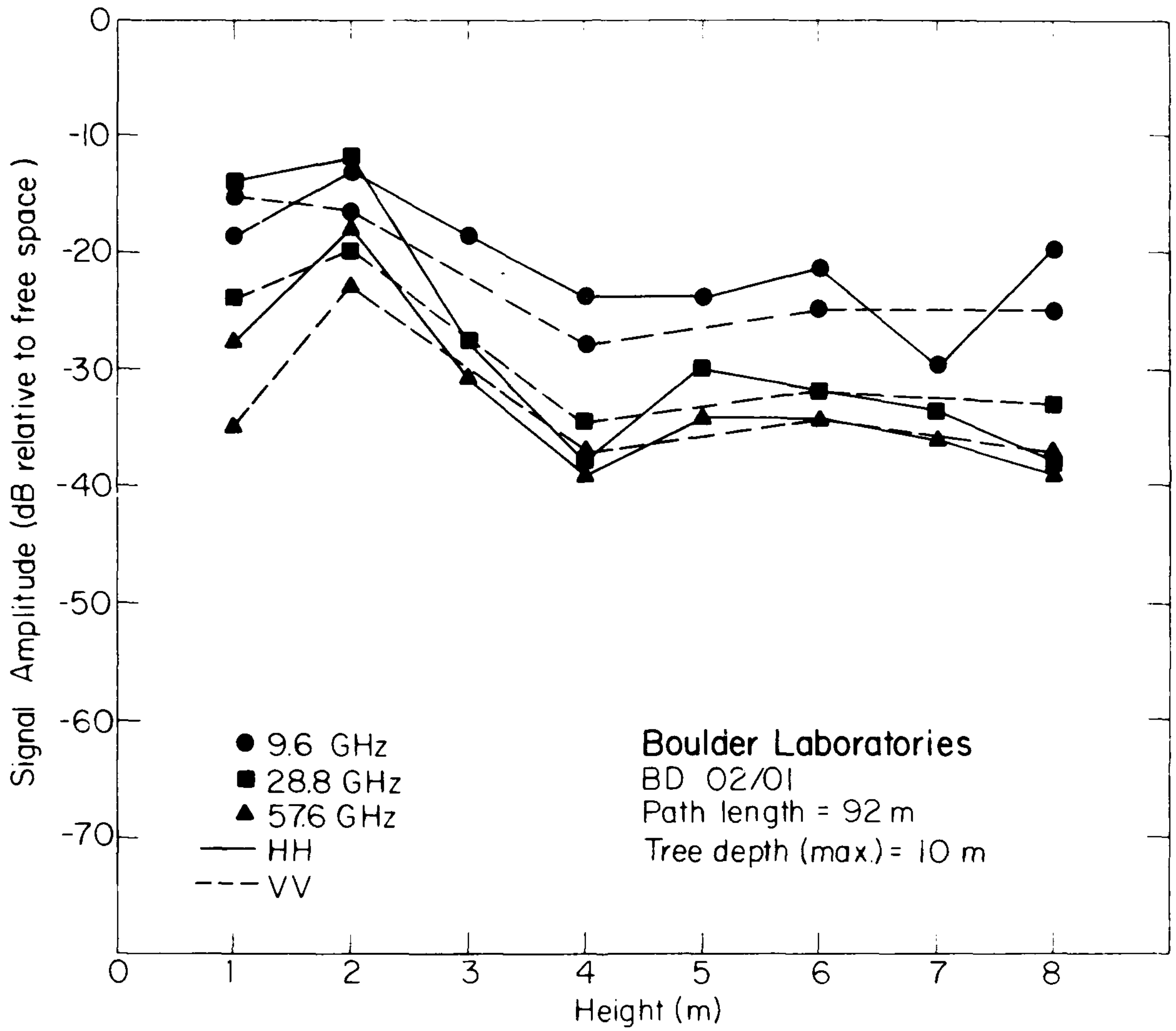

Fig. 4.1. Signal amplitudes as a function of height for a group of willow trees (HH polarization and VV polarization).

(a)

(b)

(c)

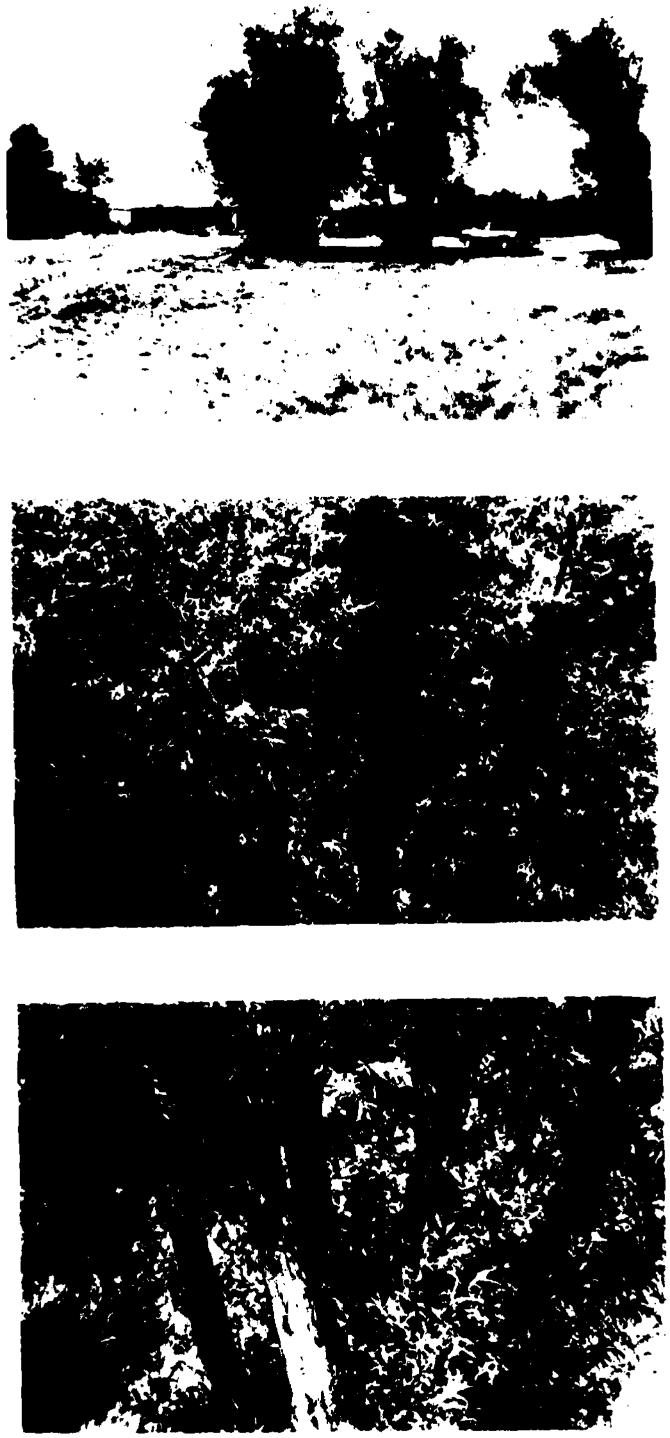

Fig. 4.2. The willow tree path at the Boulder Laboratories. The path length is 92 m and the tree coverage on the path is 10 meters.

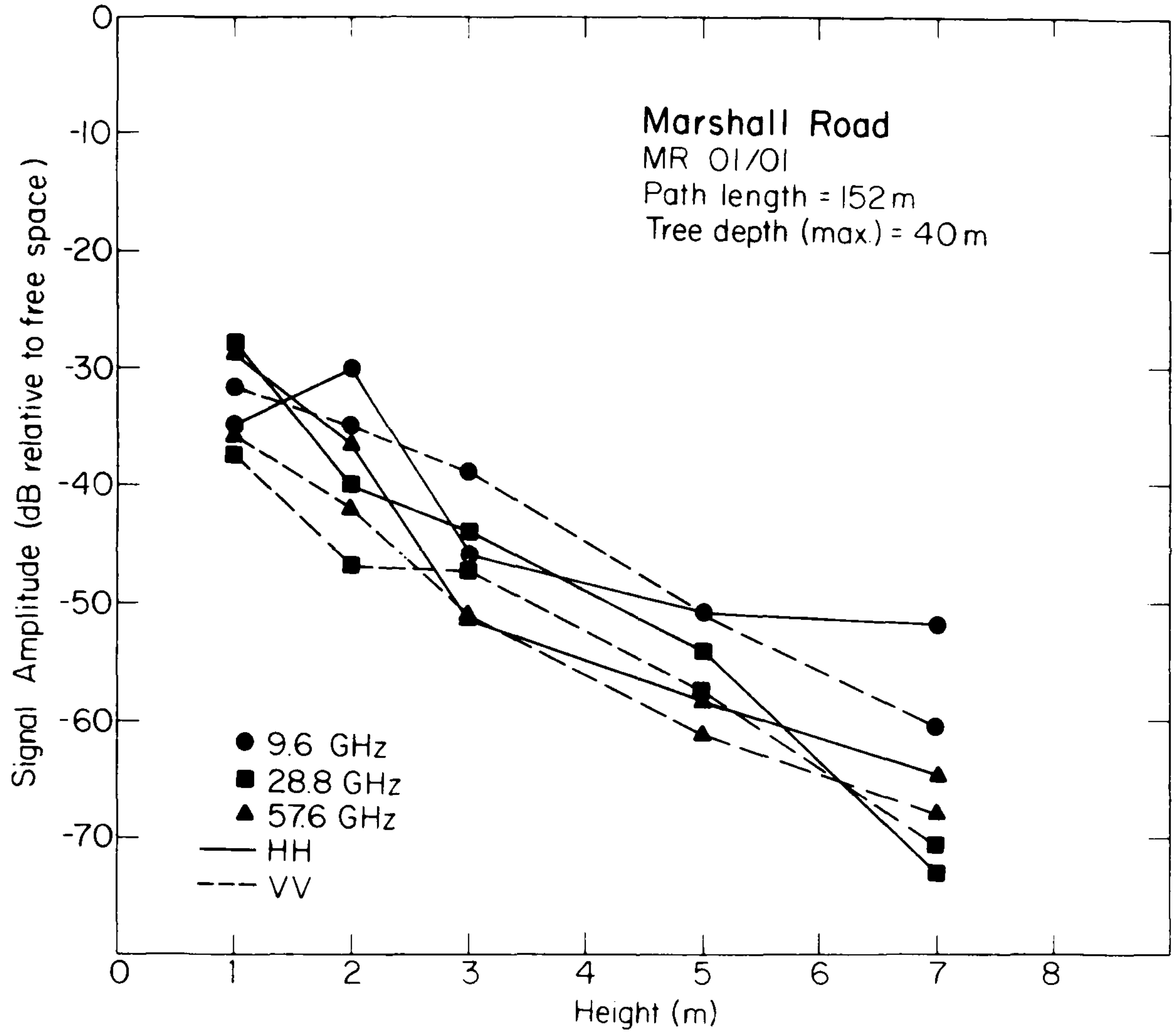

Fig. 4.3. Signal amplitude as a function of height for cottonwood trees (HH polarization and VV polarization).

a

Off-path view
looking toward
transmitter.

b

Path view from
receiver.

c

Near path
looking toward
receiver.

Fig. 4.4. A cottonwood tree path at Marshall Road. The path length is 152 meters and the tree coverage is 40 meters.

TABLE 4.1

Vegetation loss in cottonwoods.

Frequency	Signal Level
9.6 GHz	-33.5 dB at 1 m to -56.0 dB at 7 m
28.8 "	-33.0 dB at 1 m to -72.0 dB at 7 m
57.6 "	-32.5 dB at 1 m to -66.0 dB at 7 m

The third set of curves in Figure 4.5 show signal amplitude as a function of antenna height. These measurements are from a path of cottonwood trees also. The major difference between this path and the previous path of cottonwood trees is the size of trunks and density of the stand in the grove. This path was 172 meters and the coverage was 30 meter. The path is identified as TX02-RX01 on the map in Figure 3.2. Pictures of the trees are shown in Figure 4.6. The trees are a solid grove with trunk diameter of 3 to 12 cm and a dense cluster of foliage. This is in sharp contrast to the large trunks and large separation between trees in the previous path.

Perhaps it is appropriate to indicate that it was not possible to visually locate either terminal when viewing from the opposite terminal for any of the tree covered paths measured. The zero pointing angle had to be established by sighting the path in several sections, and for several paths, such as this 172 meter path. Only an estimate was possible with the final marking of the plots decided from the resulting data. But in determining signal loss or vegetation loss values, the largest recorded signal at near on-line angles were used.

Signal amplitude as a function of height on this path decreases uniformly from 1 meter to 5 meters. At 7 meters, the vegetation loss is less, which is explained by the fact that the maximum tree height on this path was 8 to 10 meters and the foliage depth at 7 meters was reduced compared to 5 meters by the crowning of the trees. The vegetation loss measured for the three frequencies are: 37 dB, 43 dB, and 43 dB below the free-space level at 9.6, 28.8, and 57.6 GHz, respectively.

2. Conifer Trees

The first set of signal amplitude curves from a path obstructed with ponderosa pine trees are shown in Figure 4.7. These data were measured on the TX05-RX01 path as indicated on the Boulder Laboratories map from Figure 3.1. This path is 150 meters long with a maximum tree depth of 13 meters. The group of ponderosa pine trees are very dense and closely clumped as can be seen from the photographs in Figure 4.8.

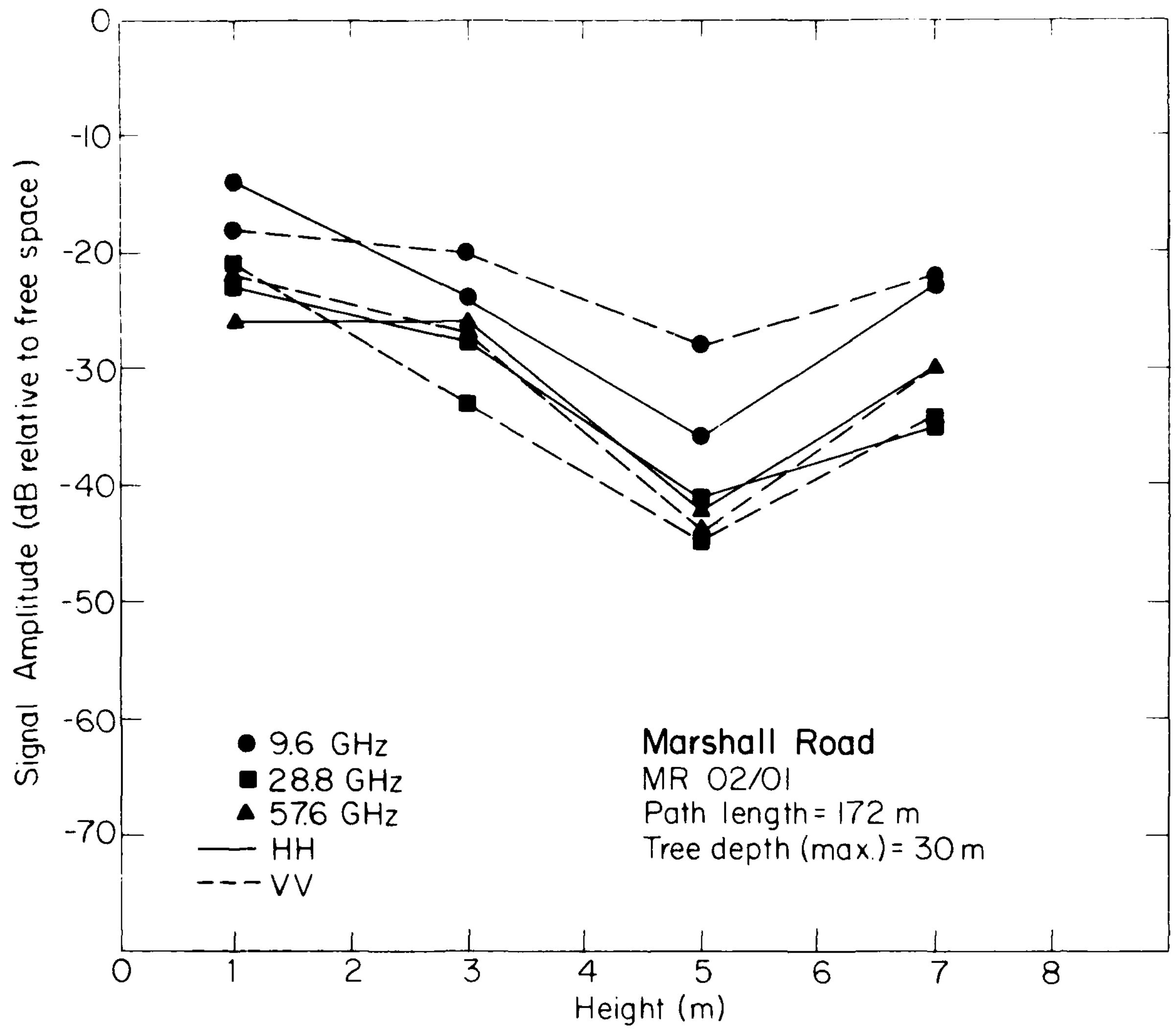

Fig. 4.5. Signal amplitude as a function of height for a cottonwood grove (HH polarization and VV polarization).

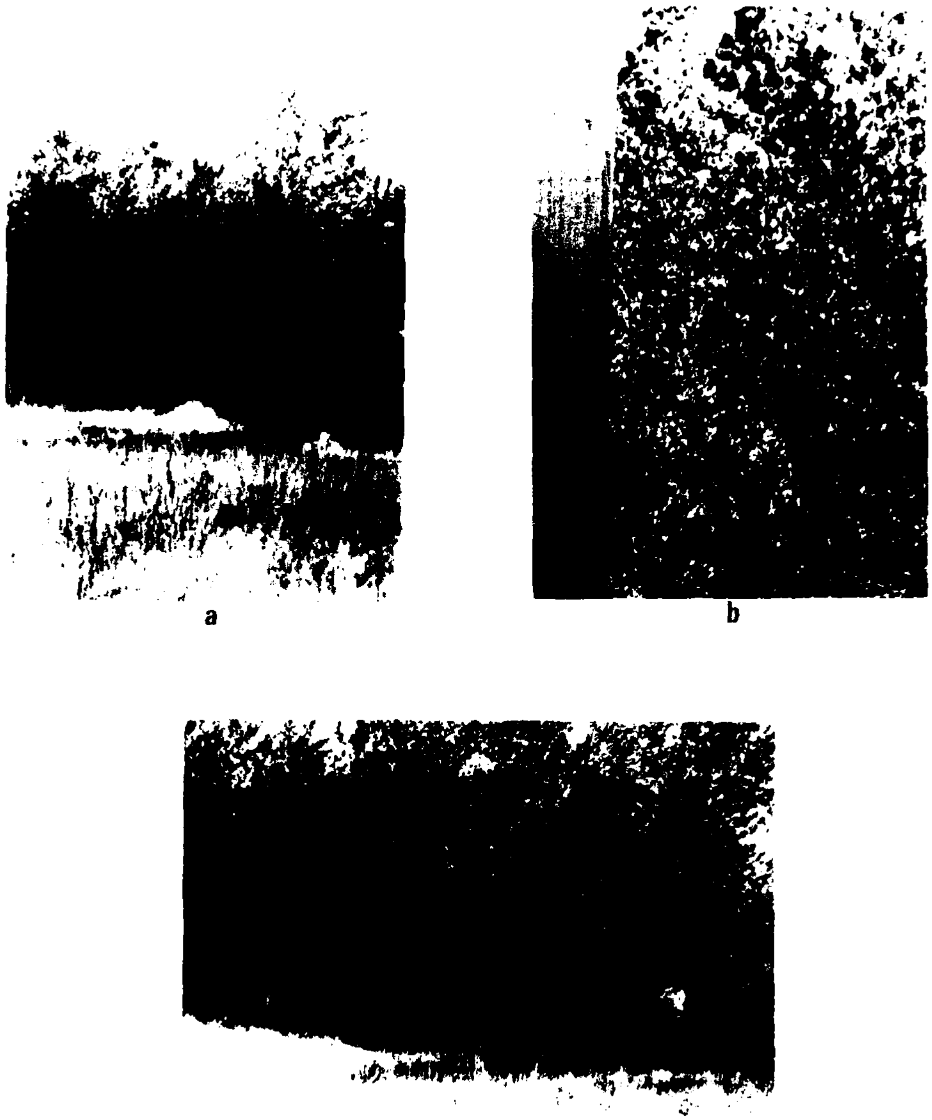

a

b

c

Fig. 4.6. A grove of cottonwood trees at Marshall Road. The path length is 172 meters and the path coverage is 30 meters.

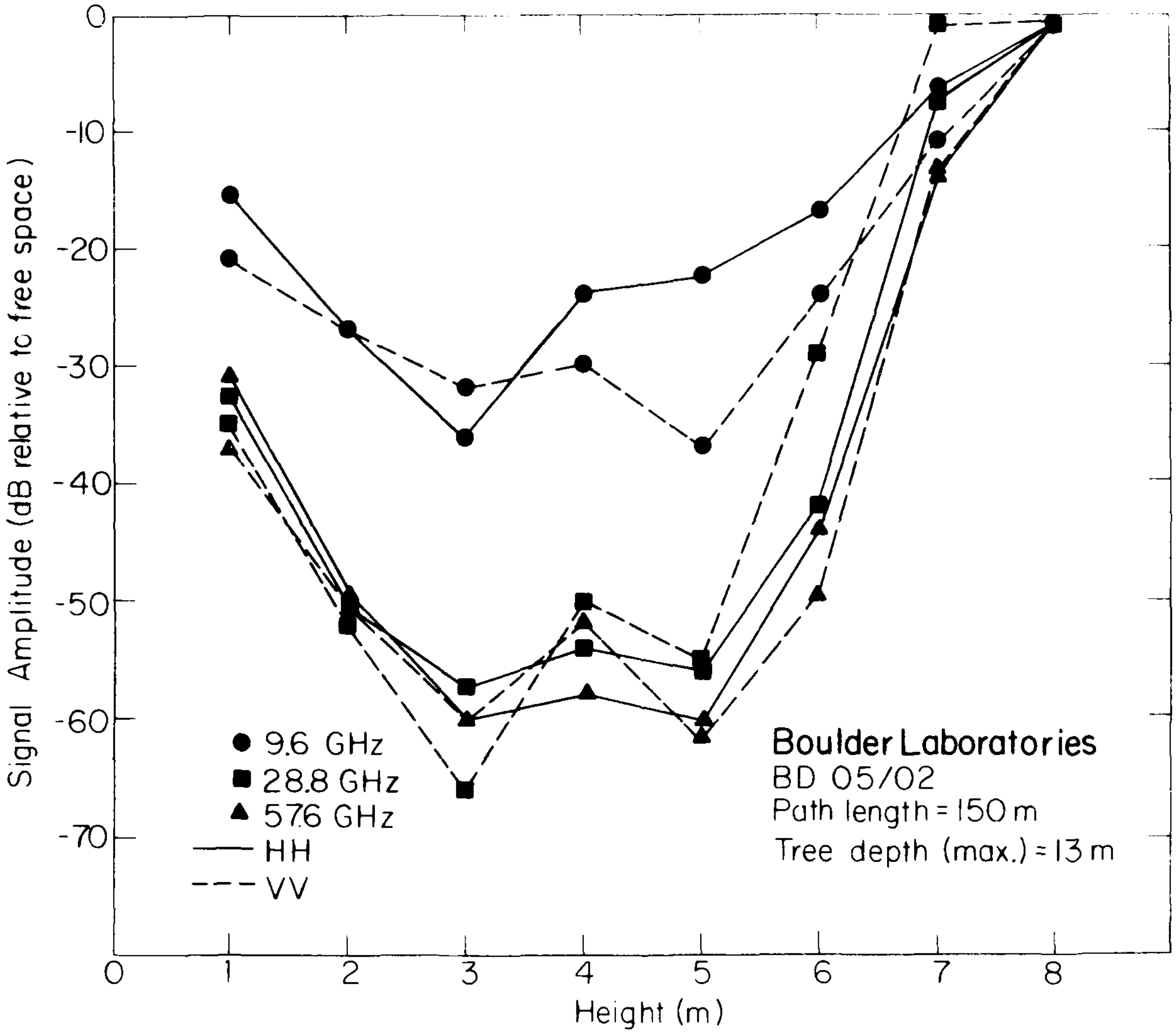

Fig. 4.7. Signal amplitude as a function of antenna height for a group of ponderosa pine (HH polarization and VV polarization).

a

At receiver looking toward transmitter.

b

Side view looking toward receiver.

c

Side view of pine grove.

Fig. 4.8. A group of large pine trees at the Boulder Laboratories. The path length is 150 meters and the path coverage is 13 meters.

The data for the two polarizations are quite similar as was the case for the previous deciduous tree measurements. The maximum tree height on path was approximately 8 meters, allowing a nearly free-space path at this height as is seen in the measured data.

Maximum signal loss was observed at the 3 to 5 meter heights, and averaging the VV and HH polarization data resulted in levels of -30 dB, -56 dB and -60 dB, respectively, at 9.6 GHz, 28.8 GHz, and 57.6 GHz. The marked difference in these data compared to the next set of measurements through conifer trees and the three previous measurements through deciduous trees is the large separation between the 9.6 GHz signal levels and the 28.8 GHz and 57.6 GHz signal levels. The reasons for the separation in frequency is not obvious, but a possible factor is the characteristic difference in the conifer in this path. The foliage on these trees was more dense than on any other path tested. There were few large (> 2 cm) branches and trunks exposed, and it is possible attenuation due primarily to live foliage may display a higher ratio of vegetation loss versus frequency compared to trees where branches and trunks are exposed. The separation between the 28.8 and 57.6 GHz does not support this, however, but perhaps physical dimensions may play a role. The dimensions are given in Table 3.2, and it was visually noted that there is a predominance of stems supporting clusters of needles which range in diameter from 0.8 to 1.3 cm. If a resonant or Mie region does exist, it would be as broad as the size distribution. Figure 5.7 gives a speculative sketch of vegetation-loss dependence on frequency due to the possible broad resonances suggested above. It is hoped that in the future a frequency scan can be incorporated to determine if a resonant tendency can be observed.

The second path of ponderosa pine trees included for measurements was the Green Mountain Mesa path TX02-RX01 in Figure 3.1. This path is 182 meters long with a maximum depth of 15 meters. The trees on the path are widely separated and exhibit sparse foliage as shown in the photographs in Figure 4.9. The signal amplitude curves for this path are in Figure 4.10.

The VV and HH polarizations are similar in this set of data as in the previous sets. The maximum tree height is estimated at 8 - 10 meters, thus the values at 8 meters in Figure 4.10 show a near free-space level. Maximum vegetation loss occurred in the 2 to 4 meter height range. Typical levels are: -26 dB at 9.6 GHz, -30 dB at 28.8 GHz, and -39 dB at 57.6 GHz. These are average values from the 2, 3, and 4 meter heights. Although the tree coverage on this path is estimated to be the same (13 m) as the Boulder Laboratories path, the vegetation loss is considerably

Far view of receiver looking toward transmitter off angle to path.

a

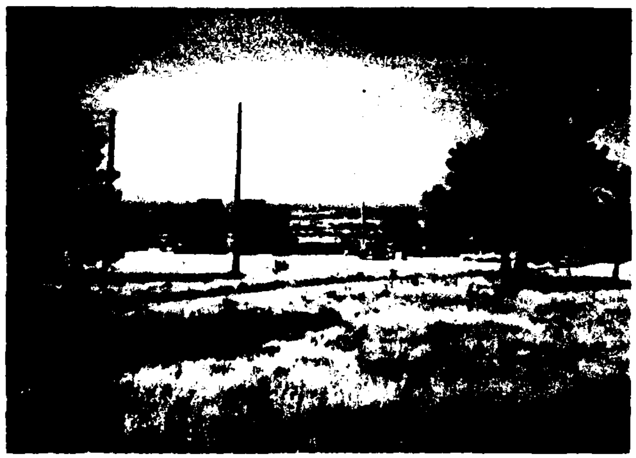

Looking toward receiver over clear portion of path.

b

Showing transmitter looking on path toward receiver.

c

Fig. 4.9. A forest of conifer trees at the Green Mountain Mesa. The path length is 182 meters and path coverage is 15 meters.

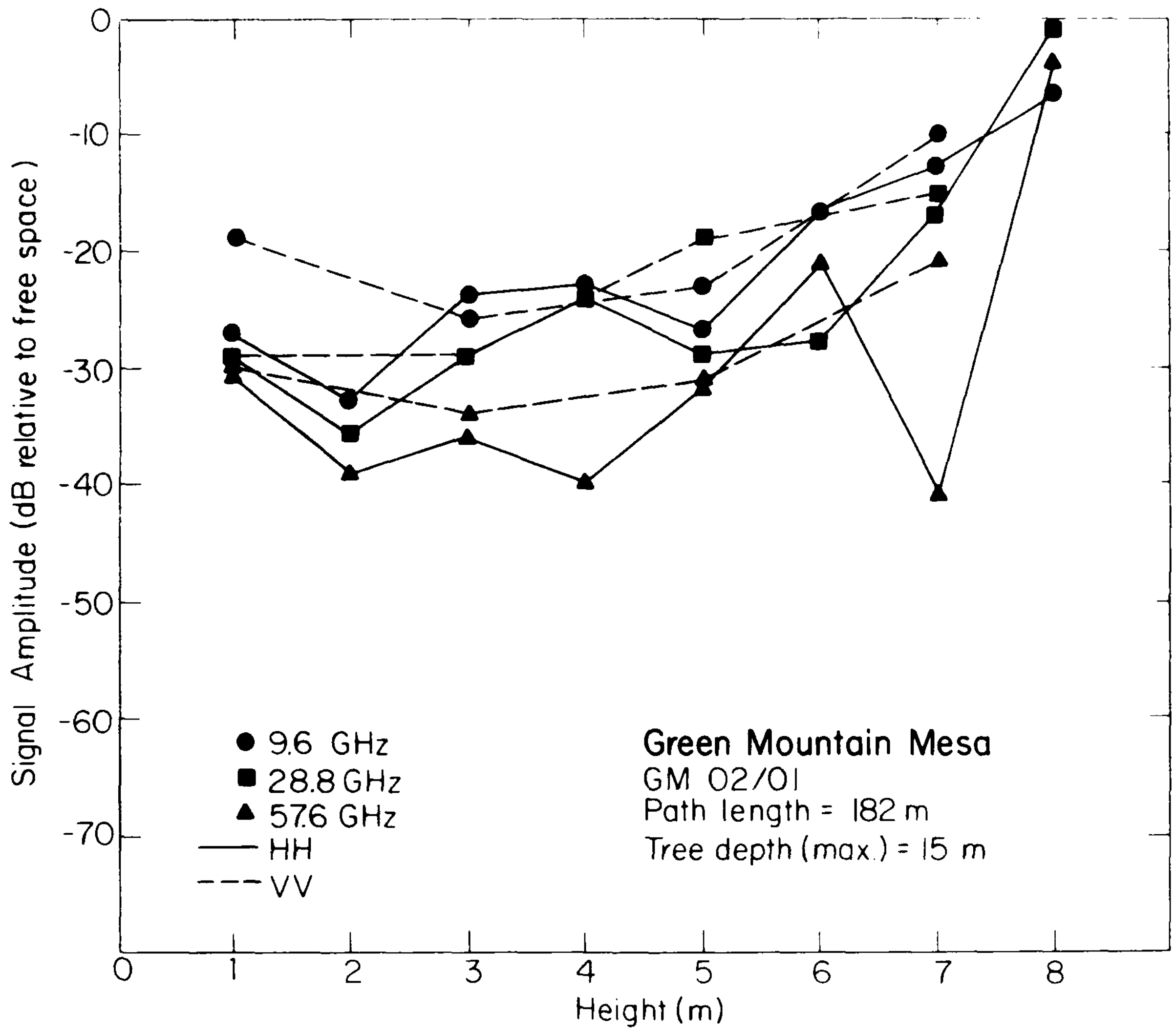

Fig. 4.10. Signal amplitude as a function of antenna height in a conifer forest (HH polarization and VV polarization).

less, particularly for the 28.8 GHz and 57.6 GHz frequencies. Differences are 4 dB, 26 dB, and 21 dB, respectively, for the 9.6 GHz 28.8 GHz, and 57.6 GHz frequencies. These differences might be explained by the large difference in foliage density. It is estimated that 10 to 15% of needles on the Green Mountain site are dead and contain very little moisture.

A third path, an extension of the previous TX02-RX01 path, doubled the depth of the ponderosa trees between transmitter and receiver. By extending the path length to 300 meters, the maximum depth of ponderosa pine foliage increased from 13 to 25 meters. The reason was to determine if the propagation loss doubles at twice the depth. However, to estimate the foliage depth at a uniform path height over an undulating terrain is difficult. The values given are the best estimates after sighting the path and measuring the coverage depth. Figure 4.11 shows the values obtained using VV polarization. Comparing results at 3, 5, and 7 meters show that at 57.6 GHz the vegetation loss came quite close to doubling and at the lower two frequencies (an average) was generally in the neighborhood of twice the loss. A listing of these values is shown in Table 4.2.

TABLE 4.2

Vegetation loss in conifers.

Frequency (GHz)	Foliage depth	Height (meters) 3m		5m		7m		Average (ratio)
9.6	13 m	26 dB	(1.4)	23 dB	(1.3)	10 dB	(2.7)	1.82
	25 m	38 dB		30 dB		27 dB		
28.8	13 m	29 dB	(1.5)	19 dB	(2.3)	15 dB	(1.7)	1.86
	25 m	44 dB		44 dB		26 dB		
57.6	13 m	34 dB	(1.7)	31 dB	(1.8)	21 dB	(2.1)	1.90
	25 m	60 dB		56 dB		45 dB		

An average of these samples provide only an indication of a trend for comparison to future observations. When comparisons as above are attempted, one must also keep in mind the data presented in Section IV C of this report, which shows a large signal variability to small position changes. The one meter height was not included because the branches at heights to 1.5 meters or so were for the most part void of needles but presented large trunks and branches as an obstruction.

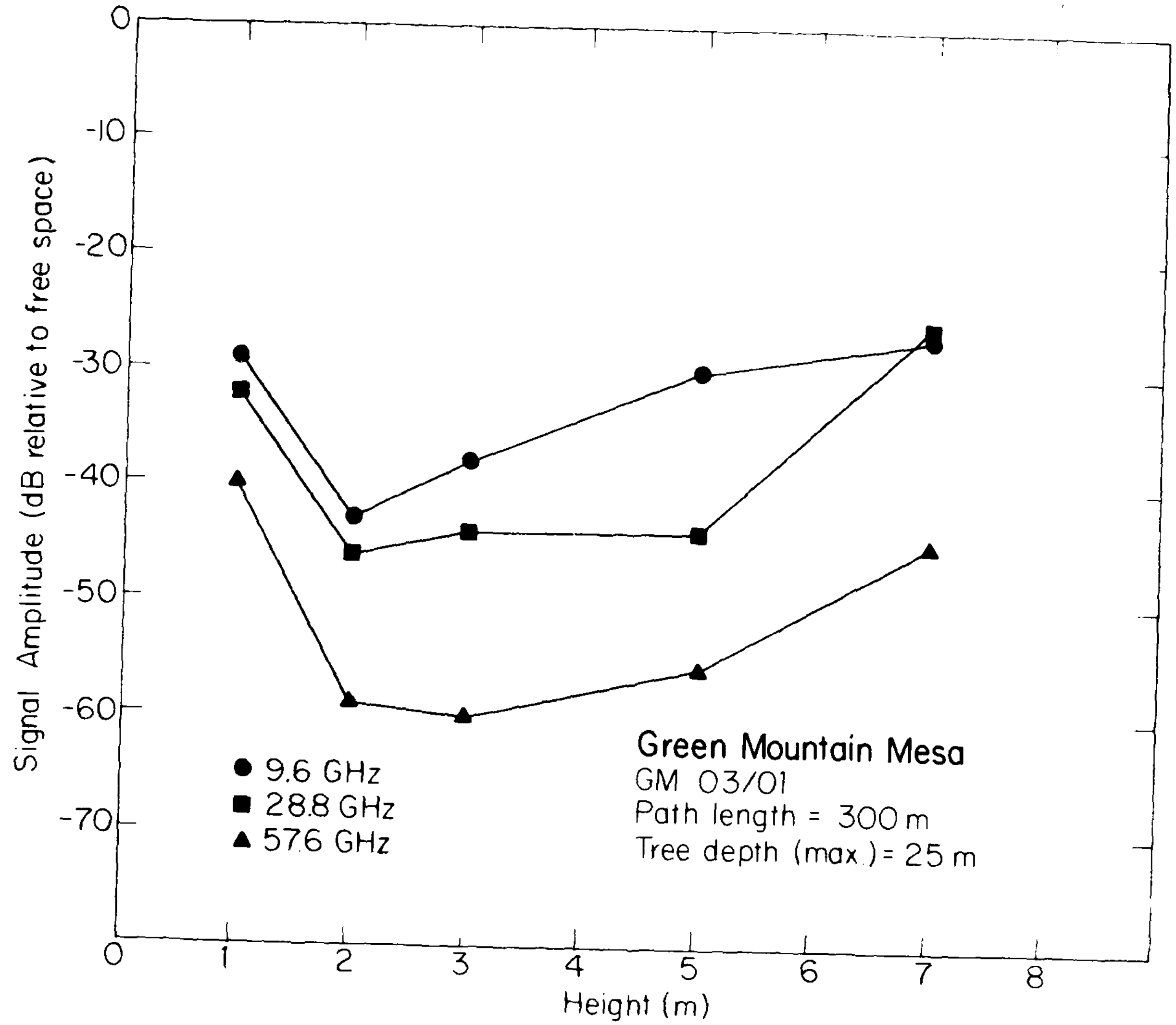

Fig. 4.11. Signal amplitude as a function of antenna height in a conifer forest (VV polarization).

B. Signal Characteristics vs. Azimuthal Pointing

A second category for discussion is the dependence of the received signal on the azimuthal pointing of the receiver antennas. The data measured by azimuthal scan on the free-space calibration paths, such as in Figure 2.4, show primarily the antenna patterns. With increasing loss on a path due to propagation through foliage, some of the antenna pattern characteristics tend to disappear, and the maximum received signal as a function of pointing may not appear at zero angle (on-path) pointing. An example of data is presented and discussed to show the pointing angle effects as a function of antenna height.

These data come from measurements on the Boulder Laboratories conifer path TX05-RX01 and are displayed in Figures 4.12, 4.13, and 4.14, representing azimuthal scans respectively at 9.6, 28.8, and 57.6 GHz. The significance of these data are not only the reduced signal levels as the foliage depth is increased, but the variability of signal level as a function of azimuthal pointing. The optimum signal level, for an arbitrarily established link such as in Figure 4.12, at -5° and 2 meters above ground is approximately 8 dB higher than at the 0° pointing. From Figure 4.13, the received signal is increased by approximately 18 dB by pointing at +4° for the 4 meter antenna height. At the 6 meter height of the same figure, a plus 11° pointing provided the maximum signal of -32 dB compared with a -47 dB at zero pointing. In Figure 4.14, an increase of approximately 18 dB is realized at 4 meters by pointing at -7°.

These off-angle results can be understood by examining the aerial photo of the Boulder Laboratories (Figure 3.3), which gives a view of the surrounding building and cars in the parking lot. On the RX01-TX05 path the cars seen in the photo are out of sight of the receiver since the receiver is elevated, on a small mesa, 15 to 20 feet above the parking area. However, the large building on the left is illuminated by the receiver beam without passing through the conifer trees. Also, at the time of the measurements shown in Figure 4.12 through 4.14, there was an aluminum trailer parked to the left of the RX01-TX02 path. Even though these objects were checked and were clearly outside the ± 5°, 3 dB beamwidth of the transmitter, the illumination was undoubtedly adequate to account for many of the off-angle signal peaks. These off-angle signals could have established a link even though foliage losses were excessive on the direct path. Even greater off-angle signal enhancement should result with judicious transmitter antenna pointing. Multipath signals from reflectors, may limit the channel bandwidth because of signal time delay spread. Signals propagating through or near foliage will

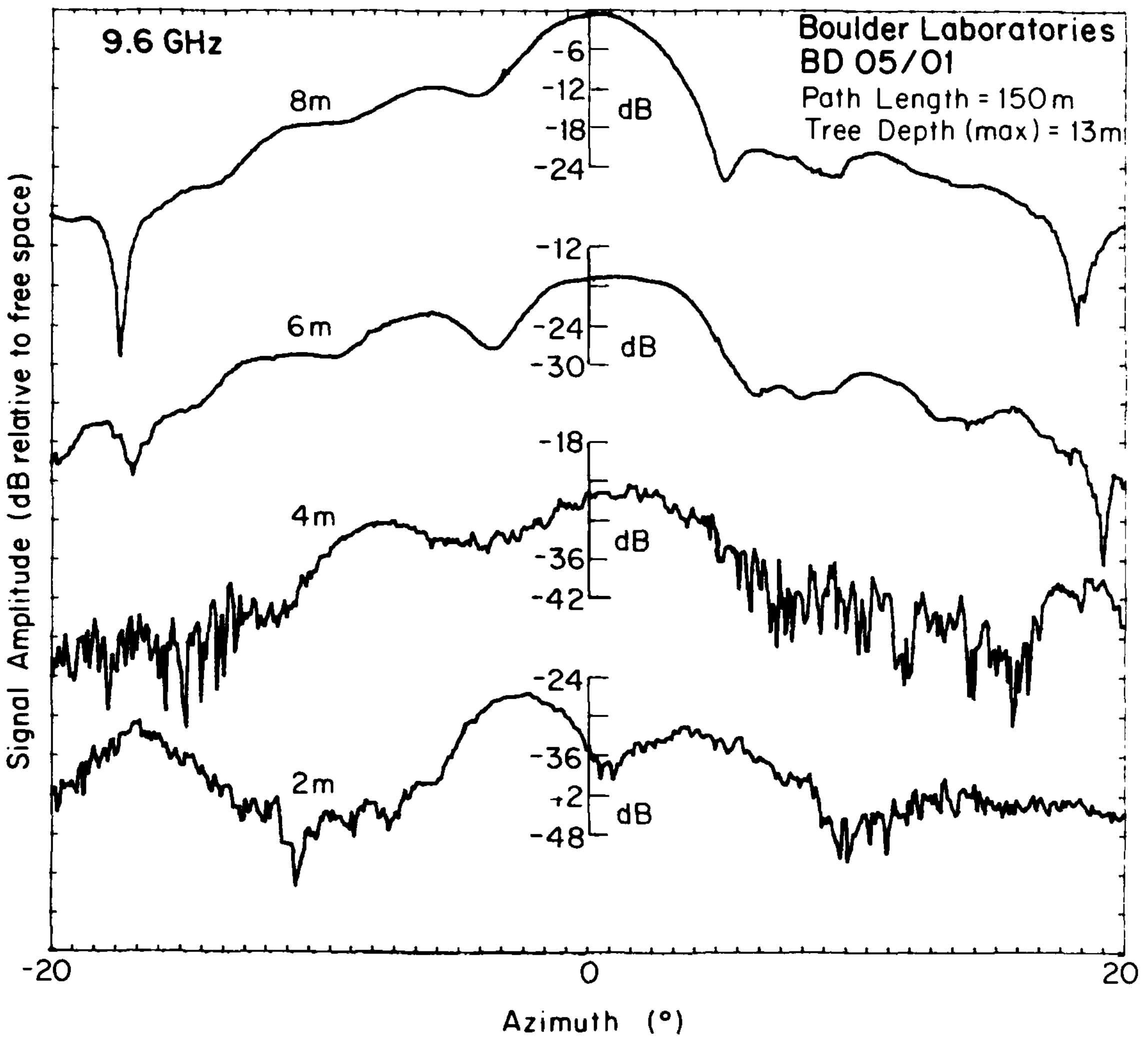

Fig. 4.12. Azimuthal scans at 8, 6, 4, and 2 meter antenna heights on the Boulder Laboratories conifer path using 9.6 GHz.

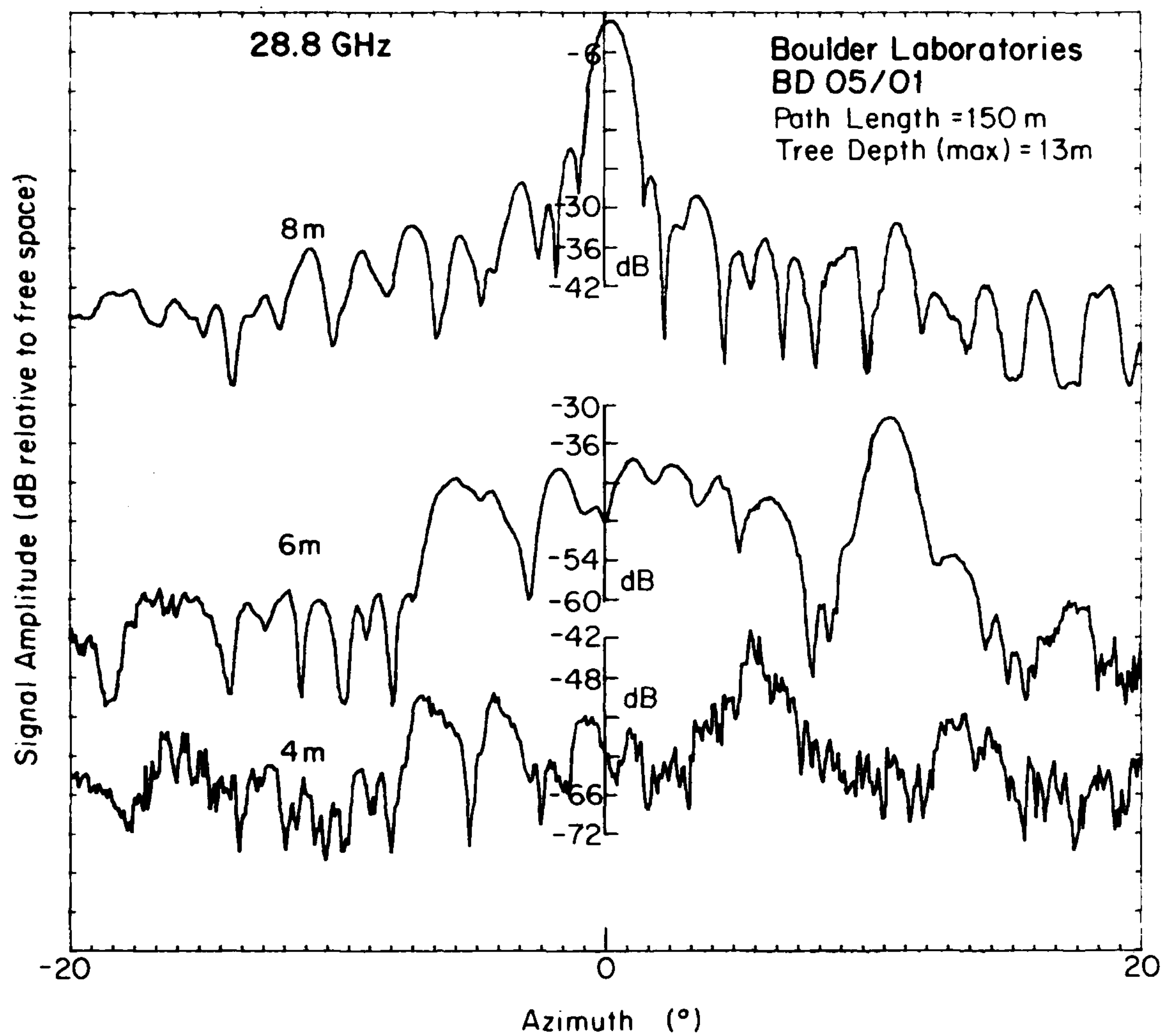

Fig. 4.13. Azimuthal scans at 8, 6, and 4 meter antenna heights on the Boulder Laboratories conifer path using 28.8 GHz.

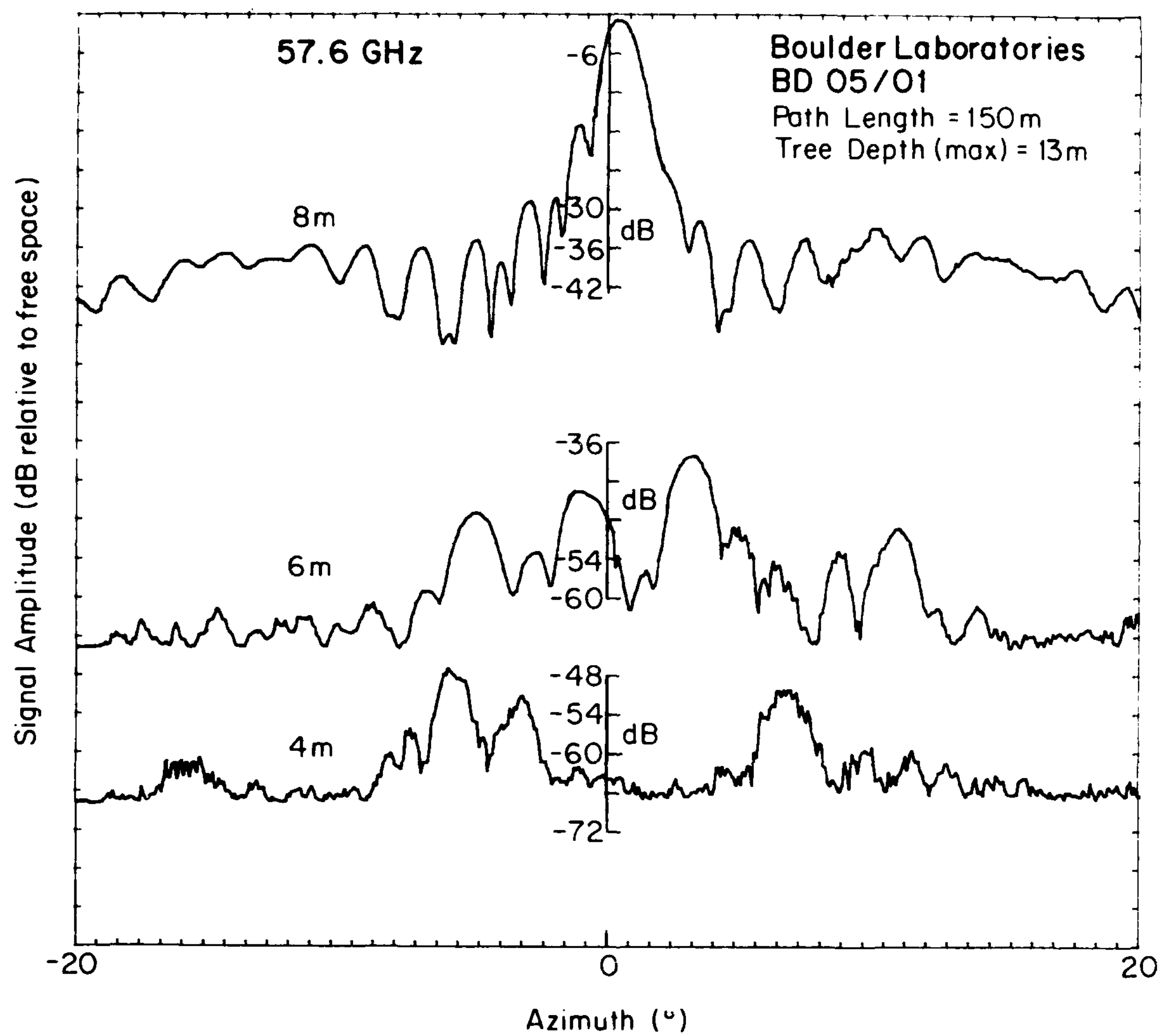

Fig. 4.14. Azimuthal scans at 8, 6, and 4 meter antenna heights on the Boulder Laboratories conifer path using 57.6 GHz.

experience delay spread due to reflections and diffraction components resulting in bandwidth limiting. Another interesting example of off-angle signals without a man-made reflector will be presented in section H, where only trees and natural terrain existed at off-angle locations.

C. Signal Amplitude as a Function of Terminal Positioning

Measurements were made to determine the variability of received signal amplitude due to changes in terminal position relative to the path. An example of signal variability caused by changes in height is shown for the Green Mountain Mesa, 181-meter conifer path in Figure 4.15. The total height change of 2.0 meters caused peak received signal variations of 36 dB, 37 dB, and 20 dB, respectively, for 9.6, 28.8, and 57.6 GHz. Sensitivity to terminal positioning is exhibited by the numerous peaks and nulls occurring for this overall height change. The signal amplitude measured at 9.6 GHz changed 30 dB from the deep null at 1.35 meters height to the next maximum at 1.45 meters. These deep fades show characteristics of multipath propagation which is very valuable information in analysis of mechanisms involved in propagation losses through foliage. Other measurements produced similar results, with typical signal variations of 20 to 30 dB.

The signal amplitude tracings in Figure 4.16 are similar to Figure 4.15, except that the position change is in the horizontal direction. These results show maximum received signal fluctuations of 42 dB, 25 dB, and 26 dB, respectively, for 9.6, 28.8, and 57.6 GHz for an over horizontal displacement of .9 meter. As in the case of the vertical displacement, the maximum rate of change occured in a displacement less than the total span.

The signal amplitudes measured at 9.6 GHz changed by 42 dB in the 10 cm displacement from the approximately .5 to .6 meter position off-set.

As previously mentioned, the results of the horizontal and vertical displacement observations give some insight on propagation modes. In order for a signal null of 30 to 40 dB to occur, two distinct paths must be present and the signal levels of the two paths must be of nearly equal strength. If a deep null occurs due to phase cancellation, then a constructive signal enhancement approaching 6 dB is likewise possible and indications of such enhancements can be seen in Figures 4.15 and 4.16. For the path geometry at the null position, the vector sum of all other scattered signals at the receiver must be no greater than the signal level at the bottom of the null. In Figure 4.16 on the 9.6 GHz plot showing the -42 dB null, the sum of all other signals can not exceed a level -66 dB below the free-space signal level

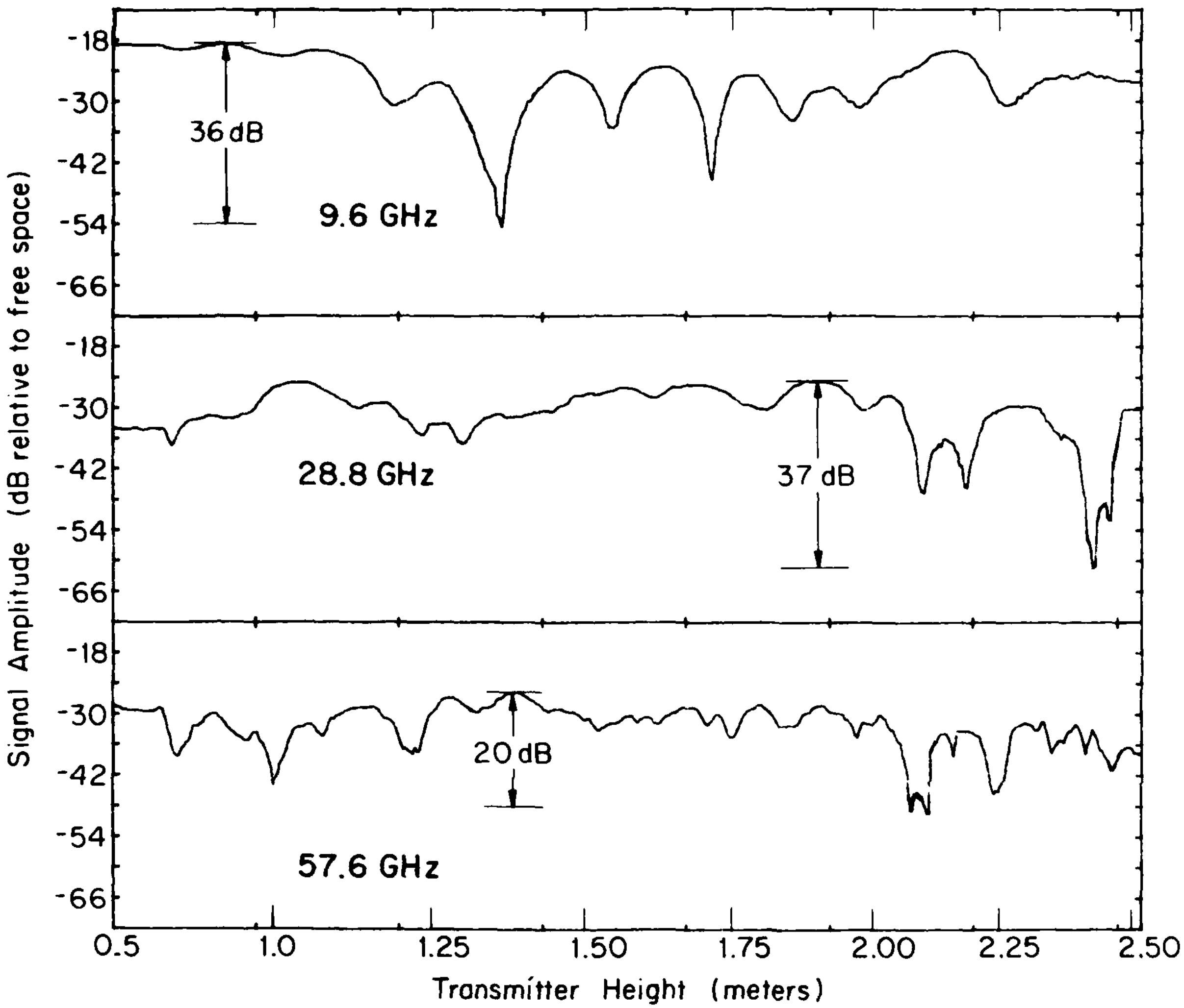

Fig. 4.15. Signal amplitude relative to transmitter antenna height displacement. (GM02/01, path length = 131 m, tree depth = 15 m, polarization = VV).

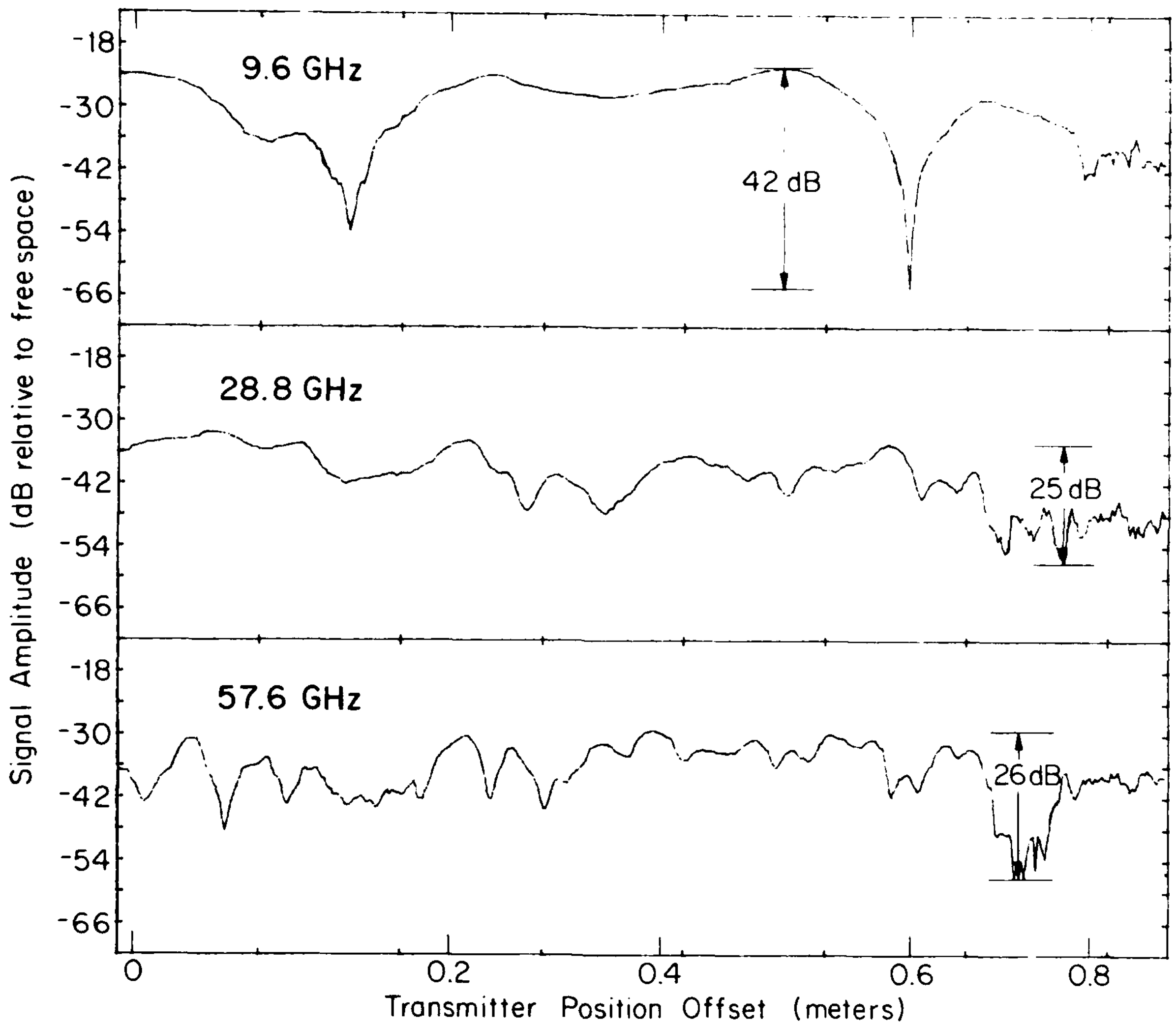

Fig. 4.16. Signal amplitude relative to transmitter antenna horizontal displacement. (MR01/01, path length = 152 m, height = 1 m, tree depth = 40 m, polarization = VV).

for the path. Note that a common factor for the two paths generating Figures 4.15 and 4.16 is that height over terrain was in the 0.5 to 2.5 meter range where large tree trunks are illuminated within the antenna beam with only sparse leave density obscuring the path, particularly at slight off-path angles. Some off-angle reflectors are likely outside the $\pm$ 0.6 degree beam of the upper two frequencies. This can account for the peak amplitude arriving off zero pointing on the azimuth scans shown in the previous section. Also note that, for the same two figures, the peak signals are -20 to -30 dB below free space value for the 9.6 GHz and -30 to -40 dB for both 28.8 and 57.6 GHz. Because of the existence of the deep null, the strongest signals are probably arriving at the receiver as reflections from, primarily, tree trunks. If this is true then the resulting signal amplitude for the cases presented is strongly related to the coefficient of reflection for a tree trunk at each frequency. It can not be verified whether or not a signal reflection from a trunk can find an open path between terminals in the above examples, but visual observations would suggest this is likely. In general, the higher frequencies shows more rapid transitions, which may indicate an increased roughness factor in addition to a greater phase change for the same movement at the shorter wavelengths. There is no reason to expect the nulls to occur at or near the same position for each frequency, not only because of the wavelength difference, but also because the antenna positions (aperture centers) are separated several centimeters on the transmitter to tens of centimeters on the receiver.

Figure 4.17 shows a height scan to 3.25 meters on the tall cottonwoods path but many exposed trunks still appear at this level and the apparent multipath fades support this. Unfortunately no displacement scans were recorded at heights where trunks and branches were covered by leaves or needles to test the difference in multipath components observed. However, the path shown in the horizontal scan plot of Figure 4.18 has a high density of small diameter tree trunks providing, one would think, a much reduced likelihood of a strong single reflection from a trunk reaching the receiver. Yet, deep signal nulls (30 dB) are seen on the 28.8 GHz amplitude versus horizontal displacement plot. The data in Figure 4.19 is from the same path as Figure 4.18, but without leaves. These horizontal displacement scans have some interesting similarities and differences. The similarities are the absence of fades at 9.6 GHz and the location and spacing of the deeper fades around 0.4 meters of displacement at 28.8 and 57.6 GHz plots. The differences are that without leaves the fades are not as deep due, probably, to the generally higher signal level from more scattering paths without the leaf coverage. These added scattering paths are also

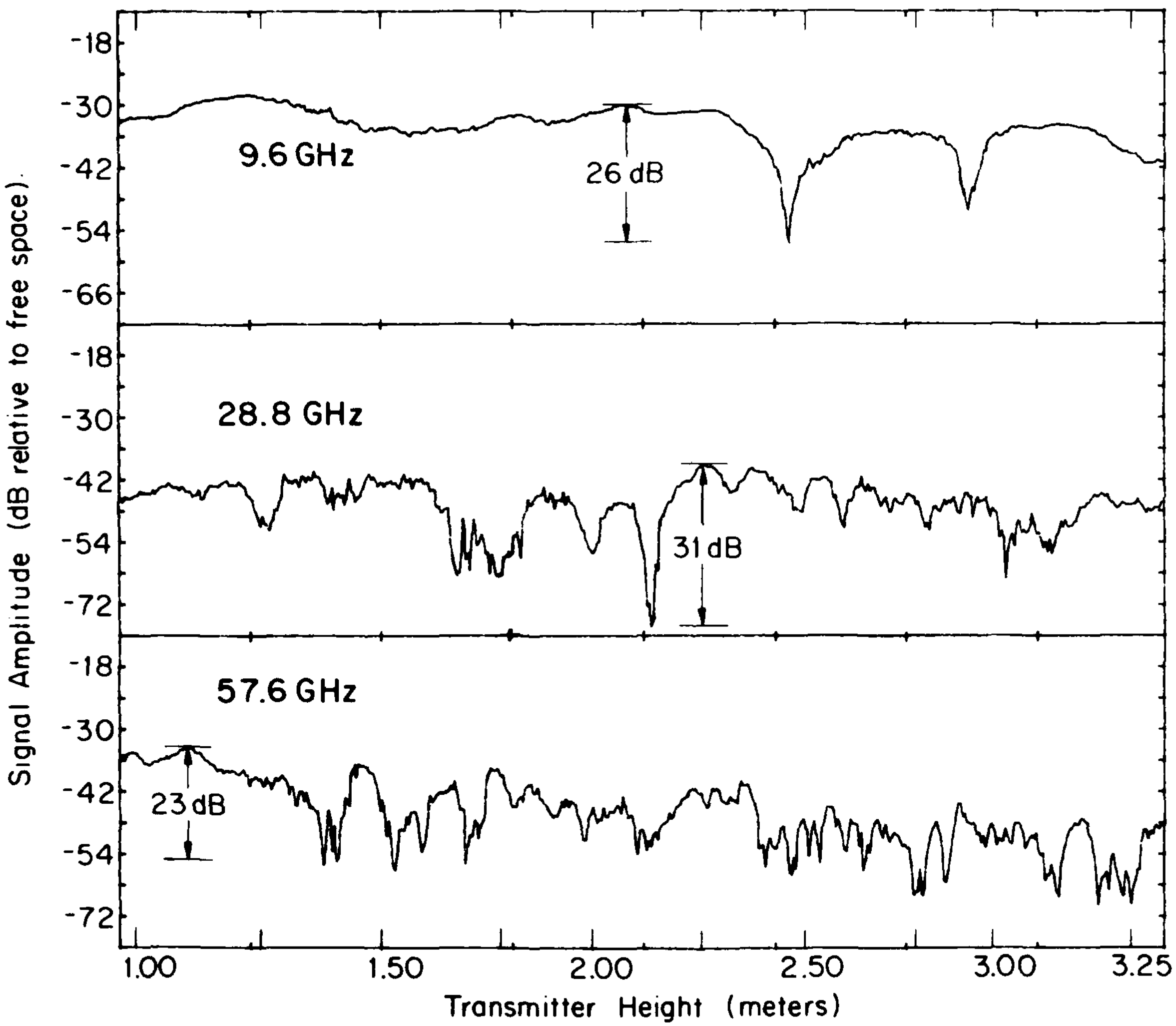

Fig. 4.17. Signal amplitude relative to transmitter antenna vertical displacement. (MR01/01, path length = 152 m, tree depth = 40 m, polarization = VV).

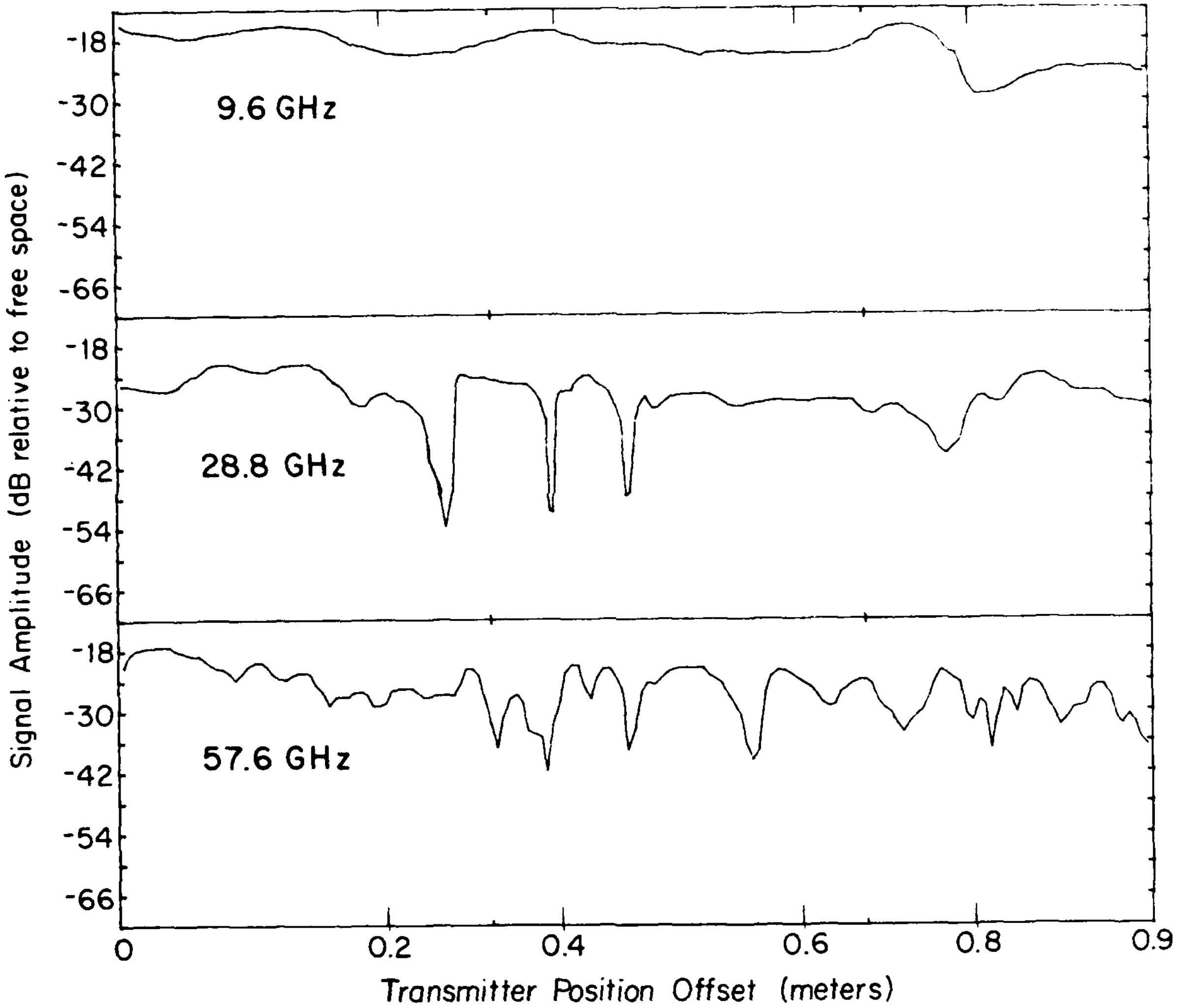

Fig. 4.18. Signal amplitude relative to transmitter antenna horizontal displacement. (MR02/01, path length = 172 m, height = 1 m, tree depth = 30 m, polarization = VV).

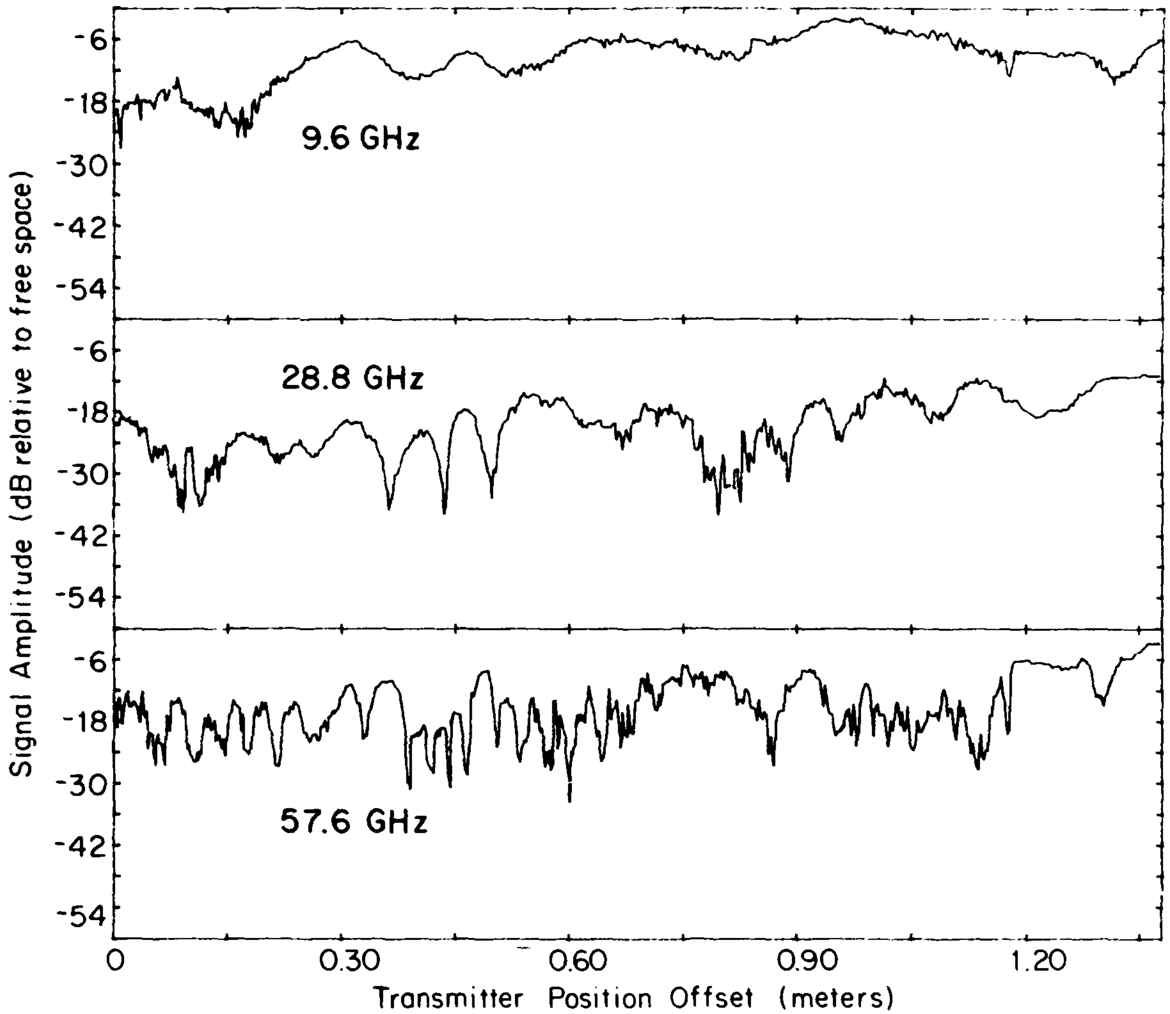

Fig. 4.19. Signal amplitude relative to transmitter antenna horizontal displacement. (MR02/01, path length = 172 m, height = 1 m, tree depth = 30 m, polarization = VV, no leaves).

very pronounced in the no leaf plots, as seen by the numerous 6 to 10 dB variations, especially for the two upper frequencies. The rapid 1 to 3 dB scintillations in Figure 4.19 are due to a somewhat windy condition at the time of recording.

Vegetation loss (in dB per meter of foliage) is a useful parameter for describing propagation characteristics through foliated paths. However, as can be seen from the figures referred to in this section these loss values can vary greatly depending on terminal position. One very consistent feature of the measurements should, however, be noted in this discussion of position sensitivity. Over all paths examined, and for any specific height or horizontal position which was remeasured (even after three or four days), the recorded signal level always repeated to within a decibel of the original value. These repeatable measurements were intentionally performed in early morning to be compared to midday and evenings, and before and a few hours after a rain (after droplets evaporated from the leaves). This suggests that differences in temperature, humidity dust coating, and physical position of branches, etc. over a period of days was not a factor.

D. Scintillation Effects

The received signals recorded on the tree-covered paths show amplitude variations (scintillations) when the wind was blowing. Examples of time series recordings are shown in Figures 4.20, 4.21, and 4.22. The signal amplitude tracings in Figure 4.20 are relatively smooth with 1 or 2 dB changes except for the brief increase between the 3.5 and 4.5 minute time period. The records in Figure 4.20 were made during a period of no-wind to very light wind. In contrast, the signal amplitude tracings in Figure 4.21 were recorded during a period of light to moderate wind (estimated velocity of 10-15 mph). These tracings exhibit short period (5-to-10 seconds) variations of 12 to 15 dB and longer period (1-2 minutes) shifts of 8 to 10 dB. These examples are typical of many taken in light-to-moderate wind conditions. The link was not operated in heavy wind, because of the wind-load limits of the antenna positioner. The data in Figure 4.22 show scintillations as signals propagate through a grove of pines during a time of moderate wind.

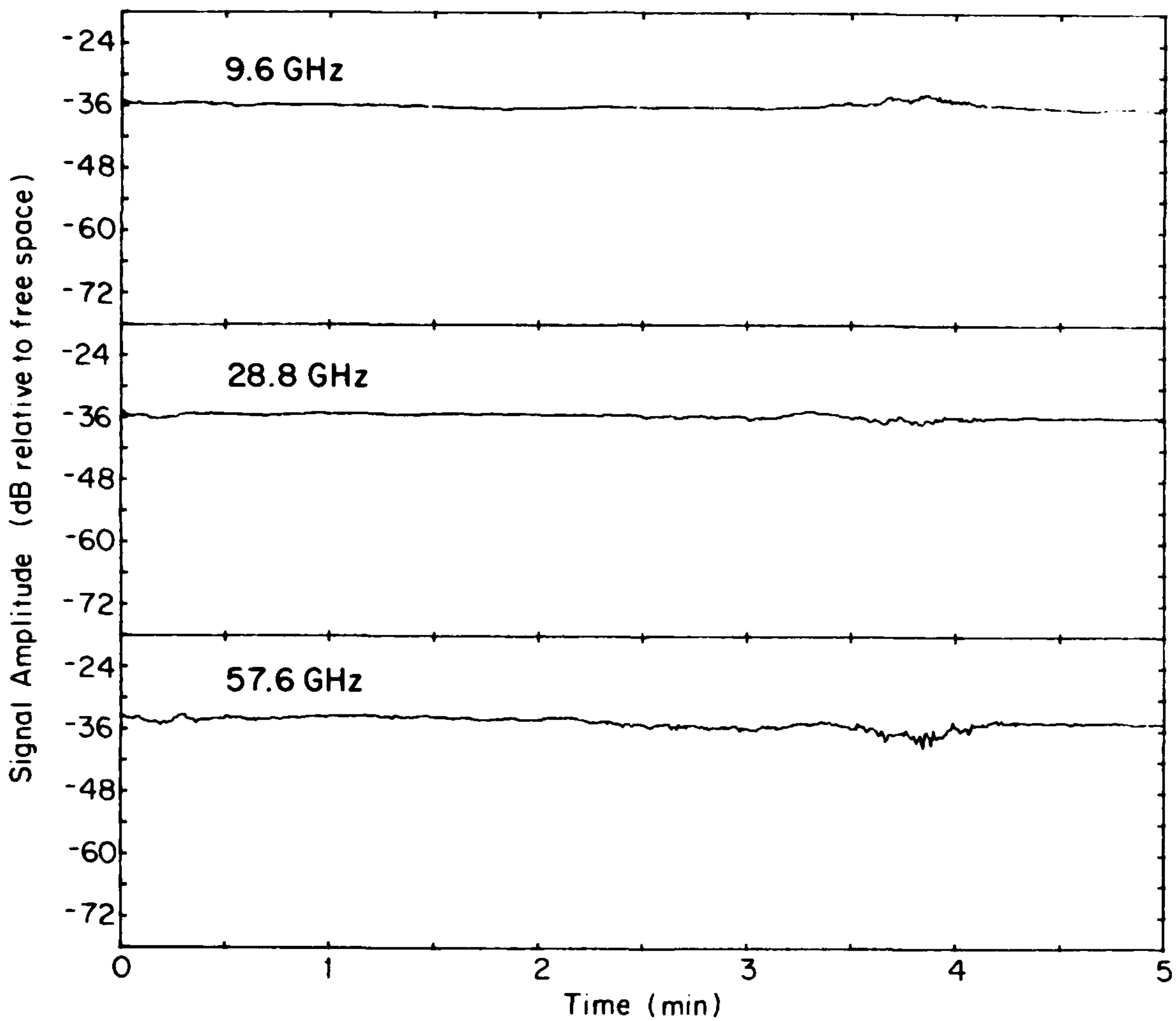

Fig. 4.20. Time series records of received signal amplitude during very light wind conditions.

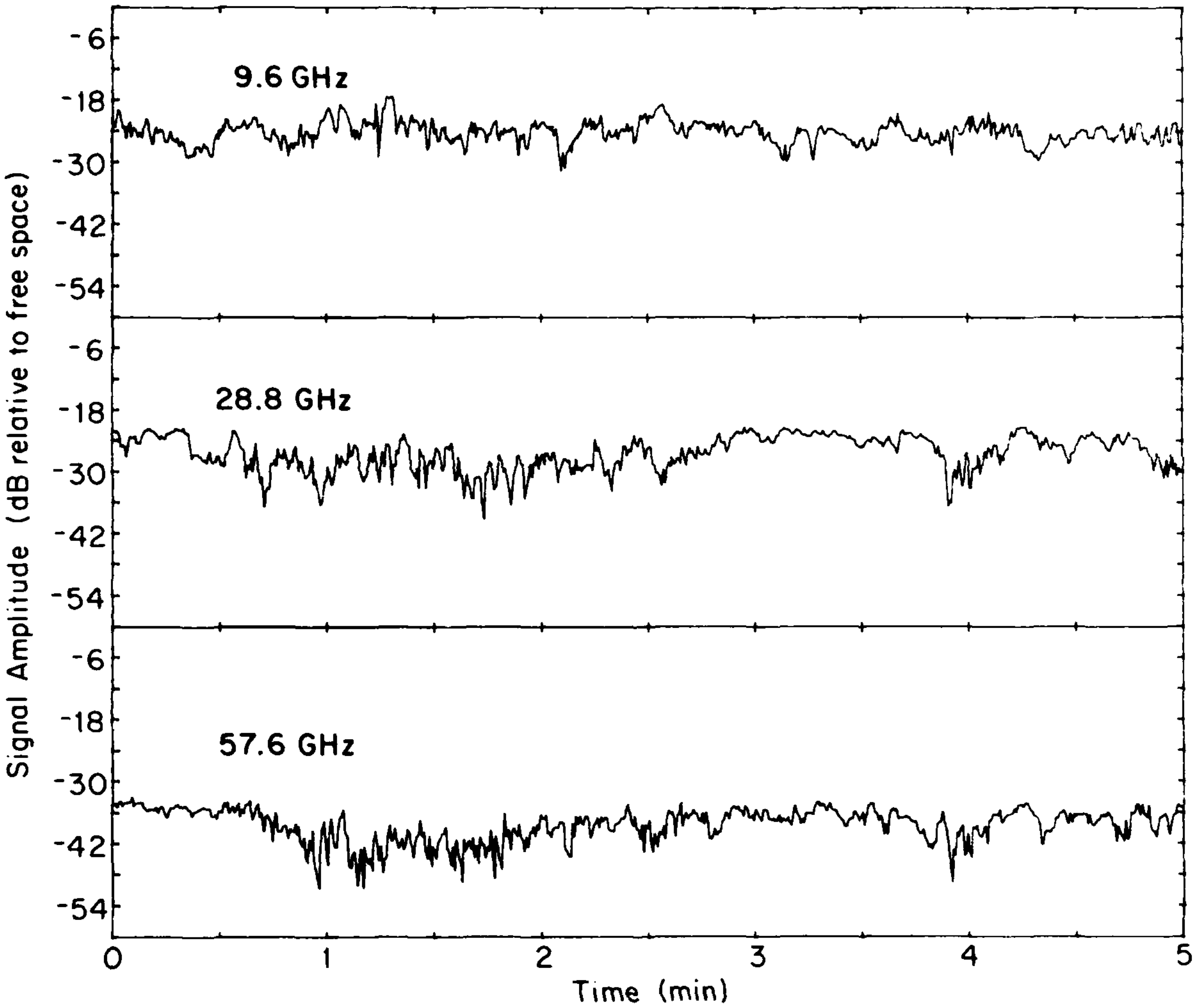

Fig. 4.21. Time series records of received signal amplitude during windy conditions.

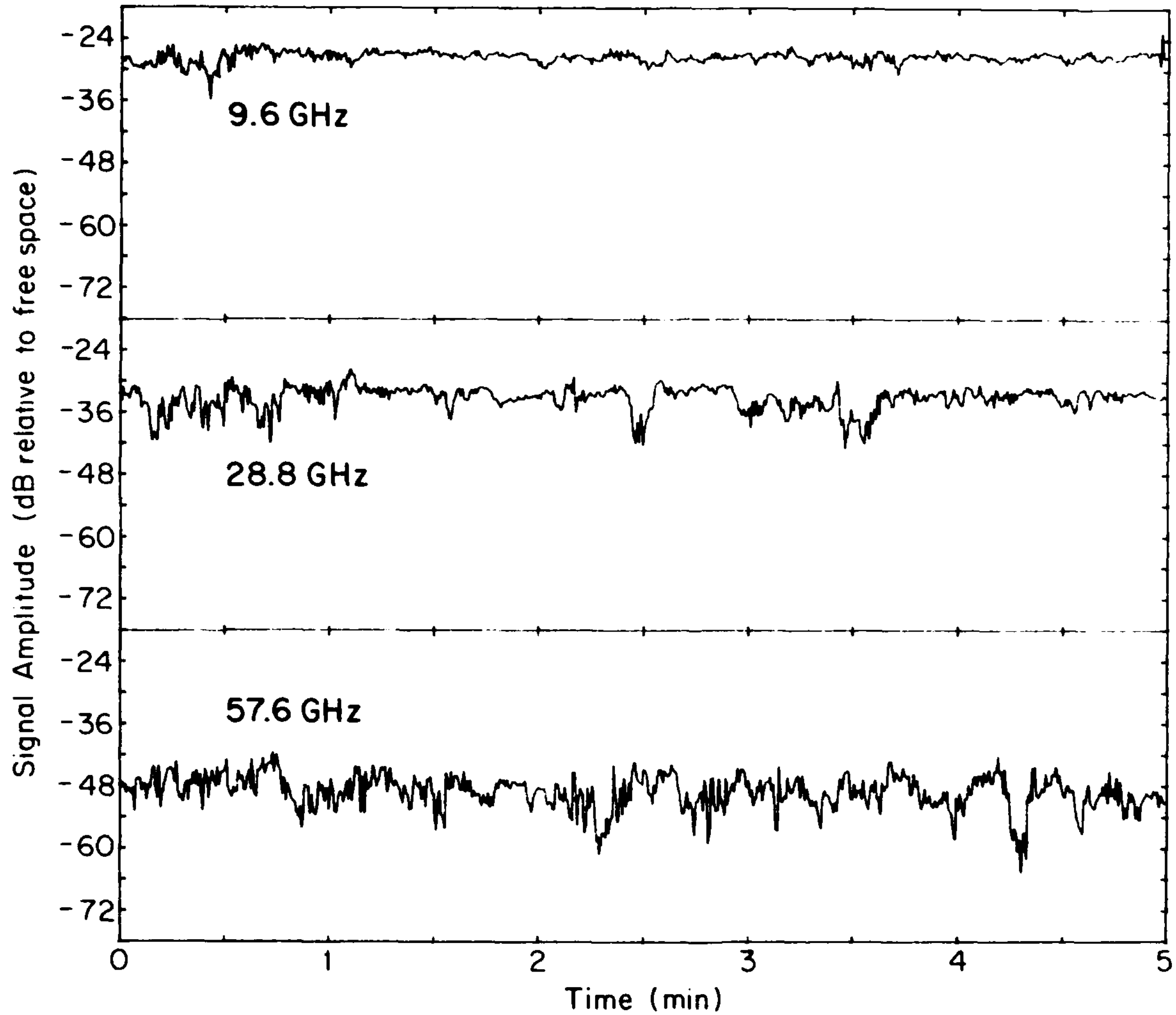

Fig. 4.22. Time series records of received signal amplitude during windy conditions.

E. Vegetation Loss as a Function of Foliage Depth

The soatial variation in Section IV C suggests that caution be used in expressing the vegetation loss as a function of foliage depth (dB/meter); however, this parameter is helpful in developing a propagation model for specific types of foliage. Conditions for measurements made in this report differ from most observations reported in the technical literature at lower frequencies [1-16]. Observations at VHF and UHF are taken with an antenna beam which illuminated the full height of the foliage (trees) and a relatively wide azimthal angle. The horizontal and vertical antenna beam in the EHF band for the data taken in this report was approximately 0.02 radians, or about a 2 meter diameter spot in a common transmitter-receiver volume at a distance of 100 meters from the receiver. Because the data presented in Figure 4.23 was taken at a height of maximum leaf or needle depth along the path (4 to 7 meters above ground), multipath effects from trunks or ground reflections are presumed small. Measured values at heights which include multipath nulls were not incorporated. The average of the vertical and horizontal signal levels was plotted for additional smoothing, as measurements throughout this study indicated vegetation loss for trees was independent of polarization.

Few opportunities are available to compare these values to those reported in the technical literature because there are differences in frequency and type of vegetation. In the case of polarization, several authors have reported a higher loss for vertical polarization in tree groves, mostly in tropical areas, for frequencies below 500 MHz. Saxton and Lane [11] reported no polarization differences in vegetation loss values for a stand of lime trees using 1.26 GHz, and they also reported on measurements made by McPetrie and Ford at 3.26 GHz indicating the loss was independent of polarization. This method of describing foliage depth was used because of the non-uniform foliage density in Colorado and because the short foliage paths at EHF make actual depth measurement practical. For these frequencies this may prove quite useful for applications involving military scenarios, since available high quality aerial photography can provide this information quite readily.

At times the maximum signal amplitude would occur at off path angles of several degrees, but for the purpose of finding vegetation loss versus foliage depth, these values were also disregarded as their probable path was outside the line of maximum foliage.

---

[11] Saxton, J.A., and Lane, J.A., "VHF and UHF Reception, Effects of Trees and Other Obstacles", Wireless World, (1955).

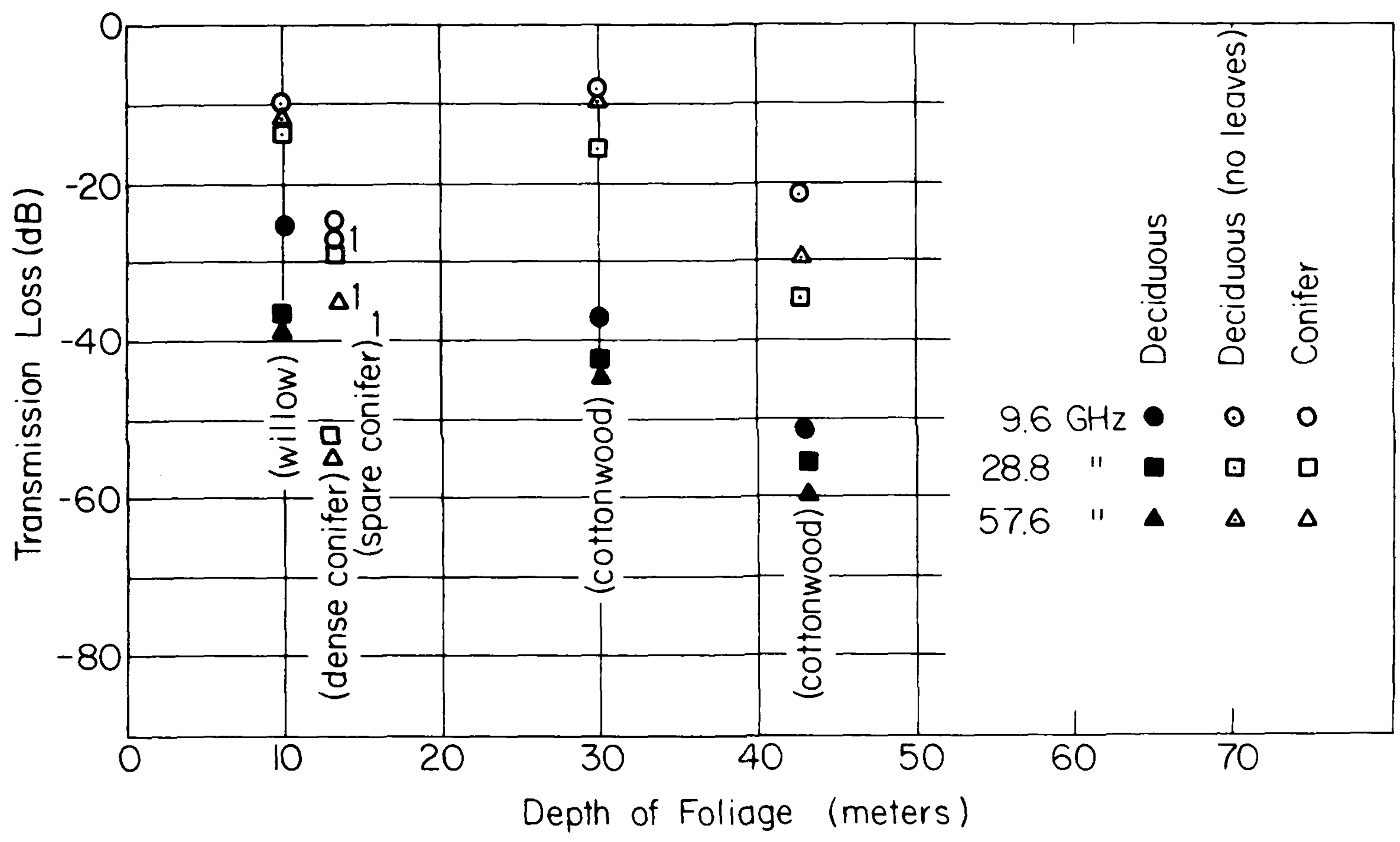

Fig. 4.23. Transmission loss as a function of foliage depth.

Data from five paths are included in Figure 4.23 and are labeled according to tree type and signal frequency. The data in Table 4.3 summarize the results of the deciduous tree measurements derived from the average dB/meter value and expressed as a normalized frequency dependent ratio.

TABLE 4.3

Vegetation loss (dB/m).

	Frequency (GHz)			Frequency dependence		dB/ (ratio)
Depth (m)	9.6	28.8	57.6	(9.6/9.6)	(28.8/9.6)	(57.6/9.6)
	dB/m	dB/m	dB/m	$\sqrt{f1/f1}=1$	$\sqrt{f2/f1}=1.7$	$\sqrt{f3/f1}=2.4$
10 (willow)	2.5	3.6	3.9	1	1.4	1.5
30 (cottonwood)	1.2	1.4	1.5	1	1.2	1.3
43 (cottonwood)	1.2	1.3	1.4	1	1.1	1.2
Average	1.6	2.1	2.3	1	1.3	1.4

No attempt is made to analyze the conifer results because only two areas were measured and, as previously mentioned, one area had lush-moist growth, while the second was drier with 10 to 15% dead needles.

The values for foliage depth were determined by measurir the maximum composite of foliage on a direct line between terminals on each path. he height at which the maximum depth occurs varies with each path but, as indicated above, this height ranged from 4 to 7 meters.

F. Signal Backscatter From Vegetation

The map in Figure 4.24 shows the relative position of the transmitter, the receiver, and two groups of trees from which significant backscatter signals were recorded. The transmitter and receiver were stationed 7 meters apart with their antenna zero angle directions parallel as indicated by the two heavy lines in Figure 4.24. Several sets of data were recorded at this site, but to demonstrate the magnitude and character of the apparent backscatter signals observed, only four sets are presented as features were quite similar. These data are shown in Figures 4.25, 4.26, and 4.27 for each of the three frequencies 9.6, 28.8, and 57.6 GHz.

In each figure, the four azimuthal scans are labelled a, b, c, and d, and represent transmitter and receiver antenna orientations as indicated in Table 4.4 below.

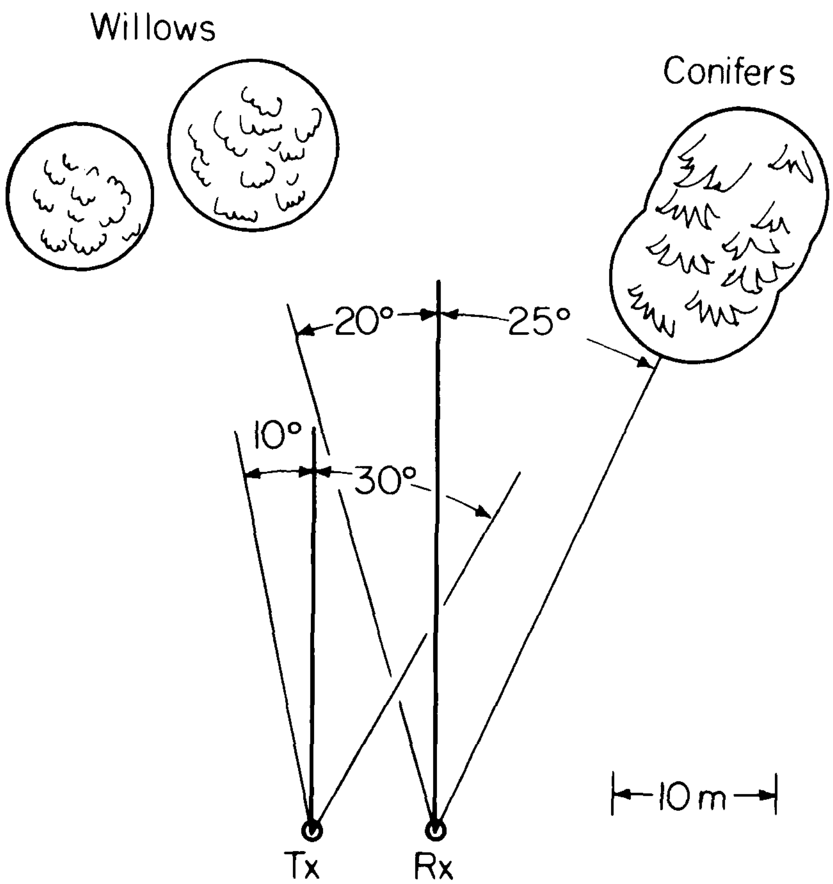

Fig. 4.24. A map showing the placement of the transmitter, receiver, and scatterers for backscatter measurements.

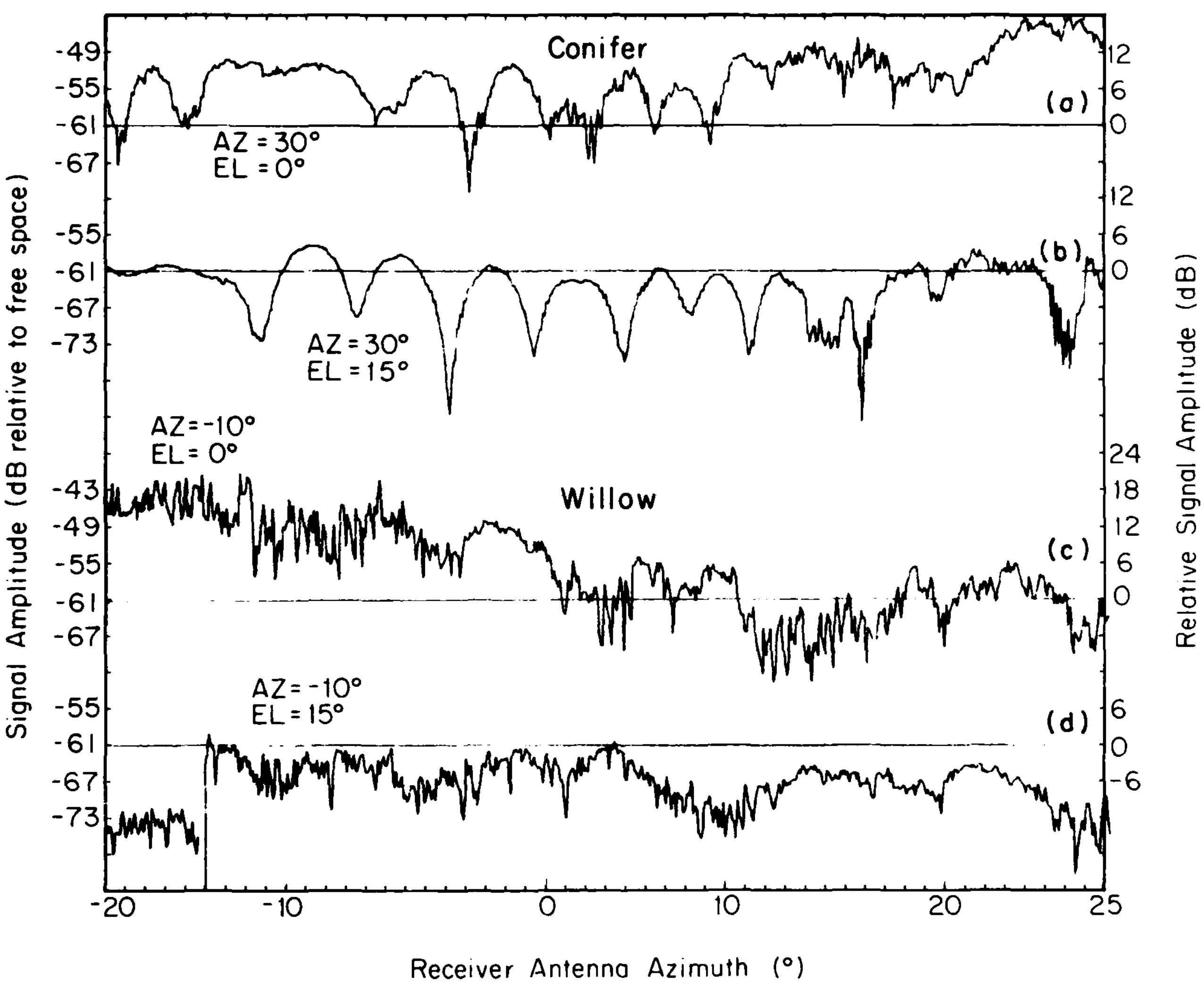

Fig. 4.25. Backscatter signals from a willow tree and a clump of conifer trees at 9.6 GHz (VV polarization).

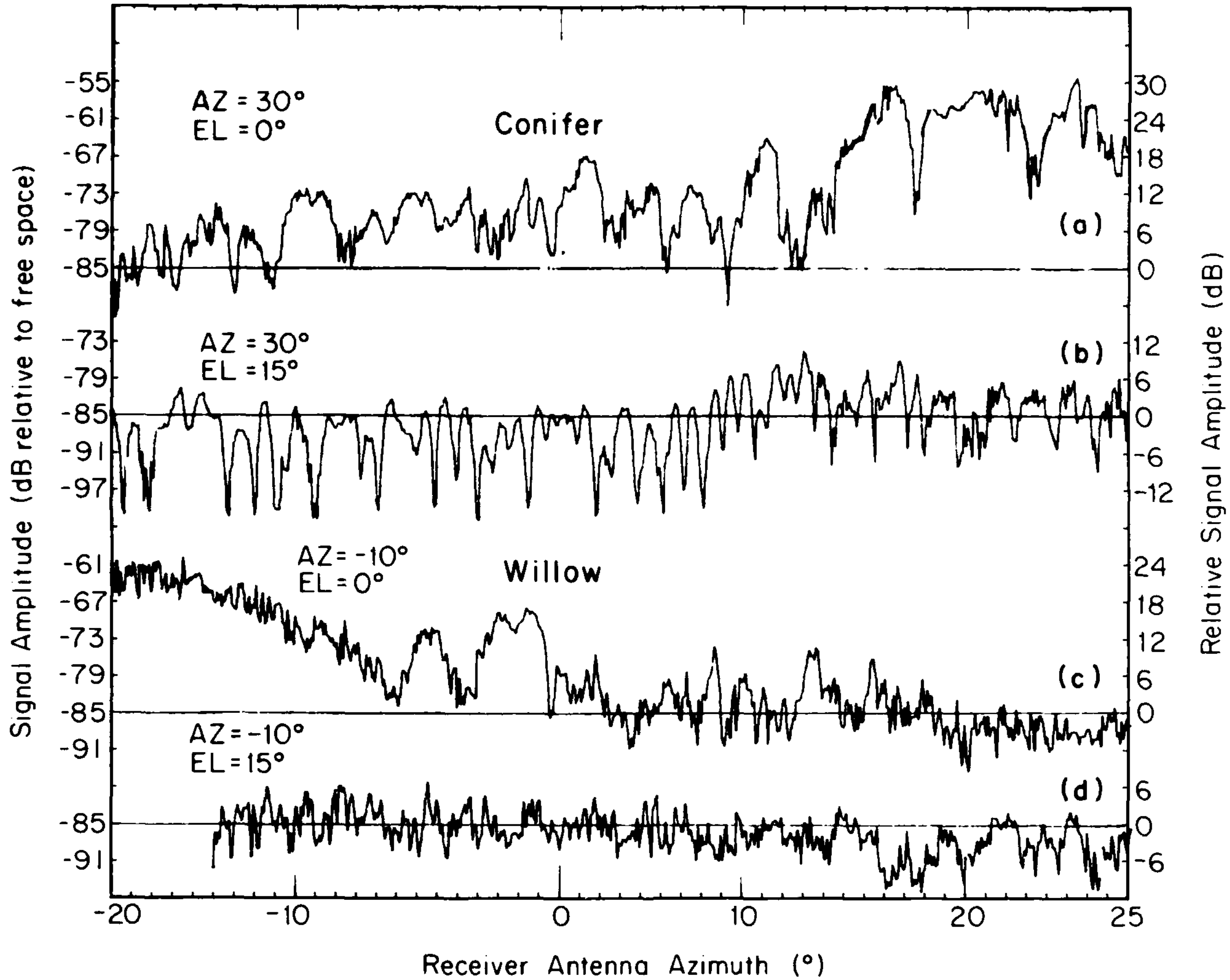

Fig. 4.26. Backscatter signals from a willow tree and a clump of conifer trees at 28.8 GHz (VV polarization).

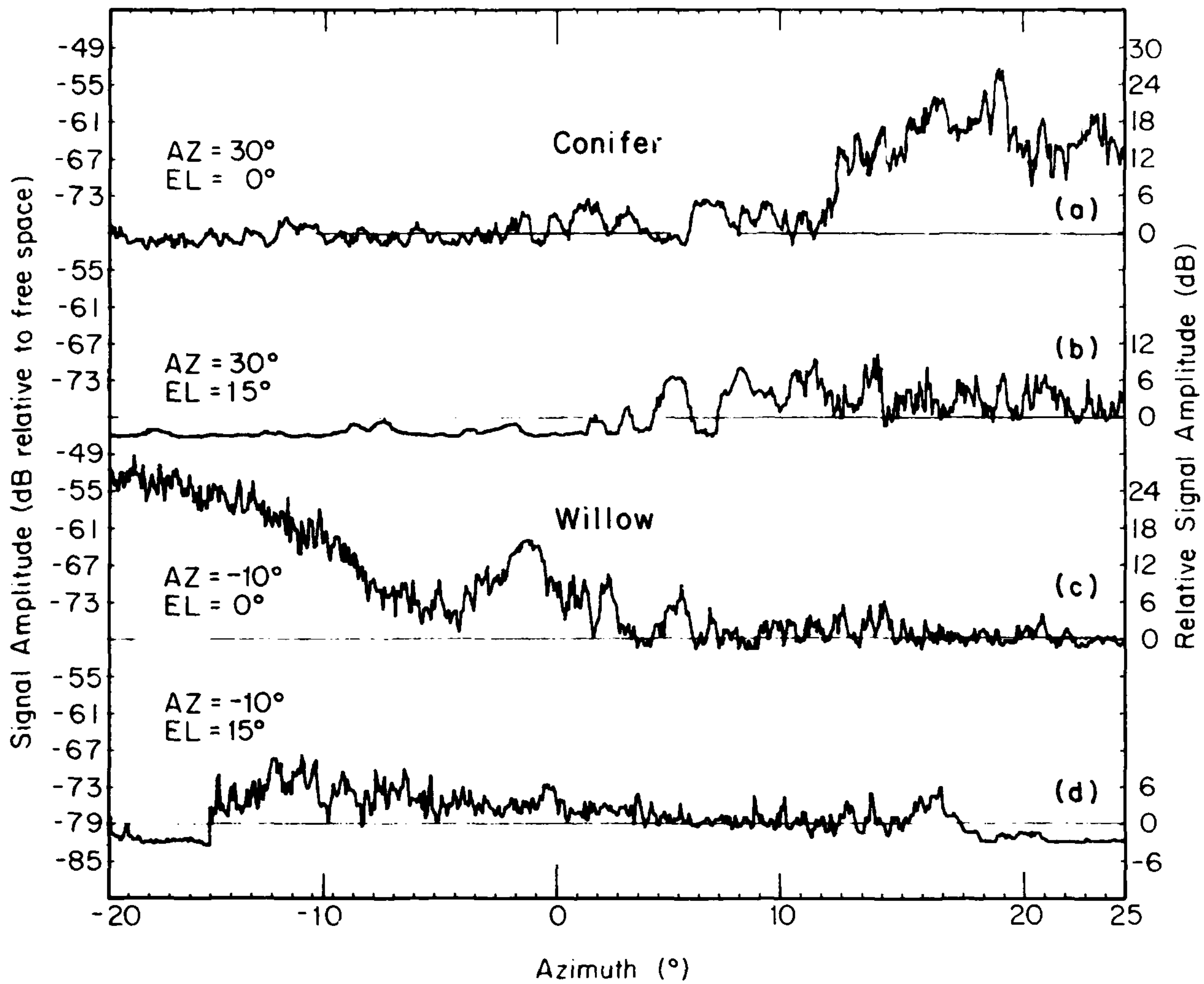

Fig. 4.27. Backscatter signals from a willow tree and a clump of conifer trees at 57.6 GHz (VV polarization).

TABLE 4.4

Antenna orientations for backscatter measurements.

	Transmitter AZ	Transmitter EL	Receiver AZ	Receiver EL	Height
Scan a)	+30°	0°	-20° to +25°	0°	6 m
Scan b)	+30°	0°	-20 to +25°	15°	8 m
Scan c)	-10°	0°	-20 to +25°	0°	6 m
Scan d)	-10°	0°	-20 to +25°	15°	8 m

Scan a) was made with the transmitter and receiver at 6 meters height and with the transmitter pointing at the conifer trees (30°). In each of the three figures, the received signal is enhanced as the receiving antenna scan approaches +15° to +20 . The enhancement boundaries are particularly apparent for frequencies 28.8 GHz and 57.6 GHz, which is due to the 1.2 degree antenna beam compared to a 5 degree receiving beam at 9.6 GHz. Scan b) was made with the transmitter at 30°, still pointing in the direction of the conifer trees, but with the receiver and transmitter both at 8 m and the receiver antenna elevation at +15°. This orientation reduced the possibility of backscatter and serves as a noise reference and/or signal leakage reference.

The vertical axes of the plots of Figures 4.25, 4.26, and 4.27 represent the backscattered signal amplitude in decibel relative to the signal amplitude present at foliage producing the backscatter. The signal amplitude at the foliage is derived from the standard path calibration computed for the distance from transmitter to the foliage using the free-space propagation equation. Comparing the received signal to the signal incident to the pine trees shows maximum backscatter levels of -46 dB, -56 dB, and -54 dB for 9.6, 28.8, and 57.6 GHz, respectively, at receiving antenna azimuthal angles between +15° to +25° of scan a).

Scan c) was made with the transmitter and receiver at 6 meters height and with the transmitter pointing at the willow trees (-10°). The received signal is enhanced as the receiving antenna covers the sector -20° to -5° which intersects the willow trees. As was the case in scan a) the enhanced signals are particularly apparent for 28.8 and 57.6 GHz. Scan d) was made with the transmitter at -10°, but with the receiver and transmitter both at 8 m and the receiver antenna elevated to 15° in the vertical plane. As before [in scan b)] this orientation reduces the possibility of backscatter and scan d) serves as reference for scan c).

Comparing the received signal of scan c) to the signal incident to the willow trees results in maximum backscatter levels of -43 dB, -62 dB, and -52 dB in order of ascending frequency. There is a drop out on all scan d) plots between -19° and -14° due to loss of phase lock at the receiver. Several sets of data were recorded at the same location for 2-meter and 4-meter heights. The results varied by only a few decibels, and the shape of the scans were very similar.

In this backscatter measurement there is a degree of uncertainity in determining the contribution due to trees and that due to other reflection from objects to the side and behind the foliage. There is an upward incline of the terrain beyond the trees which produces many potential scatterers at distances from 200 meters to several kilometers (except a building as noted below). However, the 3 dB points of the receiving beam illuminated an approximately 3-meter diameter spot at the trees (32 to 38 meters away). At 28.8 and 57.6 GHz, the 3 dB spot is only 0.75 meters in diameter. Hence, for a minimum of at least a couple of degrees of scan, the receiving beam intercepts only foliage. Since the signal loss through the foliage for these paths was never less than 17 dB at the backscatter heights at 9.6 GHz and never less than 29 dB at the two upper frequencies (Figures 4.1 and 4.7), reflections from behind the trees would suffer a minimum loss of 34 and 58 dB in passing twice through the trees. There is an additional free-space loss of 15 dB to the nearest possible reflection point of 200 meters. The sum of these numbers alone represent a signal 6 dB lower than the measured backscatter signal. In order for this signal level to produce a 1 dB error in maximum backscatter signal, the reflection would require a perfect reflecting flat plate 8.3 meters square normal to the beam and completely filling the beam at 200 meters. From the above analysis, it is felt that the peak backscatter signal observed is very near the actual backscatter from the foliage in line with each path, with scattering contributions from other sources very slight.

Note, that at the -2 to 0 degree pointing angle on scans a) and c) a reflection from a near normal surface of a 4 by 3 meter wall of a concrete aggregate building at a distance of about 120 meters is visible. This reflection is most pronounced in scan c) plots for the two upper frequencies. The degree or two displacement of the peak signal in receiver azimuth angle on the scans is likely due to the separation of antenna centers at both terminals.

Assuming most of the reflections are from the willow and pine trees at on-line pointing, it would be informative to calculate their effective scattering cross sections. The signal level incident to the willow trees at 38 meters can be derived

from the 150-meter calibration path data. The relative field intensity at the willow is found by dividing the incident signal level by the receiving antenna aperture (Ar). Thus the field intensity at the willow is $P_w = P_{R38m}/Ar$. Using this value for P_w to find the scattered power from the willow intercepted at the receiver (P_R) gives

$$P_R = \frac{P_{R\ 38m}}{Ar} \quad \frac{\sigma\ Ar}{4\pi R^2} \text{ watts/m}^2.$$

Sigma (σ) is the area of a lossless isotropic reflecting sphere and is equal to the effective scattering cross section of the trees, assuming a spherical reflector, where Ar converts the field intensity at the receiver to the signal power captured. The ratio of power received at 38 meters to the backscatter power from the willow trees (P_{R38m}/P_R) is the value recorded in the experiment and plotted in scan c) of Figures 4.25, 4.26, and 4.27. For the willow trees at 9.6 GHz, the ratio for P_R/P_{R38m} is taken from Figure 4.25 as 44 dB or 2.5×10^4 (an average peak value). Solving for effective scattering cross sections of the willow tree at 9.6 GHz gives

$$\sigma = \frac{4\pi R^2}{P_R/P_{R38m}} = 0.516 \text{ m}^2.$$

For 28.8 GHz, P_R/P_{R38m} is estimated from Figure 4.26 at 62 dB or 1.5×10^6. The (σ) becomes 8.16×10^{-3} m^2. For 57.6 GHz, the estimated P_R/P_{R38m} from Figure 4.27 is 53 dB or 2×10^5, resulting in σ of 6.45×10^{-2} m^2 for the willow trees.

For the measured backscatter signals off the pine tree which is 38 meters from the transmitter and 32 meters from the receiver, the P_R/P_{R38m} [scan a)] and σ values are listed in Table 4.5, below, with the willow values just calculated. The radii of equivalent spherical reflectors ($r = \sqrt{\frac{\sigma}{\pi}}$) are included.

TABLE 4.5

Backscatter radar cross-sections.

		9.6 GHz	28.8 GHz	57.6 GHz
Willow	P_R/P_{R38m}	44 dB	62 dB	53 dB
	σ(m^2)	0.516	8.16×10^{-3}	6.45×10^{-2}
	r(cm)	4.05	0.51	1.43
Pine	P_r/P_{R38m}	44 dB	60 dB	62 dB
	σ(m^2)	0.515	1.29×10^{-2}	8.15×10^{-3}
	r(cm)	4.05	0.64	0.509

These values illustrate the equivalent radar target size of the trees. The only comment, considering this limited sample, is that the value at 57.6 GHz for the willow stands out as large, when considering the frequency dependence shown in the other values for cross section. The reason for this apparent higher cross section is not known. It may be from a source other than the willow or perhaps a Mie region or resonant effect of leaves or stems. A point of comparison is the defoliated results of Figure 4.28 which shows a more orderly cross section as a function of frequency that may support a resonant effect.

These backscatter measurements were repeated on successive scans and even the following day. To verify that the source of the backscatter was not leakage between terminals, a panel of absorbing material was placed directly in front of the receiving antennas. This action reduced the received signal by 20 to 25 dB, demonstrating that the coupling between terminals was less than even the backscatter sidelobe level shown in scans b) and d).

The backscatter tests producing the results shown in Figures 4.25, 4.26, and 4.27 were repeated in December with the willow tree in a defoliated state. As expected, the return from the pine trees were similar to the earlier measured values. Contrary to expectations, the maximum signals from the defoliated willow were near or somewhat greater than earlier measured values, as seen in Figure 4.28. This unexpected result may be interpreted in the following way. The exposed trunks and branches act as a better reflector than the leaves, but produce fewer backscatterers, as is suggested in the figure by the smoother signal amplitude plots with deeper fades during the azimuthal scan. Also the signal loss through the willow trees was measured at approximately 20 dB less with no leaves compared to signal loss when the leaves were on the trees. This condition permits a 40 dB higher signal to penetrate the trees and reflect from the background. As previously indicated the terrain beyond the trees, in line with the path, does rise and begins intersecting the receiver beam, when at a 6 meter height, at a distance of approximately 200 meters. Also, it was not possible to guarantee that the terminals were placed at identically the same location. A displacement from the original position of a few centimeters is possible, but this amounts to several wavelengths, which can change location of multipath fades on the signal amplitude plots. On the 57.6 GHz defoliated backscatter plot, the reflection from the concrete building moved from about 0 degrees to +2 degrees on the azimuth scan, but the amplitude remained about the same. Clearly there are more rapid and less deep fluctuation with leaves than with no leaves, which primarily characterizes the differences between the two backscatter

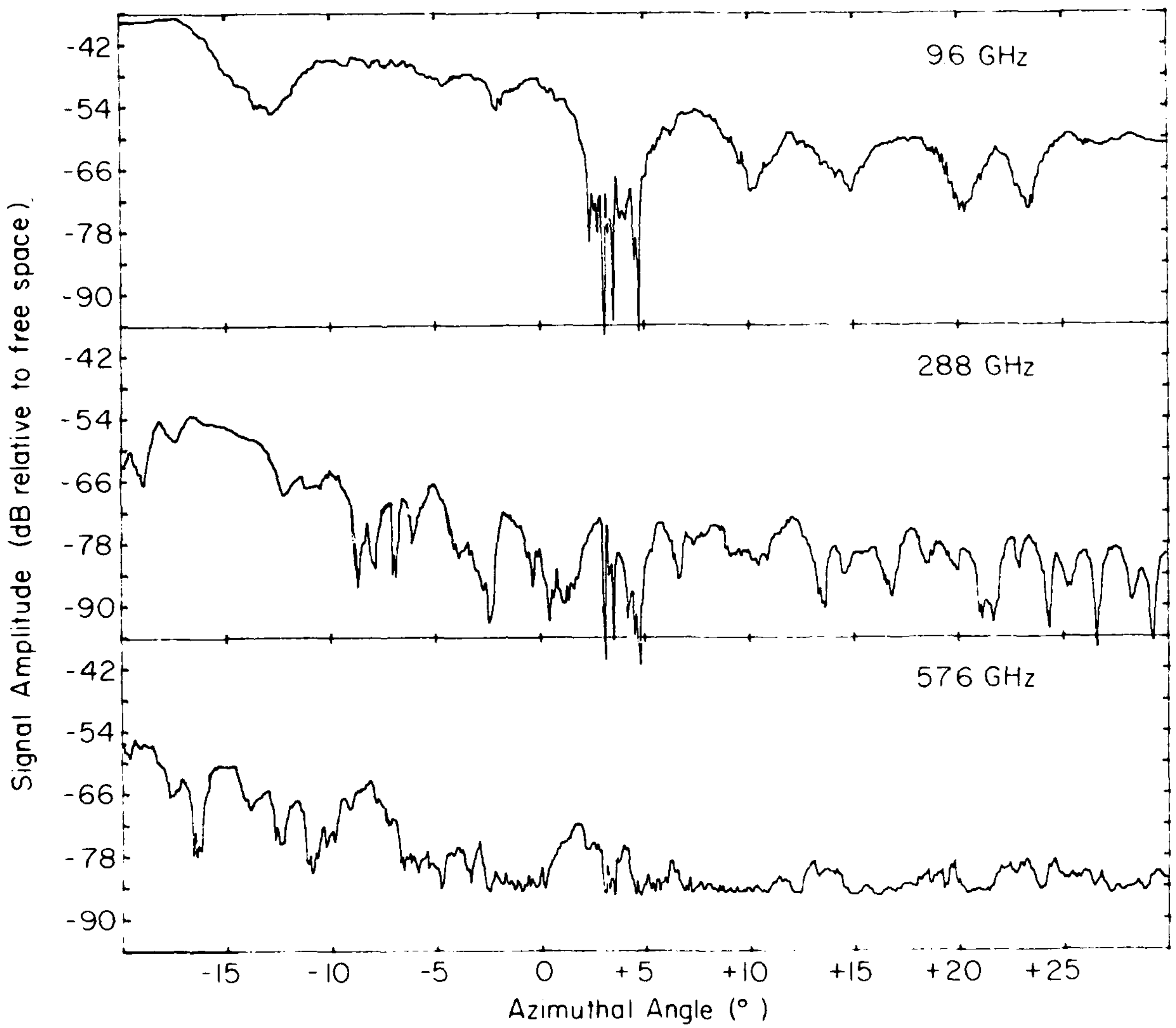

Fig. 4.28. Backscatter signals from a defoliated willow tree at 9.6, 28.8, and 57.6 GHz (VV polarization).

conditions. The relative backscatter signal amplitude from the willow trees with leaves and without leaves is given in Table 4.6, below.

TABLE 4.6

Relative backscatter signal level from willow trees.

Freq. GHz	with leaves	no leaves
9.6	-44 dB	-38 dB
28.8	-66 dB	-54 dB
57.6	-53 dB	-56 dB

G. Depolarization Effects

The majority of the received signal amplitude measurements were made with either horizontal-horizontal antenna polarization or vertical-vertical antenna polarization. However, at most locations, several scans were made to determine the effect of cross-polarization through vegetation. These measurements were made first with the antennas oriented in parallel polarization and again with the antennas oriented in cross polarization. To illustrate these effects, the data in Figures 4.29 and 4.30 show, respectively, a free-space azimuthal scan with horizontal-horizontal antenna polarization and a free-space azimuthal scan with vertical-horizontal antenna polarization. The scans in Figure 4.29 represent typical free-space calibration. The signal amplitude scales are adjusted to show 0 dB signal amplitudes at the center of the antenna major lobe. A similar scan is shown in Figure 4.30; however, due to the cross polarization antennas, the peak "near-zero" amplitudes are reduced 26, 23, and 16 dB, respectively, for frequencies 9.6, 28.8, and 57.6 GHz.

Had the elevation alignment been more precisely set and all antennas identically centered, the zero pointing null would become very sharp. The sharpness and location of the null also depends on the axial and focal alignment of the feed in the parabolic reflector. The fine adjustment of these parameters to obtain maximum cross polarization isolation was far more time consuming than it's value to the measurements. However, the cross polarization isolation values of 26, 23, and 16 dB, in order of ascending frequency, from Figure 4.30 at the near zero pointing angle represent the increased path loss with cross polarized antennas. These values are used as reference levels for the comparative parallel polarization to cross polarization measurements listed in Table 4.7 and plotted in Figure 4.31. This table contains results from eight sets of measurements through vegetation in addition to the

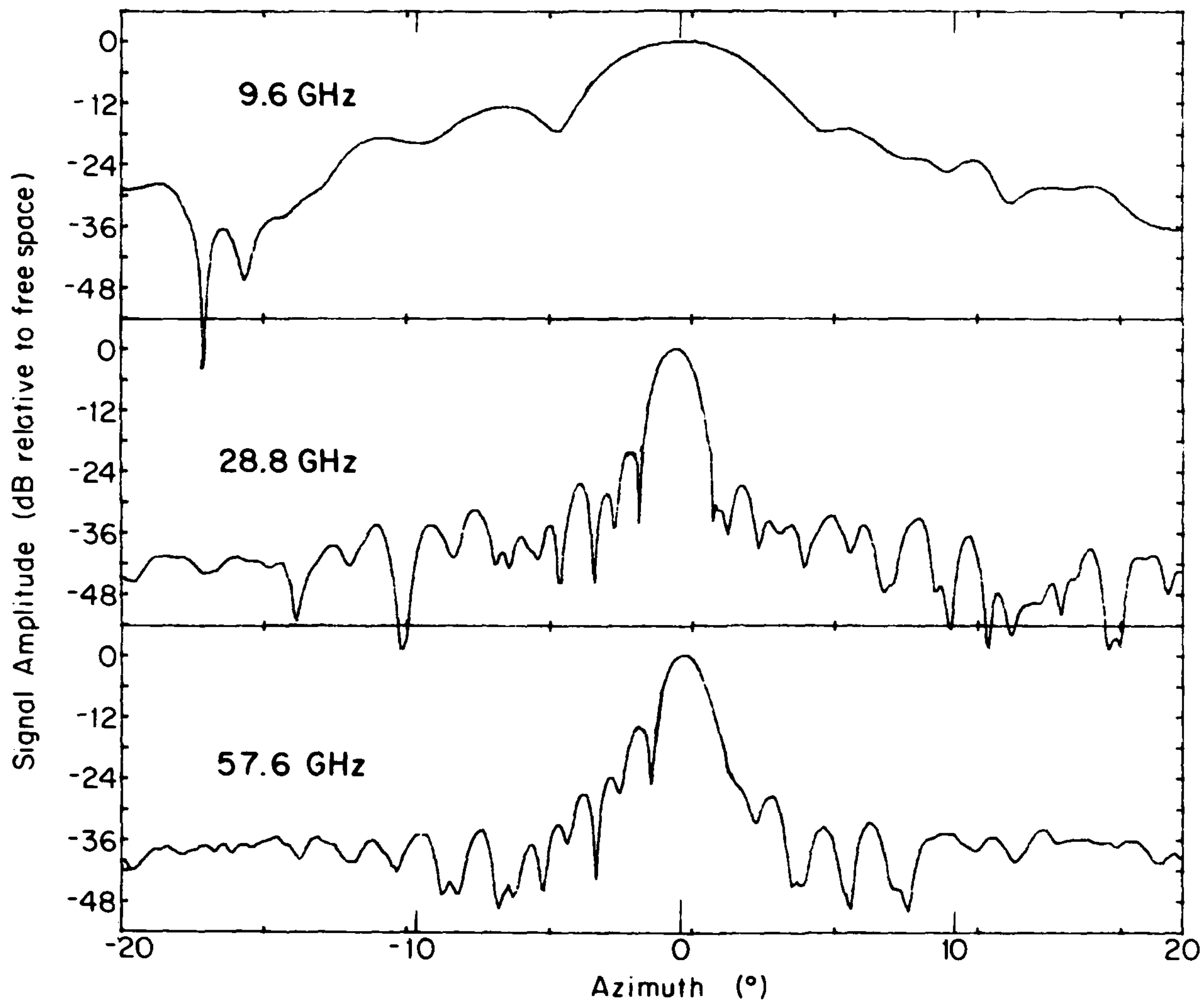

Fig. 4.29. Free-space calibration azimuthal scan (horizontal-horizontal) polarization, GM01/01, height = 1 meter, path length = 113 m).

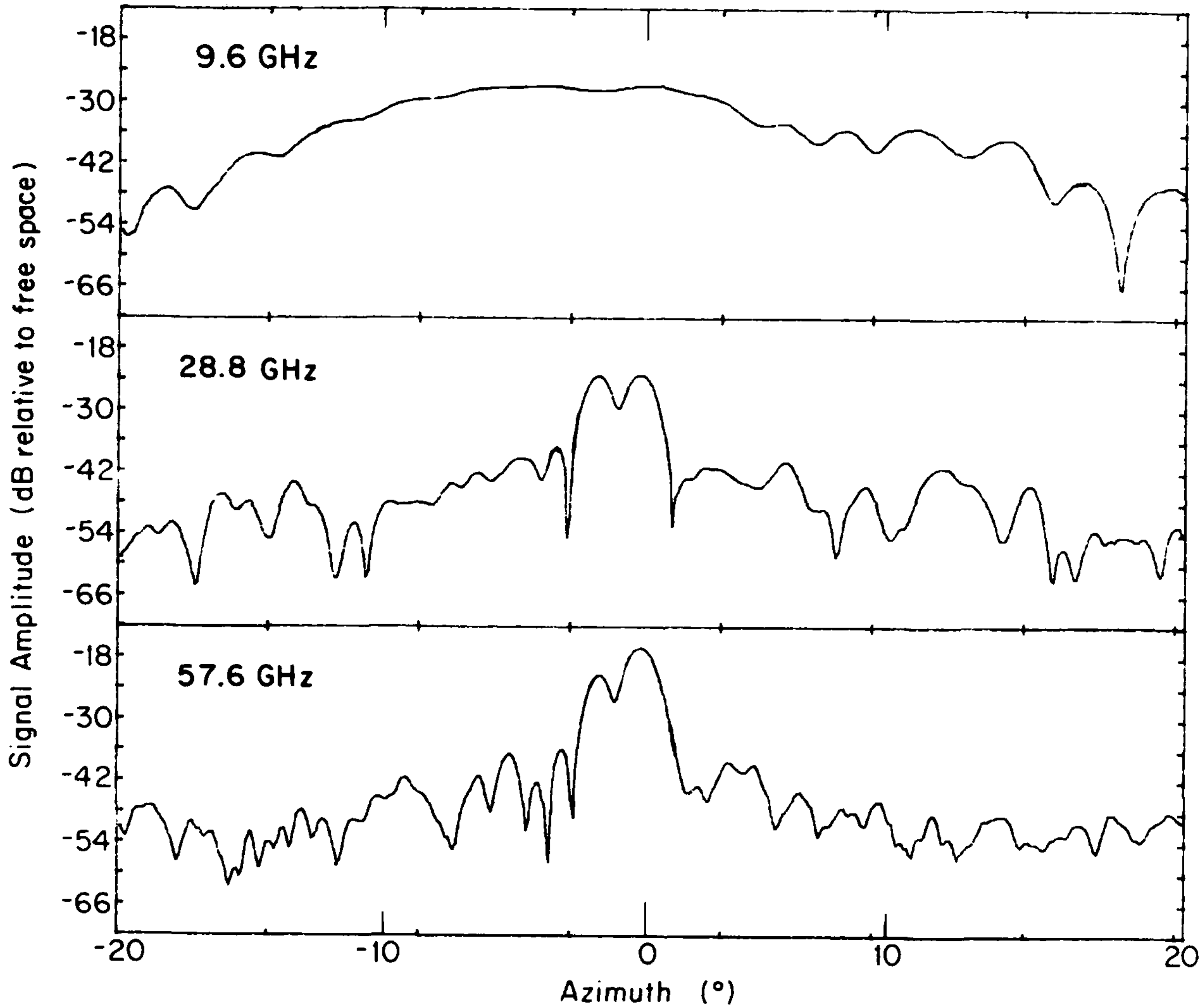

Fig. 4.30. Free-space calibration azimuthal scan (vertical-horizontal polarization, GM01/01, height = 1 meter, path length = 118 m).

TABLE 4.7

Antenna cross-polarization data.

Measurement Site		9.6 GHz VV or HH	9.6 GHz VH	9.6 GHz Difference	9.6 GHz Depolarization	28.8 GHz VV or HH	28.8 GHz VH	28.8 GHz Difference	28.8 GHz Depolarization	57.6 GHz VV or HH	57.6 GHz VH	57.6 GHz Difference	57.6 GHz Depolarization
		(dB)	(dB)	(dB)	(dB)	(dB)	(dB)	(dB)	(dB)	(dB)	(dB)	(dB)	(dB)
Calibration GM01/01 8-0-48	HH 1 Meter	0	-26	26	--	0	-23	23	--	0	-16	16	--
Willow Bd02/01 3-0-28	HH 2 Meter	-14	-38	24	2	-12	-43	31	- 8	-18	-44	26	-10
Willow Bd02/01 3-0-30	HH 6 Meter	-22	-38	16	10	-32	-46	12	11	-34	-48	14	2
Cottonwood MR02/01 7-0-28	VV 1 Meter	-18	-42	24	2	-23	-41	18	- 5	-22	-32	10	6
Cottonwood MR01/01 6-1-16	VV 1 Meter	-32	-50	18	8	-38	-53	15	8	-38	-46	8	8
Cottonwood MR01/01 6-1-18	VV 2 Meter	-35	-42	7	19	-47	-52	5	18	-42	-55	13	3
Conifer GM02/01 8-1-36	VV 1 Meter	-19	-38	19	7	-32	-42	10	13	-30	-49	19	- 3
Conifer Bd05/01 5-0-34	VV 1 Meter	-21	-27	6	20	-35	-44	9	14	-37	-48	11	5
Conifer Bd05/01 5-0-36	VV 1 Meter	-30	-36	6	20	-50	-59	9	14	-51	-57	6	10

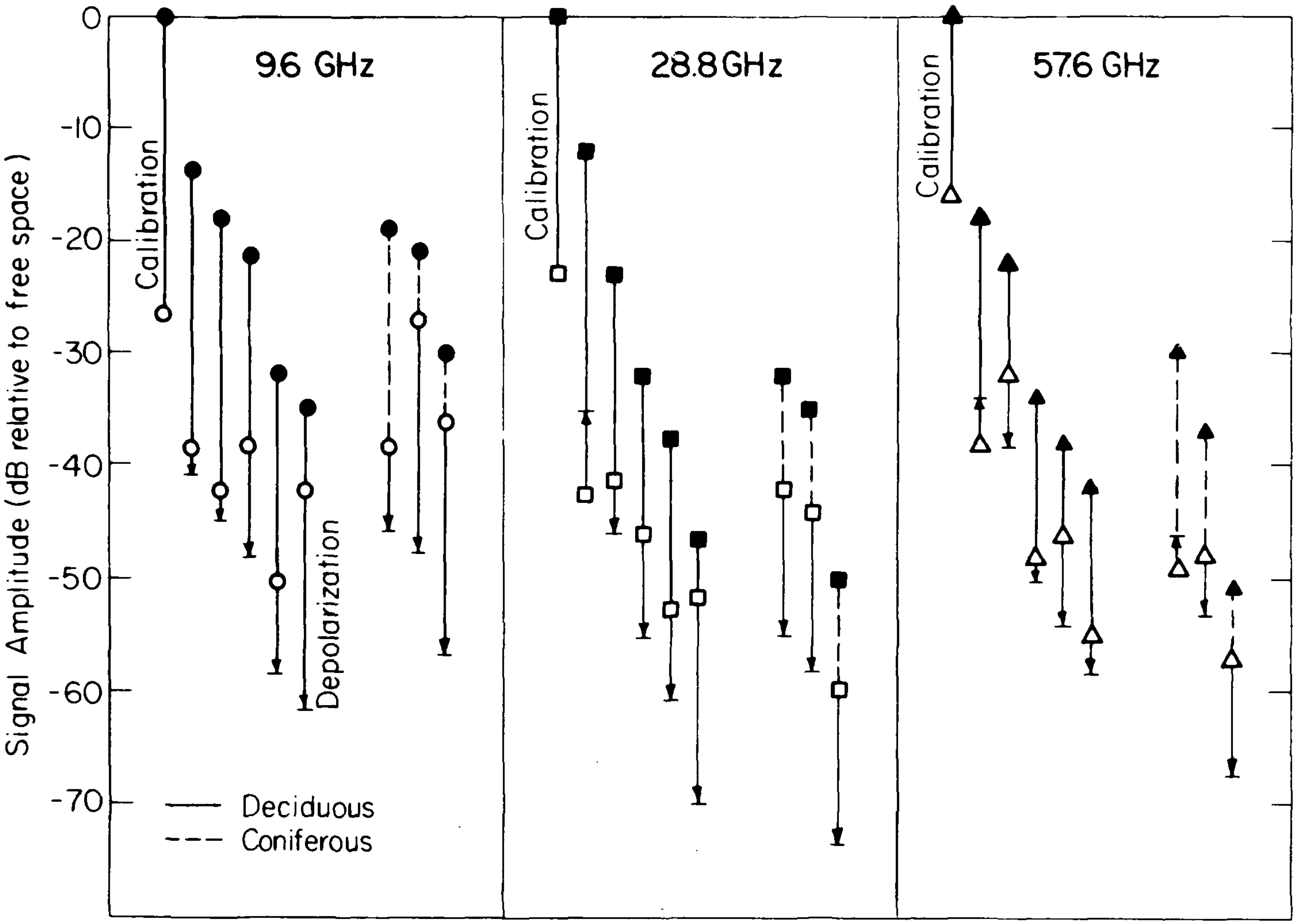

Fig. 4.31. Comparitive results of signal amplitude for parallel and cross polarization measurements. Closed symbols represent parallel polarization measurements and the open symbols represent cross polarization measurements.

calibration measurements shown in Figures 4.29 and 4.30. For each of the three frequencies, a parallel-polarization and cross-polarization value are listed as well as the difference values. Figure 4.31 displays the data from the table by frequency, type of tree (deciduous or conifer), and according to increasing vegetation loss. All bars within a frequency group are a length which represents the free-space cross-polarization isolation of the antennas. The points plotted on each bar are first the parallel-polarization loss, second the cross-polarization loss, and the extended length of the bar is the value of depolarization measured for that particular foliage path. There is a definite trend of increased depolarization with increased vegetation loss or foliage depth.

The problem of accurately accounting for depolarization effects is the same as mentioned in previous sections. In changing to cross polarization the antenna center positions are changed by as much as 10 cm. In Section IV.C, the sensitivity to terminal position is discussed, showing that a 10 cm displacement could, under certain conditions, produce up to a 10 dB shift in measured signal level for a given foliage path. Therefore, the depolarization measurements will establish order of magnitude values for a limited variety of foliage, terminal heights, and vegetation losses.

H. Off-Path Signal Enhancement

The purpose of this section is to provide facts for establishing a communications link when vegetation or other losses prevent a direct link. Even with natural terrain acting as a scatterer in a clear path within a common volume to both terminals, a suitable signal level can be acquired.

The TX04-RX02 path at Marshall Road was selected for this special test to assess off-path signal scattering for a 320-meter separation and a foliage coverage of approximately 30 meters of dense cottonwood trees. The right-hand side (positive azimuthal direction) of the transmitter-receiver path was clear of trees, and the left-hand side (negative azimuthal direction) was heavily wooded.

The map in Figure 4.32 shows the site orientation and the transmitter pointing angles from -10° to +25°. The two receiver center angles for the normal -20° to +20° receiver antenna scans are indicated at 0° and -15°. Curves showing the received signal for the eight transmitter pointing angles, and the two receiver center-pointing angles are plotted in Figures 4.33, 4.34, and 4.35, respectively, for 9.6, 28.8, and 57.6 GHz. These measurements were made with both the transmitter and receiver antennas at 1 m above ground.

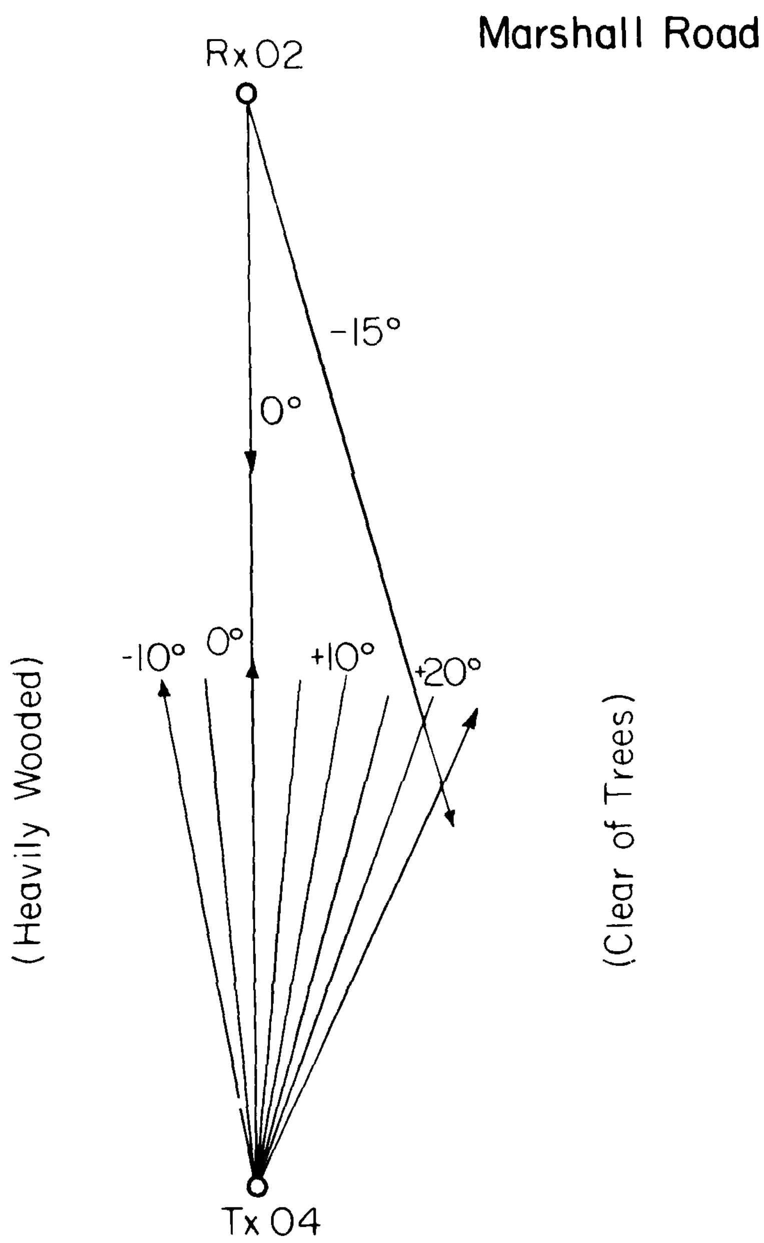

Fig. 4.32. Map of off-path measurements at Marshall Road.

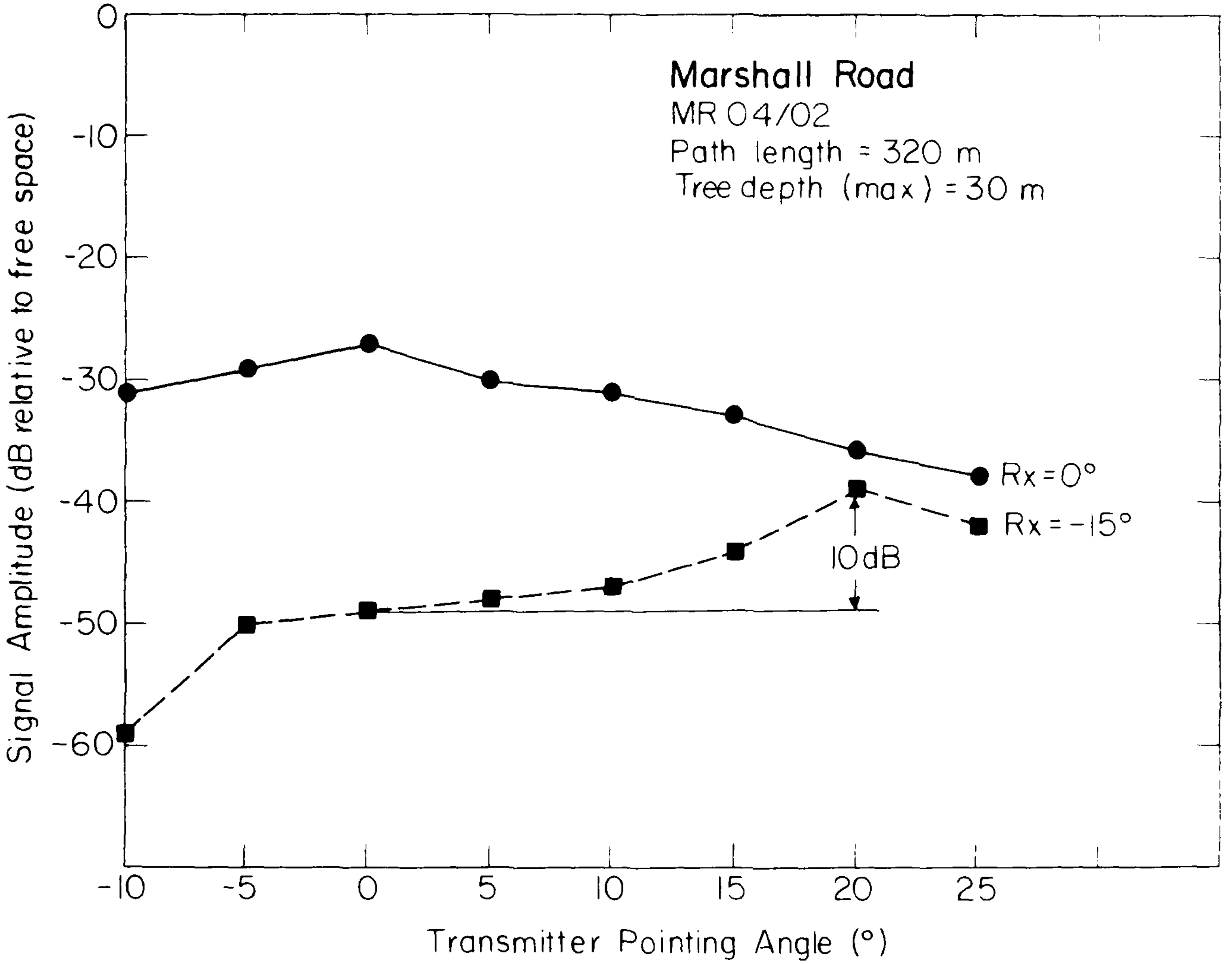

Fig. 4.33. Signal amplitude for off-path measurements using VV polarization at 9.6 GHz.

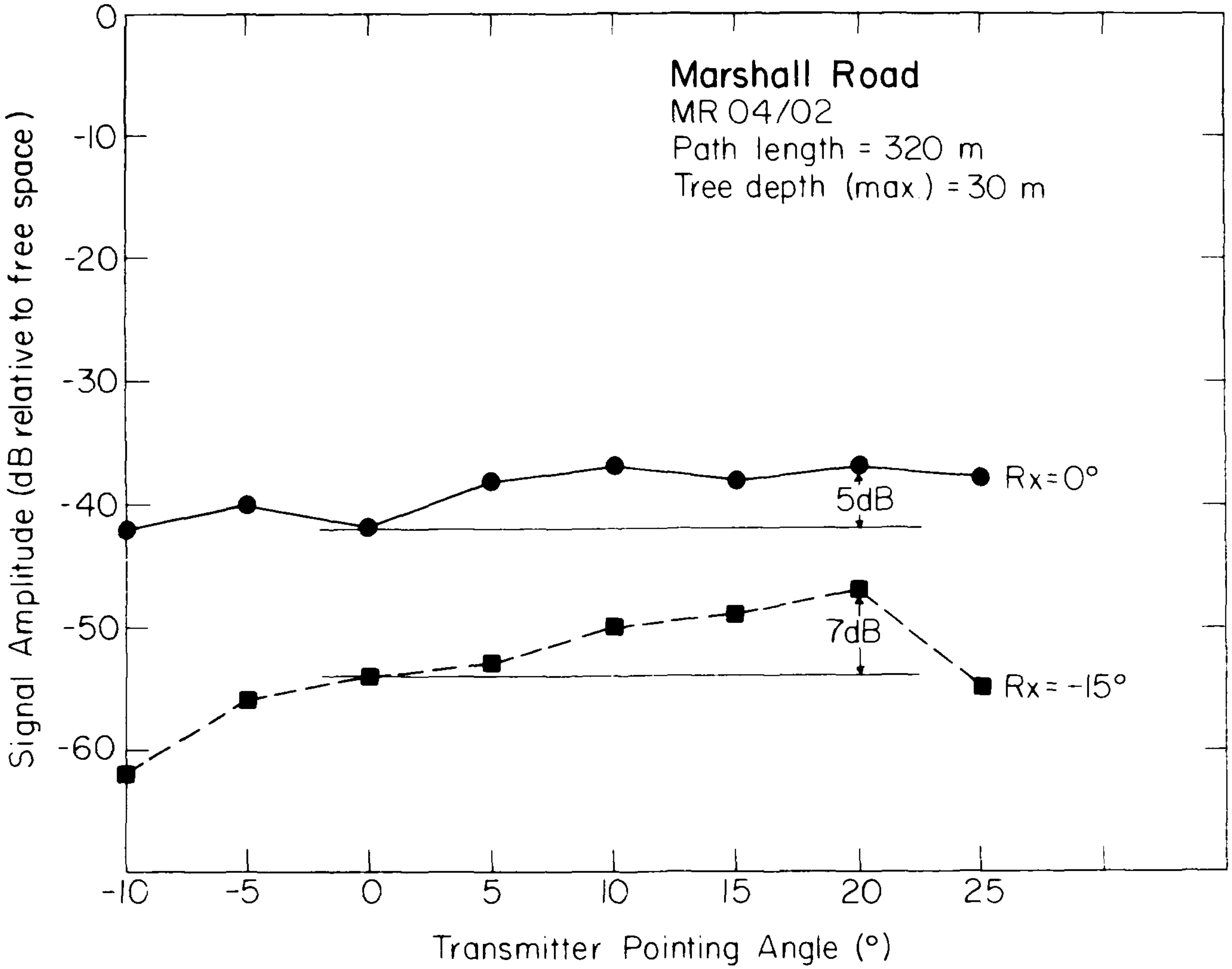

Fig. 4.34. Signal amplitude for off-path measurements using VV polarization at 28.8 GHz.

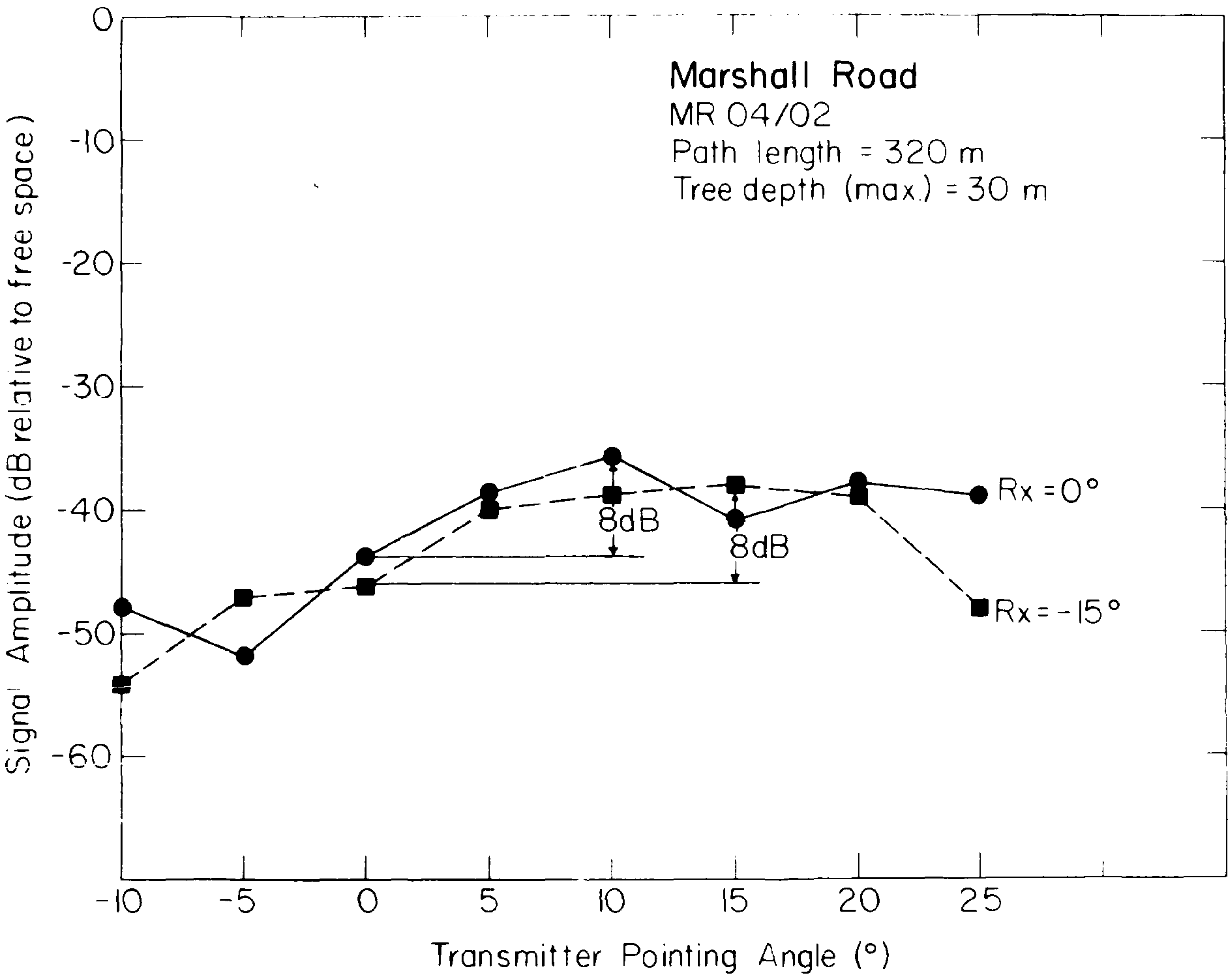

Fig. 4.35. Signal amplitude for off-path measurements using VV polarization at 57.6 GHz.

In this case, the common volume encompassed at -15° receiving pointing and +15 to 25 degrees transmitter pointing in gently rolling ground was covered by approximately 1/2 meter high grass and an occasional small bush.

In Figure 4.35 (for 57.6 GHz), the direct path vegetation loss exceeds the off-path scattered signal return. If the terminal positions had been chosen so that the vegetation depth was about 1/3 greater, the largest received signal would easily have been from the off-path scatterer. Additional advantage could be made of this situation by placing reflecting objects in the common volume to increase the signal received from outside the vegetation path.

I. Grass Measurements

One set of measurements was taken on the TX03c-TX02 path at Marshall Road to observe vegetation loss in grass. To produce a near or slightly below grazing angle path, the height of the transmitting antenna was lowered to 0.5 meter. The total path was 320 meters and grass coverage on path was estimated at 75 meters. The photographs in Figure 4.36 show the grass coverage. The receiver height was 1 meter and the results for the two parallel-polarization measurements are given in Table 4.8.

TABLE 4.8

Vegetation loss in grass.

	Frequency (GHz)		
Antenna Polarization	9.6	28.8	57.6
Vertical-Vertical	13.0 dB	21.0 dB	25.0 dB
Horizontal-Horizontal	6.0 dB	9.0 dB	16.0 dB

Visual blockage existed between terminals at the antenna heights chosen. An estimate, in sighting between terminals, is that the antenna centers were 0.7 to 0.9 meters below the visual grazing angle. The data presented in Table 4.8 show vegetation losses and polarization dependences for this condition.

J. Rain and Snow Effects

Only one rain shower occurred during the summer measurements, which was on August 25th starting about 2010 MDT, while measuring losses on the 92 meter willow path at a height of 4 meters. Instrumentation for rain rate was not set up on the path, so the actual rain rate is not known. The 57.6 GHz data were lost because of condensation in the receiver terminal waveguide and the signal did not recover until disassembled and cleared. At a rain rate of 150 mm/hr, which far exceeded the rain rate observed, the rain attenuation for a 92 meter could not be greater

a

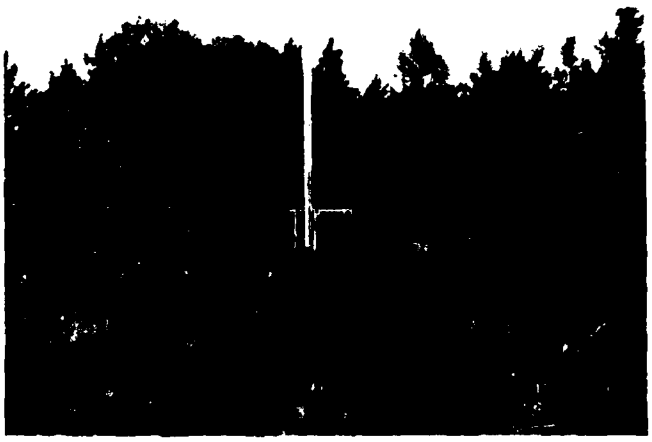

b

Fig. 4.36. These photographs show the grass and shrubs on the (TX03c-RX02) path at Marshall Road.

than 0.5 dB at 9.6 GHz, or 2 dB at 28.8 GHz. All dish feeds and horn apertures were covered with a thin plastic. Losses due to rain and condensation on the plastic is known not to exceed 0.75 dB at any of the three frequencies as determined by covering to capacity the plastic protectors with water from an atomizer, in addition to other free-space observations following a rain. The worse case signal drop due to rain and to water on the antenna is calculated to be 1.25 dB at 9.6 GHz and 2.75 dB at 28.8 GHz.

Figure 4.37 shows a plot of the received signal over the path before, during, and after the rain shower. The starting time of the rain is believed to be around 2010 hrs, and at 2015 the rain was observed to be the highest (estimated 40 to 50 mm/hr). However, at 2015, the increased loss was almost imperceptible with the signal scintillation caused by brisk-gusty winds. By 2100 hrs, 9.6 GHz showed a maximum signal drop of 8 dB and a much larger 23 dB at 28.8 GHz. It could be assumed that this delay in signal loss is the time taken for the rain water to sheet the sheltered leaves, trunks, and branches if these elements are the source of additional signal loss when wet. The 57.6 GHz channel fell greater than 20 dB within about ten minutes after the start of the rain. One would think that the condensation must have occurred by moist air being pulled in through porous openings and then collecting due to cooling on the guide interior. If true, the action may have taken a much greater interval than ten minutes but there is no way to verify this. The 9.6 and 28.8 GHz signals showed essentially full return to pre-rain level within a short time after the rain stopped. but an exact correlation was not made. The rain rate diminished slowly before stopping. and the signal level appeared to increase with the diminishing rain rate. After the signal levels had returned to pre-rain levels on the two lower frequency channels, it was observed that most leaves had several large water droplets still clinging to them. A comparison of moisture on the leaves during the rain was not done.

While taking data on the 181-meter dry conifer path in October a 3 to 5 inch snowfall occurred. The snow was quite wet and much of it stuck to the pine branches, however, very little change in path loss could be detected.

K. Lateral Wave Tree Top Diffraction Measurements

An attempt was made to measure a low-loss diffraction mode over the tree tops. The path chosen was 172 meters in length with 30 meters of dense cottonwoods standing at a reasonably uniform height. A measurement of signal amplitude was performed with the transmitter at 9 meters in height, near tree top height, and the receiver at 1 meter. The geometry requires the line-of-sight path to pass through dense foliage,

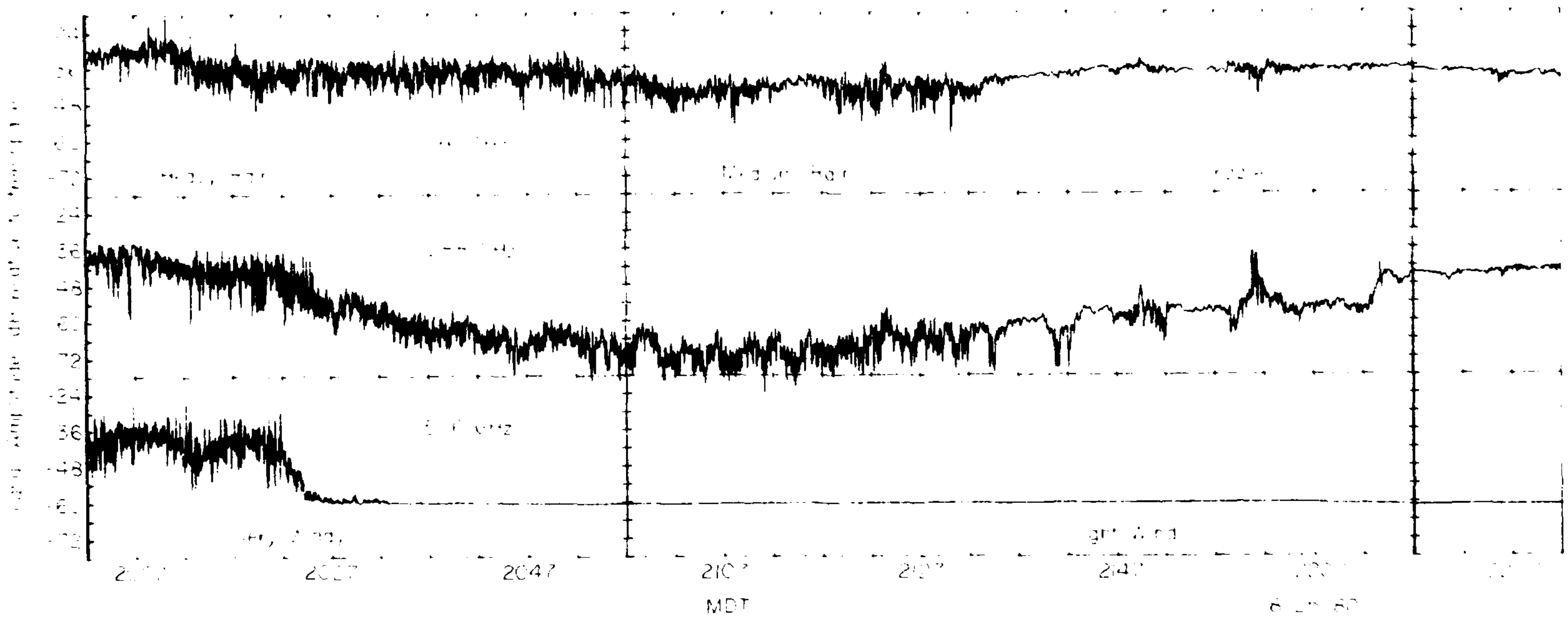

Fig. 4.37. Received signals on the path with willows at Boulder Laboratories (Bd02/01). The path is 92 meters long with 10 meters (depth) of willows.

with an equivalent vegetation loss of 30 to 40 dB, depending on frequency. The receiver was scanned in elevation and azimuth seeking a diffracting edge which would provide a lower loss. None could be identified within the constraints of the geometry available.

In this case, and probably in most forested areas, it is obvious the tree top roughness is large compared to the wavelength of the measuring frequencies making it unlikely that a layer boundary or a knife edge reradiation would be prevalant.

L. Measurements at VHF

To maintain voice communications between the receiving and transmitting terminals, a pair of 163.3 MHz FM transceivers was employed. This provided an opportunity to compare effects of vegetation at a frequency at which data already exists.

A calibration was performed by first recording the AGC voltage of one of the 163.3 MHz receivers as a function of dBm input from a rf signal generator. A pair of vertically positioned, 18 inch rod (1/8 inch diameter) antennas were mounted on a 30 inch square ground plane and attached to the carriage of each terminal. The AGC voltage of the VHF receiver was recorded for each height position at the time the micromillimeter wave system was calibrated. Received signals on a non-obstructed calibration path were very dependent on height over ground and position of large metal objects to the side and behind the terminals such as tripod stands and vehicle doors, so care was taken in duplicating each measurement set-up in this regard. Data for five vegetation paths at VHF are shown in Figure 4.38. It is not surprising that the vegetation losses are only a fraction of those at 9.6 GHz and above. The small, but dense, pine grove that produced the largest signal losses at EHF (see Figure 4.7) produced the smallest at VHF. Vegetation losses at VHF appeared to be more a function of tree heights and area covered between and to the sides of each path rather than the actual foliage density in line-of-sight. An example is the tall-large trunk cottonwood stand (MR01/01) where approximately 20 dB loss occurred, about the same as the EHF loss in the defoliated state. Results at 163.3 MHz demonstrate that much higher loss factors were encountered at frequencies where the size of scatterers is near the rf wavelength.

M. Light Propagation Over a Path with Vegetation

A high intensity spot light was mounted on the transmitter carriage and a seat with camera mount was installed on the receiver carriage. The location of the spot light and camera were set to duplicate the position of transmitting and receiving antennas. The camera used a zoom lens set at 205 mm to restrict the field of view. Only the 92-meter willow tree path (BL01/01) was explored with the light beam.

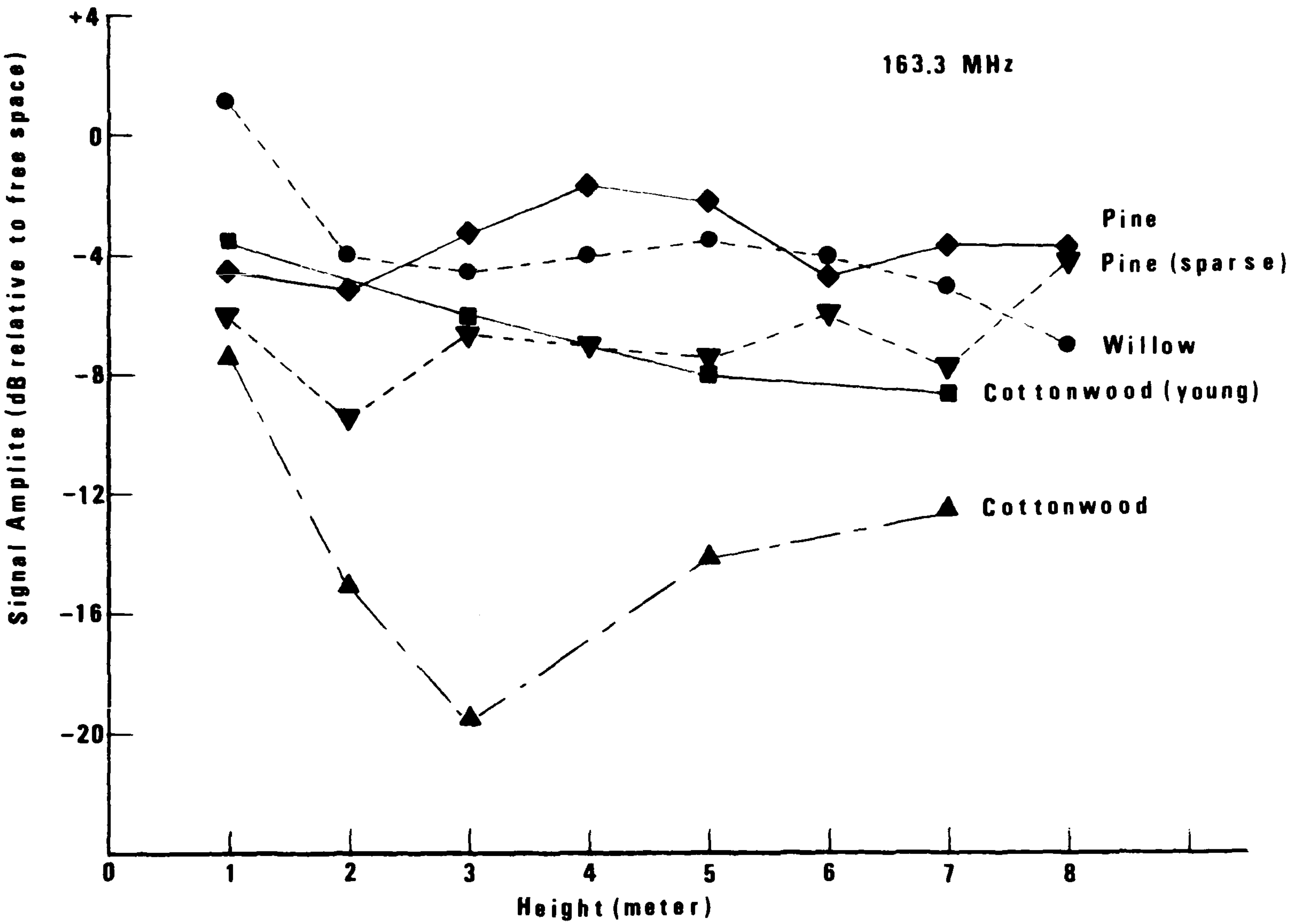

Fig. 4.38. Signal amplitude as a function of height measured at 163.3 MHz for several groves.

Figure 4.39 shows the resulting series of photographic prints. Print No. 0 is a view of the light source in the clear, 10 meters to the side of the receiving terminal, with both spot light and camera at a height of 1 meter. Print 1 is on path through the trunk portion of the willow at a 1 meter height. The halo effect is not understood, but is presumed to be a diffraction pattern from trunks and branches which produced illumination outside the main light beam. Print 2, taken at 2 meters, shows the outline of one of the main supporting trunks screening a segment of the center of the lighted regions. This also shows in Print 3 at 3 meters and even in Print 4, but careful inspection shows lighted portions in the center area of the 4 meter photo.

By use of an enlarger with the negatives and the prints shown, the relative light area and intensity in terms of decibels below that of the clear path photo was estimated. These values are tabulated in Table 4.9 along with the measured rf values.

TABLE 4.9

Vegetation loss on willow path.

Terminal Height Meters	Vegetation Loss (dB)			
	9.6 GHz	28.8 GHz	57.6 GHz	Light (Estimated)
1	-14	-19	-27	- 6
2	-12	-14	-18	-13
3	-18	-27	-30	-20
4	-24	-38	-39	-30
5	-24	-30	-34	-33
6	-21	-32	-34	-23
7	-30	-33	-36	-26
8	-20	-38	-38	-13

This photographic light presentation permits one to see the degree of coverage and density of the vegetation obstruction and determines if any similarities are apparent to propagation at millimeter wavelengths. Considering the data in Table 4.9, the rf losses were quite uniform from 3 to 8 meters, but it seems the light suffered less loss at 8 meters. The estimated light loss at 1 meter also is less than that experienced by the rf at the same height. Other height values are in reasonable agreement. It was of interest to see the variation in the light paths and to obtain some feel for the differences in the trunk and leaf regions.

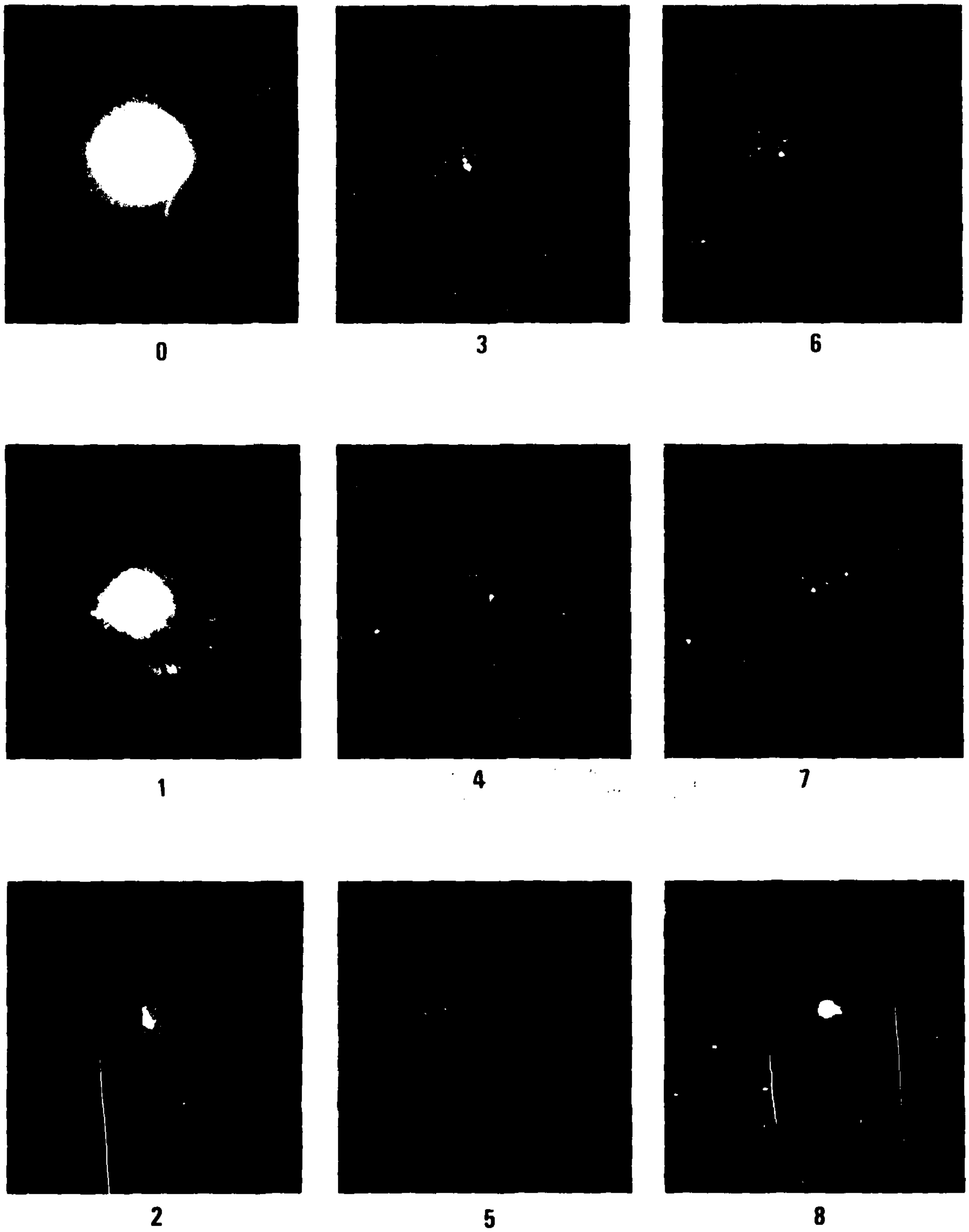

Fig. 4.39. Photographs of light through vegetation.

V. ANALYSIS OF ATTENUATION THROUGH LEAFLESS TREES

Signal amplitude measurements were repeated on three of the paths with deciduous tree coverage when the leaves had fallen to compare vegetation loss between trees with foliage and trees without foliage. These paths were Bd02/01 (willow) in Figure 3.1 and MR01/01 (cottonwood) and MR02/01 (cottonwood) in Figure 3.2. For each path, the transmitter and receiver were repositioned and realigned to faithfully duplicate (within centimeters) the original setting.

A. Comparative Results (Leaves vs. No Leaves)

The data in Figures 5.1 through 5.6 are from measurements at the three deciduous locations. The received signal amplitude at 9.6, 28.8, and 57.6 GHz are shown when measured with the trees in leaf and when the leaves had fallen. The data in Figures 5.1, 5.3, and 5.5 were measured with vertical-vertical polarization, and the data in 5.2, 5.4, and 5.6 were measured with horizontal-horizontal polarization. The data points connected with broken lines represent signal amplitude levels measured without leaves and solid lines represent signal amplitude levels measured with leaves.

A general observation is that, for every set of measurements at all frequencies, the vegetation loss with foliage was greater than that without foliage. These differences range from approximately 10 dB to 40 dB, with the smaller differences at the lower heights, the regions of least foliage density. A second observation is that the slope of the plot of signal amplitude vs. height is not as steep for the defoliated conditions as in the foliage condition. This condition is particularly evident in Figures 5.3 and 5.4.

A comparison of results relative to antenna polarizations show insignificant differences as a function of polarization. These results are similar to polarizations effects observed with foliage.

In the 3 to 8 meter height range, there is an indication of reversal of order of signal loss as a function of frequency between foliage and no-foliage data at 28.8 GHz and 57.6 GHz. In Figures 5.2, 5.4, and 5.6, the average loss of signal with foliage at 57.6 GHz is slightly greater than the loss of signal at 28.3 GHz. Without foliage, however, average signal loss was slightly greater at 28.8 GHz than at 57.6 GHz.

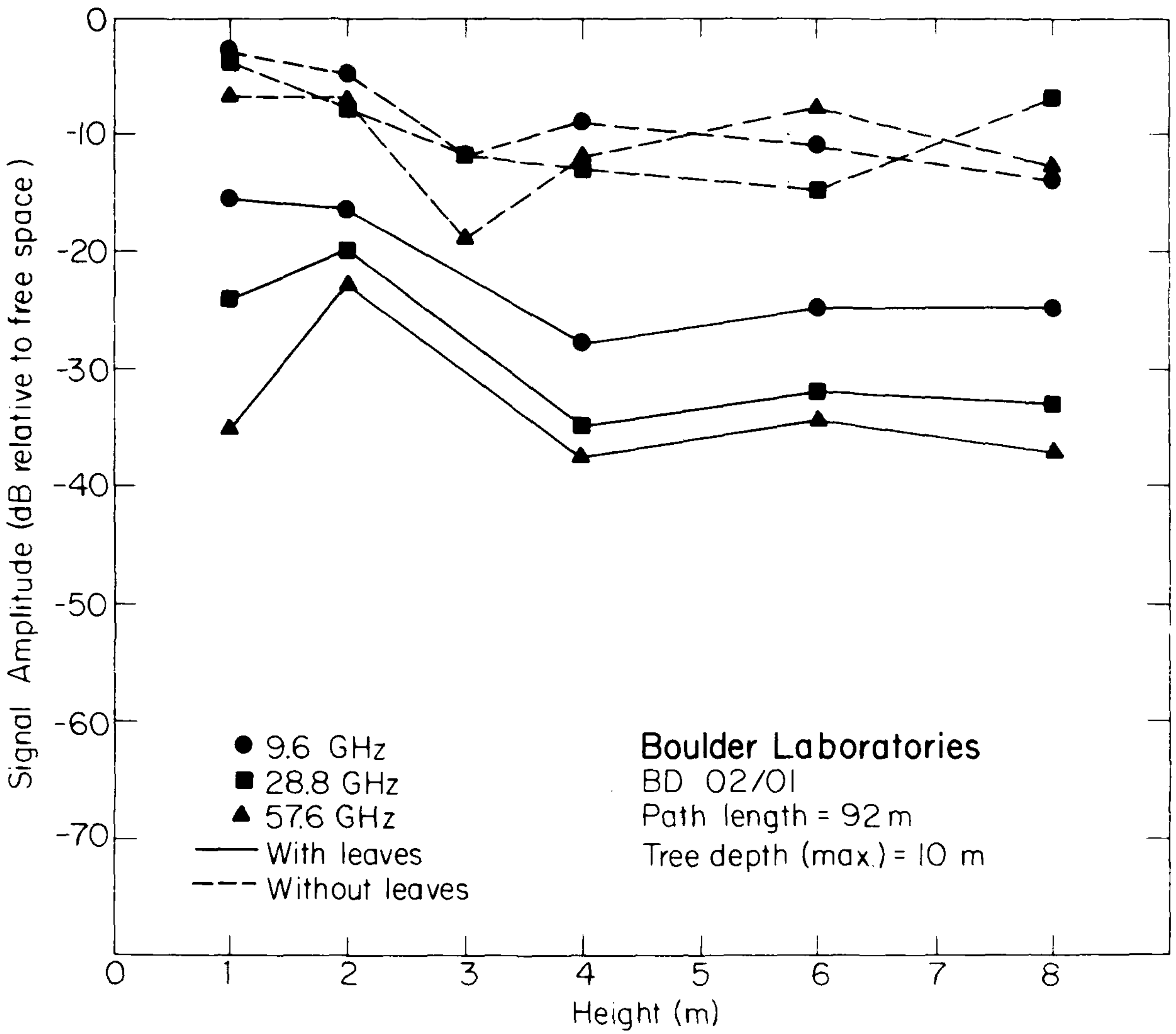

Fig. 5.1. Signal amplitude as a function of height for a group of willow trees, with and without foliage (VV polarization).

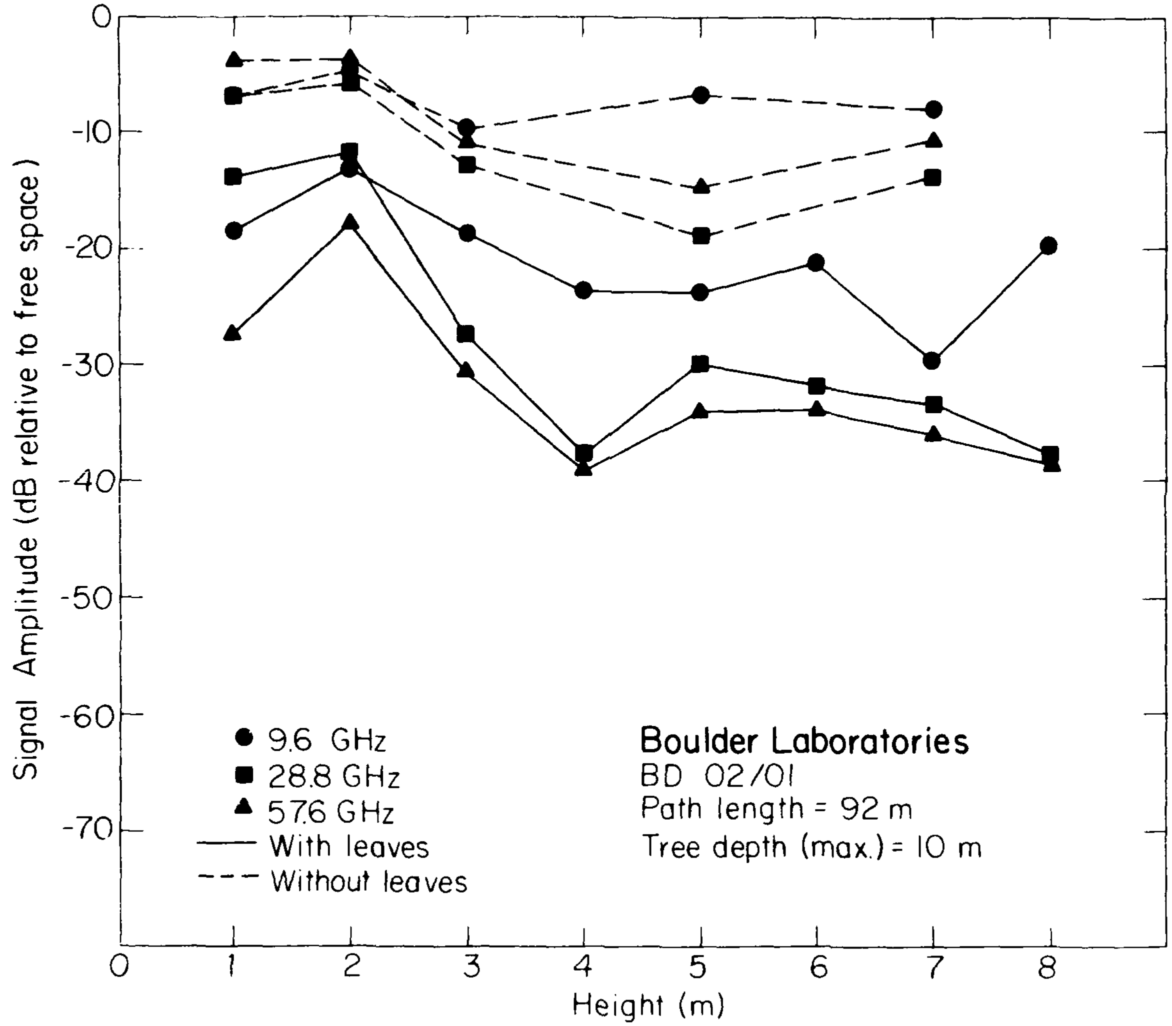

Fig. 5.2. Signal amplitude as a function of height for a group of willow trees, with and without foliage (HH polarization).

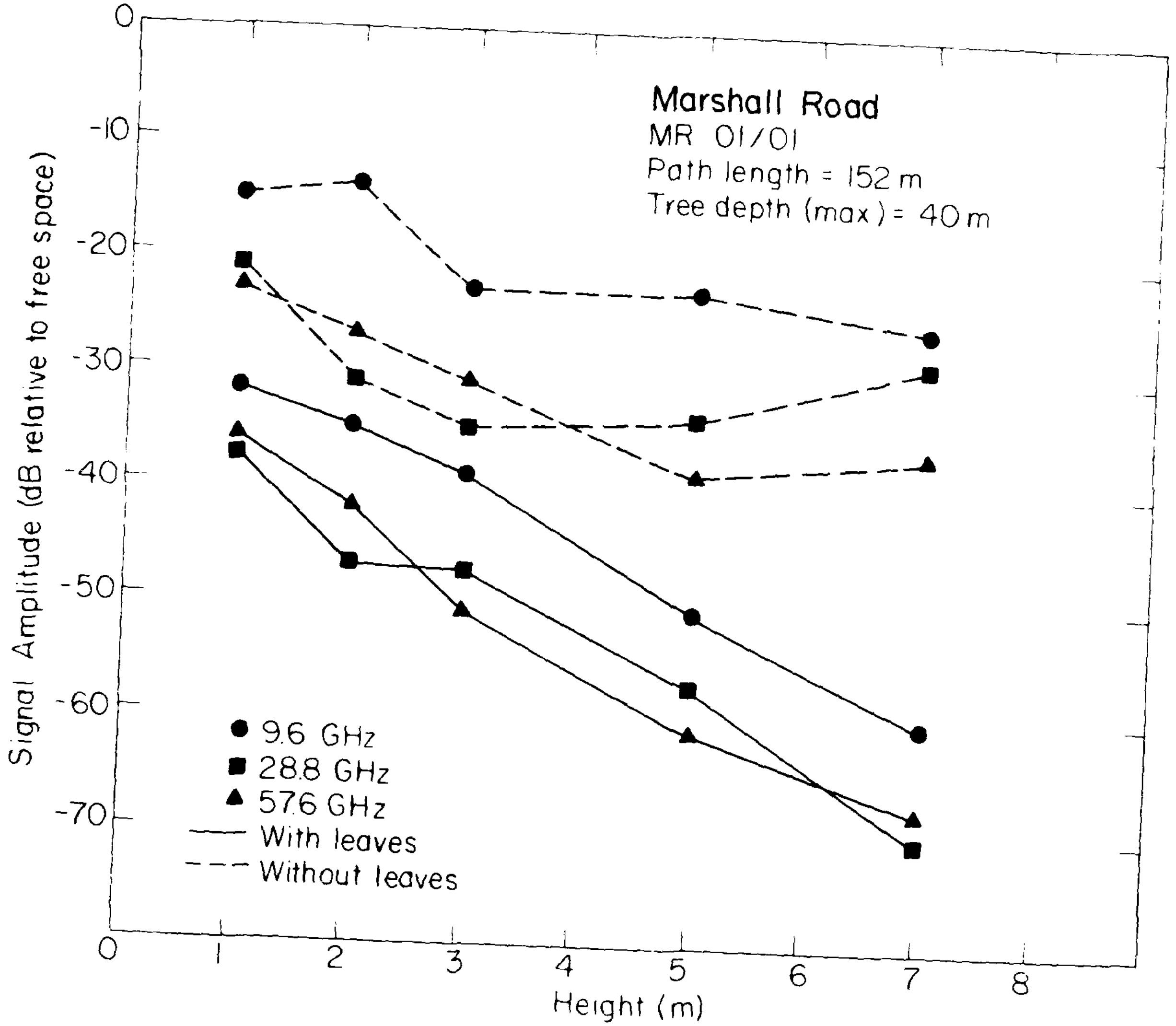

Fig. 5.3. Signal amplitude as a function of height for cottonwood trees, with and without foliage (VV polarization).

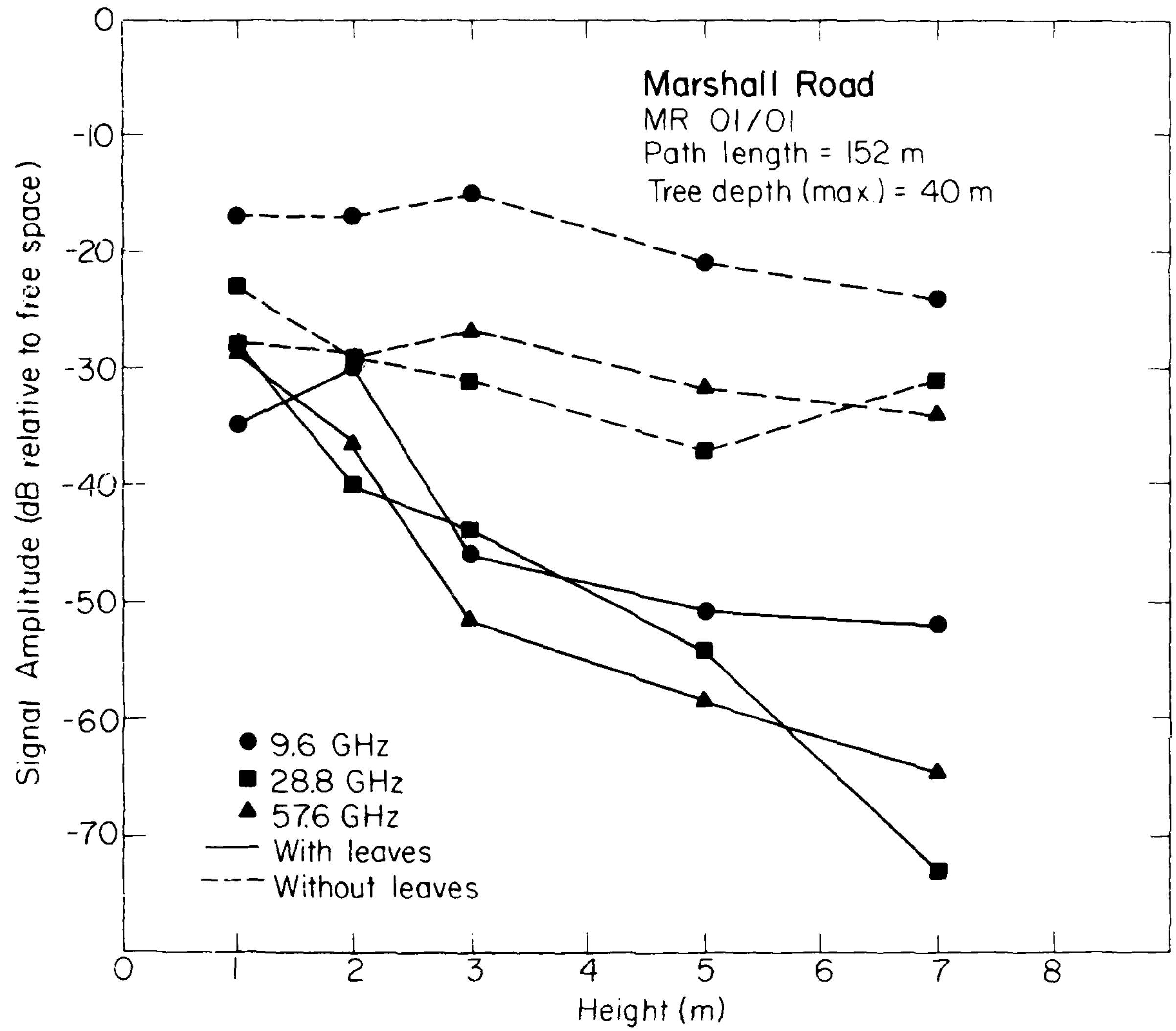

Fig. 5.4. Signal amplitude as a function of height for cottonwood trees, with and without foliage (HH polarization).

AD-A105 672 NATIONAL TELECOMMUNICATIONS/INFORMATION ADMINISTRATIO--ETC F/G 20/14
SHF-EHF PROPAGATION THROUGH VEGETATION ON COLORADO EAST SLOPE.(U)
JUN 81 E J VIOLETTE, R H ESPELAND
UNCLASSIFIED CECOM-81-CS020-F NL

2 OF 2
AD
A105672

END
DATE
FILMED
11-81
DTIC

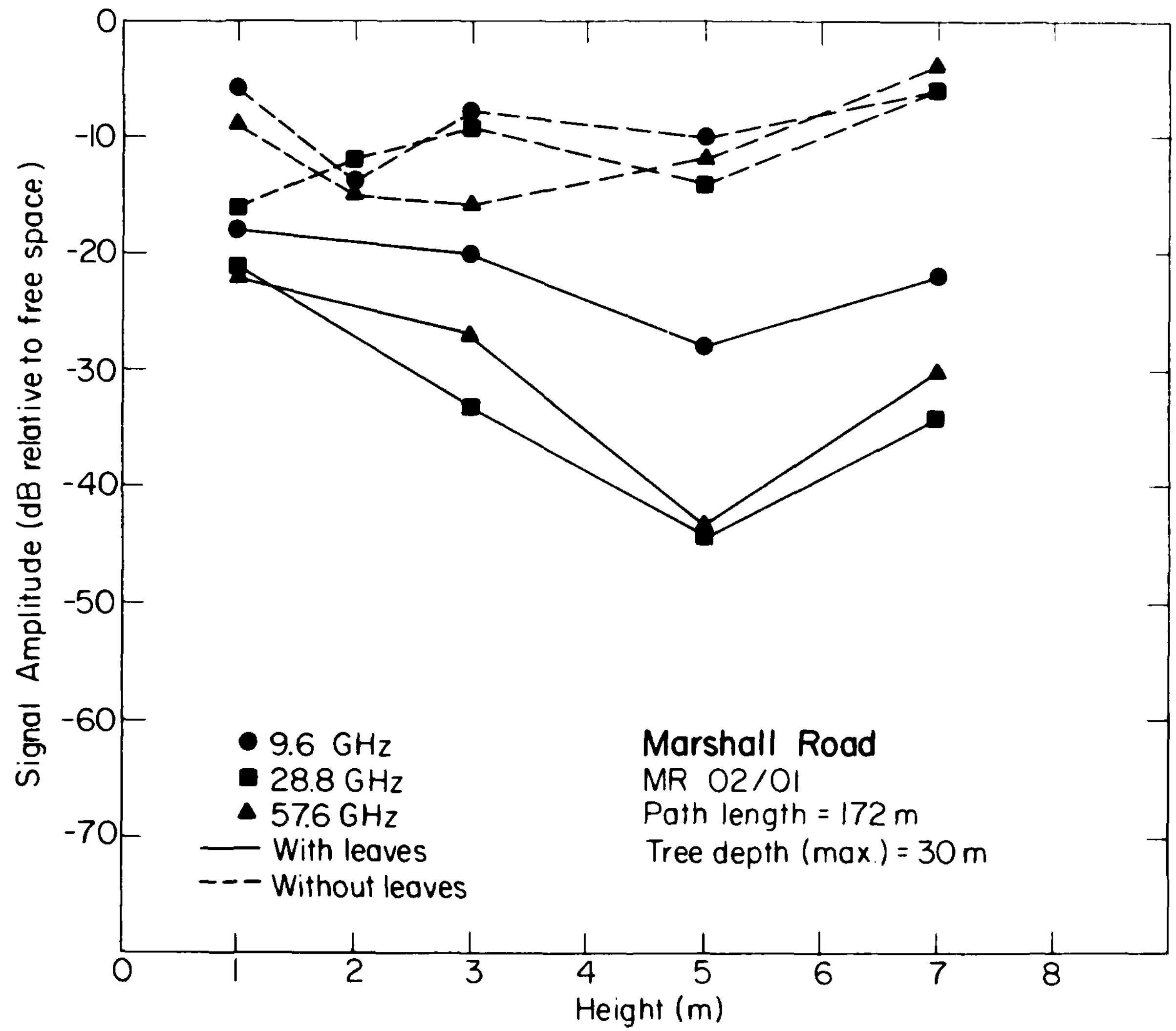

Fig. 5.5. Signal amplitude as a function of height for a cottonwood tree grove, with and without foliage (VV polarization).

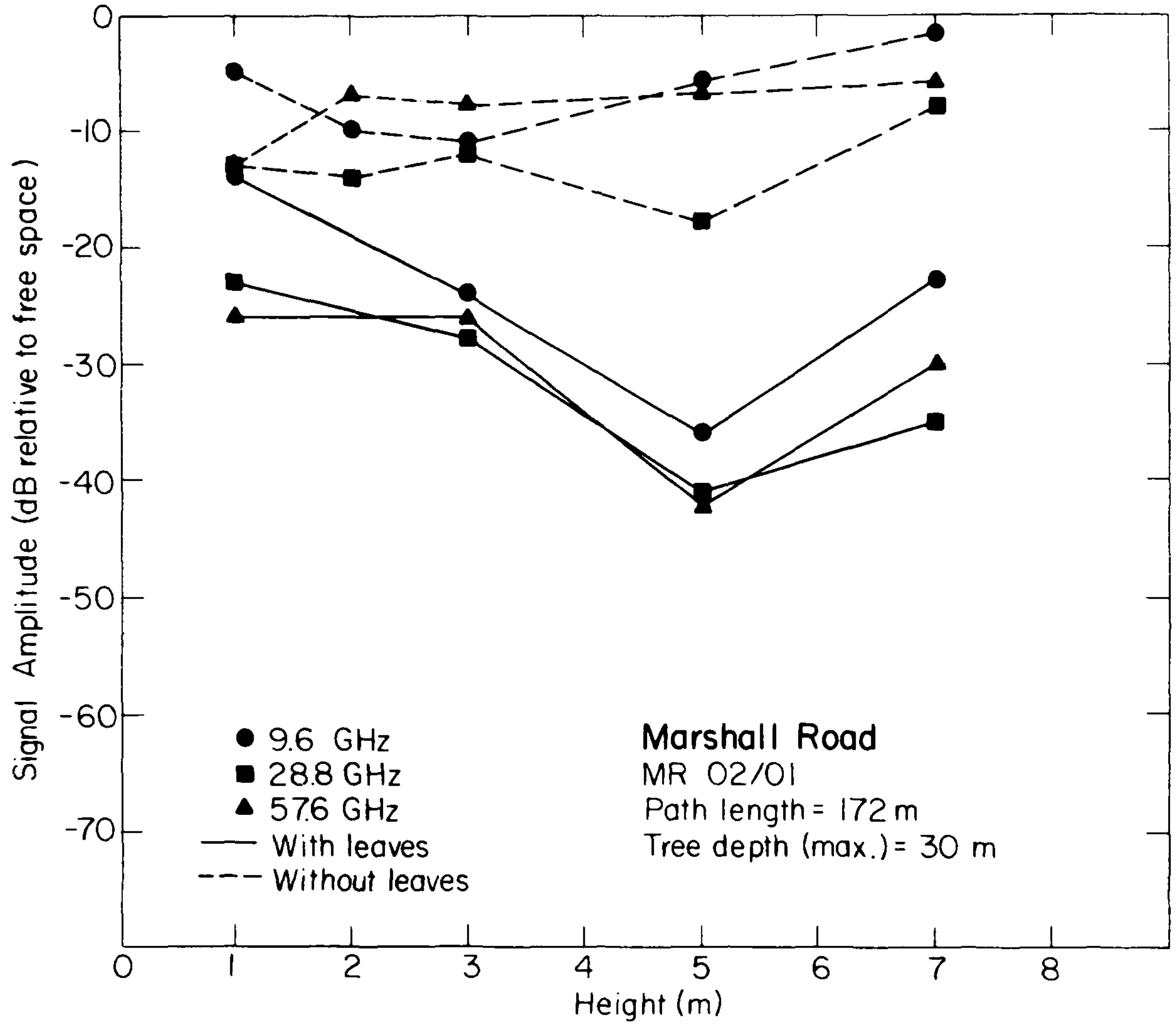

Fig. 5.6. Signal amplitude as a function of height for a cottonwood tree grove, with and without foliage (HH polarization).

The question of a possible resonant effect is of interest to modelling efforts, and for this reason the above data is significant. Plots of the vegetation loss for summer and winter measurements at three depths of vegetation in Figure 5.7 show the frequency dependence in these data between the trees with leaves and the same trees without leaves. Figure 5.7 is generated by using average values of both polarizations and height measurements limited to the height region of near maximum loss. If one assumes a resonant effect due to the multitude of twigs, which range in diameter from 0.2 to 0.8 cm, the sketch on the right side of Figure 5.7 shows a possible resonant bandwidth. However in this conjecture it is not possible to know if the resonant effect takes place in the region around 28.8 or around 57.6 GHz. With leaves, the frequency reversal trend is still apparent, but not as pronounced, perhaps because of partial shielding of the branches by leaves. The readers should note this trend and it will be kept in mind in conducting further measurements and in follow-up forward scattering analysis. Defoliated measurements of signal amplitude level changes relative to transmitter terminal displacement are shown in Figure 4.19 in Section IV C.

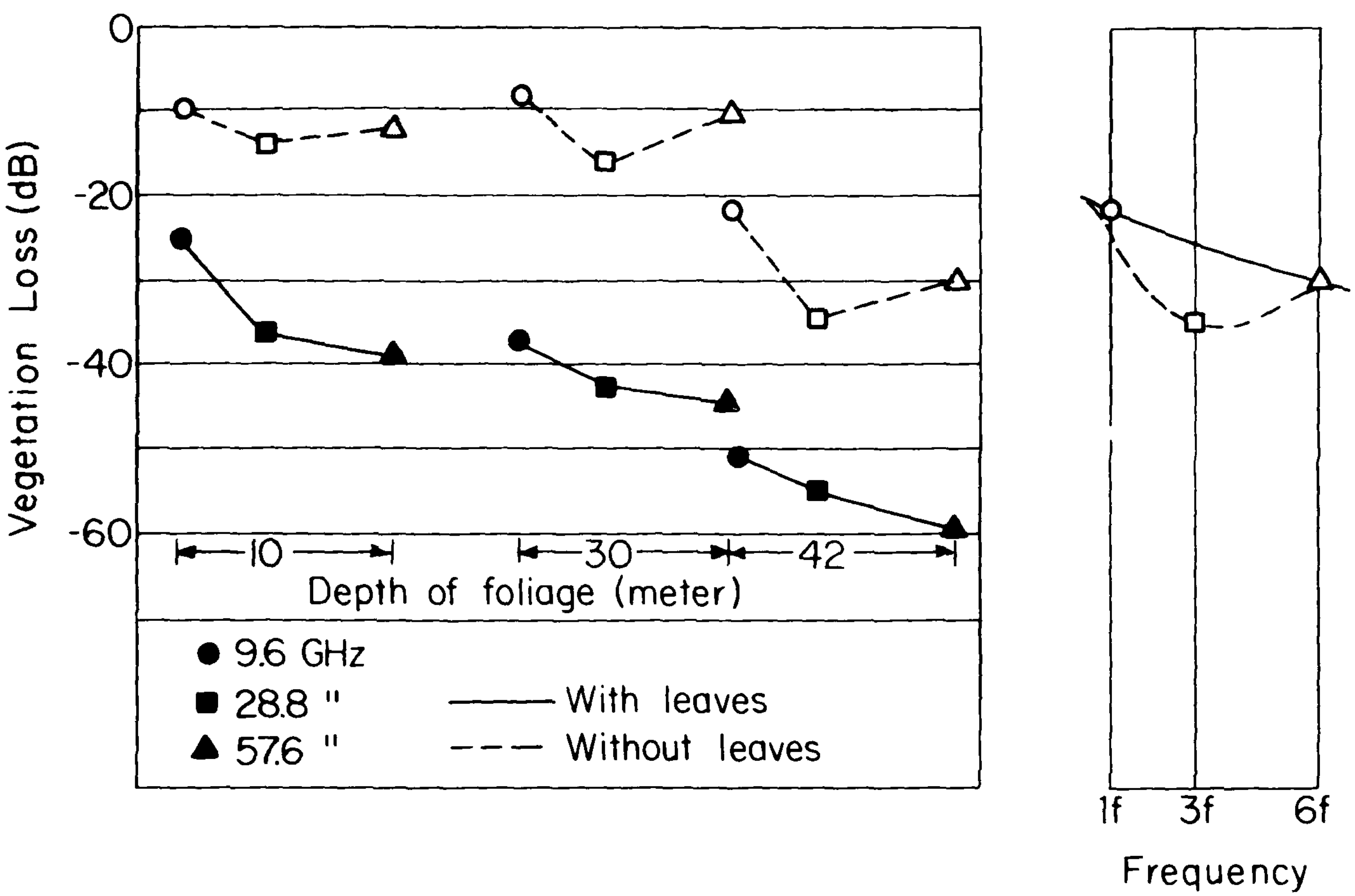

Fig. 5.7. Comparison of vegetation loss for deciduous trees with and without foliage. The depth of foliage scale in the figure means that the three values within the depth limit bars, were measured at that depth.

VI. COMPARISON OF ANTENNA BEAMWIDTH EFFECTS

This experiment was originally designed to use widebeam antennas (10°) at the transmitter and narrowbeam antennas (4.8° at 9.6 GHz and 1.2° at 28.8 and 57.6 GHz) at the receiver. This configuration offered non-critical pointing at the transmitter (fixed in azimuthal and elevation positions) and greater resolution at the receiver (scanned azimuthal and elevation positions). This mode of operation left unanswered the question of effect of antenna beamwidth in the presence of dense vegetation. A second operating procedure placed the receiver in or near the vegetation and placed the transmitter in a cleared area. Two special tests were conducted to evaluate the use of a narrowbeam antenna in the presence of vegetation. In the first, the transmitter and receiver remained in their original locations (transmitter in the trees and receiver in the clearing) and the 57.6 GHz 10° transmitting antenna was replaced by a 1.3° antenna. In the second test, the antennas were unchanged and the locations of transmitter and receiver were interchanged, which placed the narrow-beam receiving antennas in the vegetated area. Measurements from both of these tests, with the trees in this defoliated state, are presented and compared below.

A. Narrow-beam Transmitter and Receiver Antennas

The second test, conducted at the 57.6 GHz frequency only, included measurements at 1 meter for both the MR01/01 and MR02/01 sites. Measurements were made using the 1.2° beamwidth antenna at the receiver and, alternately, 10° and 1.3° antennas at the transmitter, with the transmitter near the vegetation and the receiver in a clear area. The results show a 2 dB stronger signal with the narrowbeam antenna compared to the wide-beam antenna at the MR01/01 site and a 3 dB stronger signal at the MR02/01 site for the same comparison. The signal amplitude plots in Figure 6.1 and 6.2 show the azimuthal patterns using the 10° and 1.3° transmitting antennas.

In addition to the small increase in signal amplitude, the narrow transmitting beam also reduced significantly the off-angle signal levels. There may be a reduction in scattered signals that find a path to the receiver at zero pointing, which could account for the amplitude difference. Also, a somewhat better coherent bandwidth should be available due to reduced time delay spread. These results were as anticipated in signal amplitude characteristics, but channel performance relative to beamwidth through a scattering medium was not determined.

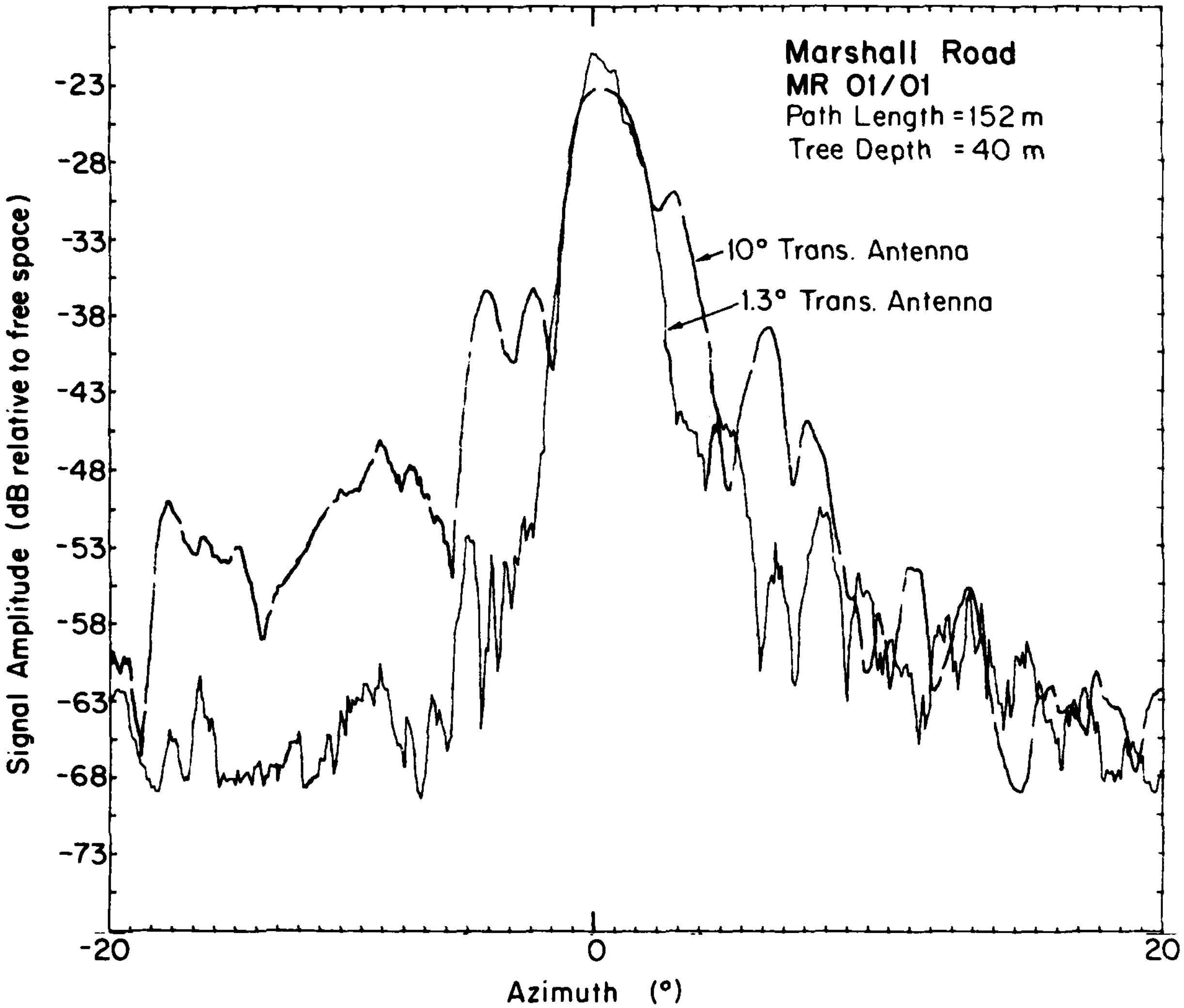

Fig. 6.1. Signal amplitude recorded from received azimuthal scans using a widebeam (10°) transmitting antenna and a narrowbeam (1.3°) transmitting antenna. The recording site was MR01/01 with VV polarization.

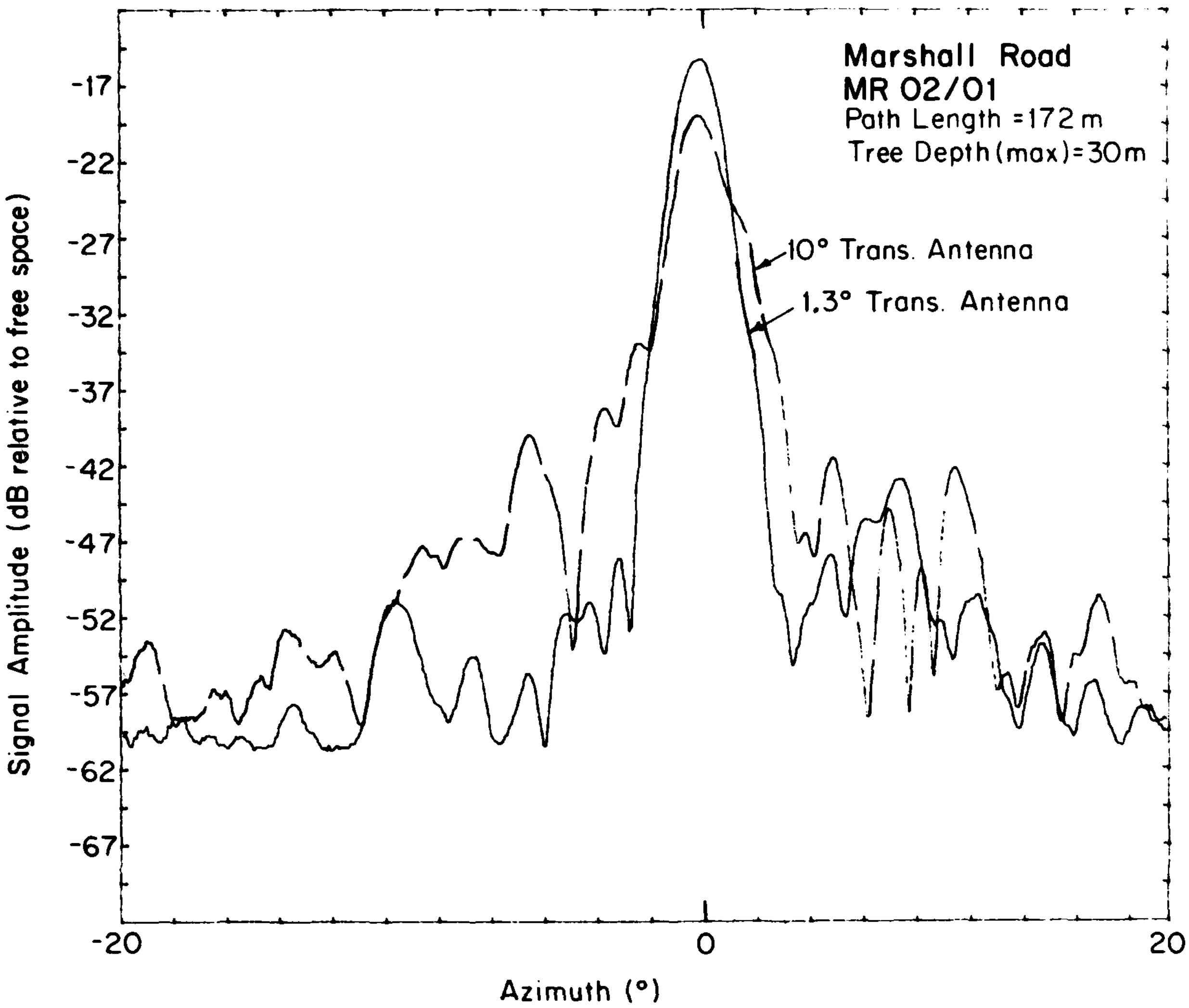

Fig. 6.2. Signal amplitude recorded from receiver azimuthal scans using a widebeam (10°) transmitting antenna and a narrowbeam (1.3°) transmitting antenna. The recording site was MR02/01 with VV polarization.

B. Reversal of Transmitter and Receiver Locations

At the Marshall Road site (MR02/01), a set of signal amplitudes was recorded for the no foliage measurement. The locations of the transmitter and receiver were then reversed and the transmitter and receiver were carefully aligned to accurately duplicate the original measurements. The results of this test are shown in Table 6.1.

TABLE 6.1

Signal amplitudes at MR02/01 for first set and reversed transmitter and receiver locations.

Height	Location	9.6 GHz		28.8 GHz		57.6 GHz	
2 m	First Set	-14 dB		-12 dB		-15 dB	
	Reverse	- 9 dB		-12 dB		-11 dB	
	ΔdB		+5		0		+4
3 m	First Set	- 9 dB		- 9 dB		-16 dB	
	Reverse	-10 dB		-13 dB		- 8 dB	
	ΔdB		-2		-4		+8
5 m	First Set	-10 dB		-14 dB		-12 dB	
	Reverse	-14 dB		-12 dB		-12 dB	
	ΔdB		-4		+2		0

The values in Table 6.1 are normalized for antenna gain differences and are relative to a free-space calibration.

The results from the three frequencies measured at three heights indicates a variation in the data showing no clear trend.

VII. CONCLUSIONS

The results presented are but a sample of vegetation types and climates necessary to make a comprehensive model of SHF-EHF propagation through foliage. These measurements provide order of magnitude estimates which must be used with certain cautions. For instance, the trees of the east slope of Colorado are obviously less dense in leaf or needle cover than in rainer-warmer climates. Humidity conditions, which relates to moisture content of the foliage and elevation also effect foliage size and density and likewise signal propagation through them. Overall the east slope of the Rocky Mountains and the southwest region of the U.S. are likely to show lower absorption losses per meter depth than most regions in the U.S. In the near future additional measurements may follow in contrasting climatological regions to obtain a better data base on these questions and for comparison to other parts of the world.

An important factor identified by these measurements is that terminal position changes of the order of a few rf wavelengths produced large variations in SHF-EHF propagation parameters. To describe this variable, more data is required to construct a probability density function of propagation properties relative to position change.

VIII. REFERENCES

[1] E.P.W. Anttema and F.T. Ulaby, "Vegetation Modeled as a Water Cloud," Radio Science, Vol. 13, No. 2, pp 357-364 (1978).

[2] G.S. Brown and W.J. Curry, "An Analytical Study of Wave Propagation Through Foliage," RADC-TR-79-359, Rome Air Development Center AFSC, Griffis Air Force Base, NY 13441 (1980).

[3] C.R. Burrows, "Ultra-Short-Wave Propagation in the Jungle," IEEE Transactions on Antenna and Propagation, Vol. AP-14, No. 3, pp. 386-388 (1966).

[4] T.F. Bush and F.T. Ulaby, "Radar Return from a Continuous Vegetation Canopy," IEEE Transactions on Antenna and Propagation, Vol. AP-24, No. 3, pp. 269-276 (1976).

[5] A.K. Fung, "Scattering from a Vegetation Layering," IEEE Transactions on Geoscience Electronics, Vol. GS-17, No. 1, pp. 1-6 (1979).

[6] C.M. Horwitz, "Optimization of Radio Tracking Frequencies," IEEE Transactions on Antennas and Propagation, Vol. AP-27, No. 3, pp. 393-397 (1979).

[7] A.H. LaGrone and C.W. Chapman, "Some Propagation Characteristics of High UHF Signals in the Immediate Vicinity of Trees," IRE Transactions on Antennas and Propagation, September Issue, pp. 487-491 (1961).

[8] A.H. LaGrone, "Propagation of VHF and UHF Electromagnetic Waves over a Grove of Trees in Full Leaf," IEEE Transactions on Antennas and Propagation, Vol. AP-25, No. 6, pp. 866-869 (1977).

[9] P.L. McQuate, J.M. Harman, and M.E. McClanahan, "Tabulations of Propagation Data Over Irregular Terrain in the 239- to 9200 MHz Frequency Range," Part IV: Receiver Site in Grove of Trees, U.S. Department of Commerce, Office of Telecommunications, OT/TRER 19 (1971).

[10] D.O. Rendink and M.F. Wazowica, "Some Propagation Experiments Relating Foliage Loss and Diffraction Loss at X-Band and UHF Frequencies," IEEE Transactions on Vehicular Technology, Vol. VT-22, No. 4, pp. 114-122 (1973).

[11] J.A. Saxton and J.A. Lane, "VHF and UHF Reception, Effects of Trees and Other Obstacles," Wireless World, May (1955).

[12] W.L. Stutzman, F.W. Colliver, and H.S. Crawford, "Microwave Transmission Measurements for Estimation of the Weight of Standing Pine Trees," IEEE Transactions on Antennas and Propagation, Vol. AP-27, No. 1, pp. 22-26 (1979).

[13] S. Swarup and R.K. Tewari, "Depolarization of Radio Waves in Jungle Environment," IEEE Transactions on Antennas and Propagation, Vol. AP-27, No. 1, pp. 113-16 (1979).

[14] T. Tamir, "Radio Wave Propagation Along Mixed Paths in Forest Environments," IEEE Transactions on Antennas and Propagation, Vol. VP-25, No. 4, pp. 471-477 (1977).

[15] J.R. Wait, R.H. Ott, and T. Telfer, "Work Shop on Radio Systems in Forested and or Vegetated Environments," TR ACC-ACO-1-74, Advanced Concepts Office, U.S. Army Communications Command, Fort Huachuca, AZ 85613 (1974).

[16] M.A. Weissberger, "An Initial Critical Summary of Models for Predicting the Attenuation of Radio Waves by Foliage," ECAC-CR-80-035, Electromagnetic Compatibility Analysis Center, Annapolis, MD 21402 (1980).

☆ U.S. GOVERNMENT PRINTING OFFICE:1981—781-840 / 531

ATE
LMED
– 8